



**CARIBOU MONITORING STUDY FOR THE BEAR TOOTH
UNIT PROGRAM, ARCTIC COASTAL PLAIN, ALASKA, 2020**

Prepared for
ConocoPhillips Alaska, Inc.
Anchorage, Alaska

Prepared by
ABR, Inc.—Environmental Research & Services
Fairbanks, Alaska

**CARIBOU MONITORING STUDY FOR THE BEAR TOOTH UNIT
PROGRAM, ARCTIC COASTAL PLAIN, ALASKA, 2020**

Prepared for

ConocoPhillips Alaska, Inc.
P.O. Box 100360
Anchorage, Alaska 99510-0360

Prepared by

Joseph H. Welch
Alexander K. Prichard
Matthew J. Macander

ABR, Inc.—Environmental Research & Services
P.O. Box 80410
Fairbanks, Alaska 99708-0410

July 2021

EXECUTIVE SUMMARY

- Caribou use of the Bear Tooth Unit area has been studied since 2001 using a combination of aerial surveys, analysis of telemetry data, and remote sensing in order to understand caribou distribution and movements prior to development in the area. This report summarizes field research conducted in 2020 and analyses of data collected over the life of the project.
- Spring 2020 air temperatures were near the 30-year average and snow melted slightly earlier than usual at the Kuparuk airport. Temperatures were variable during early and mid-June but were generally below average. From June through early August, strong winds (>10 mph) occurred frequently and temperatures were often below average. Therefore, weather conditions were generally not conducive to high insect activity for much of the 2020 insect season. Temperatures were generally above average from mid- through late-August.
- We completed 6 of 8 planned aerial transect surveys of the Bear Tooth North (BTN) survey area between February and October 2020. The estimated density ranged from a maximum of 2.02 caribou/km² on 18–19 June to a minimum of 0.12 caribou/km² on 6 October. We observed 13 calves in the BTN survey area during the calving survey on 8–9 June.
- We completed 6 of 8 planned aerial transect surveys of the Bear Tooth South (BTS) survey area between February and October 2020. The estimated density ranged from a maximum of 2.41 caribou/km² on 26 February to a minimum of 0.11 caribou/km² on 18–19 June. We observed 11 calves in the BTS survey area during the calving survey on 8–10 June.
- We analyzed telemetry data using kernel density analysis, dynamic Brownian Bridge movement models, and species distribution models to examine seasonal patterns of movements and distribution for caribou from both the Teshekpuk Caribou Herd (TCH) and the Central Arctic Herd (CAH).
- We examined annual and seasonal spatial patterns in vegetative biomass (based on NDVI) and snow cover and snow water equivalent calculated on a regional scale using satellite imagery. We also estimated forage metrics including forage biomass and nitrogen levels based on NDVI and phenology.
- The BTN and BTS survey areas get some use by TCH females throughout the year, but the BTS survey area gets little use by females in June and July; use of the survey areas by male caribou of the TCH is highest during June–September with little winter use. Use of the BTN or BTS area by caribou of the CAH is rare.
- Species distribution models indicated that broad geographic patterns were important factors influencing caribou distribution during all seasons, but caribou distribution can also be explained by differences in vegetative biomass, landscape topography, snow cover, and habitat type.
- We assessed caribou movements around ice roads during the winters of 2018–2019 and 2019–2020, years when there were both extensive ice roads constructed and caribou use of the area, using an integrated step-selection analysis. There was some indication of avoidance of the area within approximately 5 km of ice roads in 2018–2019, but no similar response was detected in 2019–2020.
- We observed 9 grizzly bears in 5 groups in the BTN survey area, primarily along Fish or Judy creek and 5 bears in 2 groups in the BTS survey area. Three bear observations were in June, 2 were in August, and 2 were in October. A single wolverine was observed on 19 June.

TABLE OF CONTENTS

Executive Summary	iii
List of Figures	vi
List of Tables	vii
List of Appendices	viii
Acknowledgments	viii
Introduction.....	1
Background	1
Study Objectives	3
Study Area	4
Methods	5
Weather And Insect Conditions	5
Caribou Distribution and Movements.....	6
Aerial Transect Surveys.....	6
Density Mapping.....	6
Radio Telemetry	7
Seasonal Occurrence in the Study Area.....	7
Remote Sensing.....	9
Snow Cover.....	9
Vegetative Biomass	9
Forage Modeling.....	10
Habitat Classification.....	10
Species Distribution Modeling.....	10
Distribution Relative to Ice Roads.....	14
Results.....	16
Weather Conditions	16
Caribou Distribution and Movements.....	16
Aerial Transect Surveys.....	16
Radio Telemetry	21
Movements Near Proposed Willow Infrastructure	30
Remote Sensing.....	30
Snow Cover.....	30
Vegetative Biomass	34
Species Distribution Modeling.....	34
General Suitability	34
Suitability by Season	34
Distribution Near Ice Roads.....	51
Other Mammals.....	51
Discussion.....	53
Weather, Snow, and Insect Conditions	53
Caribou Distribution and Movements.....	56
Species Distribution Model.....	57
Distribution Near Ice Roads.....	61
Other Mammals.....	62
Conclusion	62
Literature Cited.....	63

LIST OF FIGURES

Figure 1.	Location of the caribou monitoring study area on the central North Slope of Alaska and detailed view showing locations of the Bear Tooth North and Bear Tooth South survey areas, 2001–2020	2
Figure 2.	Population size of the Teshekpuk and Central Arctic caribou herds, 1975–2020, based on Alaska Department of Fish and Game census estimates	3
Figure 3.	Habitat types used for caribou habitat-selection analysis in the Bear Tooth Unit study areas, National Petroleum Reserve-Alaska.....	11
Figure 4.	Snow depth, long-term mean, and 95% confidence interval at the Kuparuk airstrip, May–June 2020 and daily average air temperature, long-term mean, and 95% confidence interval at Kuparuk, May–September 2020.....	17
Figure 5.	Hourly air temperature, wind speed, mosquito probability index, and oestrid fly probability index at Nuiqsut, 15 June–1 September 2020.....	18
Figure 6.	Distribution and size of caribou groups observed during aerial surveys in seven seasons in the Bear Tooth North and Bear Tooth South survey areas, February–October 2020	19
Figure 7.	Mean seasonal densities of caribou in the NPRA caribou survey areas based on inverse distance-weighting interpolation of aerial survey results, 2002–2020	22
Figure 8.	Seasonal distribution of Central Arctic Herd female caribou based on fixed-kernel density estimation of telemetry locations, 2001–2020	24
Figure 9.	Seasonal distribution of Teshekpuk Caribou Herd females based on fixed-kernel density estimation of telemetry locations, 1990–2020.....	25
Figure 10.	Seasonal distribution of Teshekpuk Caribou Herd males based on fixed-kernel density estimation of telemetry locations, 1997–2020.....	26
Figure 11.	Distribution of parturient females of the Teshekpuk Caribou Herd during calving based on fixed-kernel density estimation of telemetry locations, 1990–2020.....	27
Figure 12.	Proportion of CAH and TCH caribou within the Bear Tooth Unit North and Bear Tooth Unit South survey areas, based on fixed-kernel density estimation, 1990–2020	28
Figure 13.	Movements of GPS-collared female caribou of the Teshekpuk Herd in the vicinity of the proposed Willow development during each of 8 seasons based on 95% isopleths of dynamic Brownian Bridge movement models	29
Figure 14.	Movements of GPS-collared caribou from the Teshekpuk Herd and Central Arctic Herd in the vicinity of the proposed Willow development during each of 8 seasons	31
Figure 15.	Proportion of caribou from the Teshekpuk Herd within 4 km of the proposed Willow development alignments, based on fixed-kernel density estimation, 1990–2020	33
Figure 16.	Extent of snow cover between early May and mid-June on the central Arctic Coastal Plain of Alaska in 2020, as estimated from MODIS satellite imagery.....	35
Figure 17.	Median snowmelt date and vegetation index metrics, as estimated from MODIS satellite imagery time series, on the central Arctic Coastal Plain of Alaska, 2000–2020.....	36
Figure 18.	Departure of 2020 values from median snowmelt date and vegetation index metrics, as estimated from MODIS satellite imagery time series, on the central Arctic Coastal Plain of Alaska.....	37
Figure 19.	Metrics of relative vegetation biomass during the 2020 growing season on the central North Slope of Alaska, as estimated from NDVI calculated from MODIS satellite imagery.....	38

Figure 20.	Predicted relative suitability for use of the GMT, BTN, and BTS survey areas by caribou during 8 different seasons, 2002–2020, based on Maxent analysis.....	40
Figure 21.	Response curves and permutation importance of the top 15 variables included in models to predict caribou suitability in the GMT, BTN, and BTS surveys areas during the winter season	41
Figure 22.	Response curves and permutation importance of the top 15 variables included in models to predict caribou suitability in the GMT, BTN, and BTS surveys areas during the spring migration season	42
Figure 23.	Response curves and permutation importance of the top 15 variables included in models to predict caribou suitability in the GMT, BTN, and BTS surveys areas during the calving season.....	43
Figure 24.	Response curves and permutation importance of the top 15 variables included in models to predict caribou suitability in the GMT, BTN, and BTS surveys areas during the postcalving season	44
Figure 25.	Response curves and permutation importance of the top 15 variables included in models to predict caribou suitability in the GMT, BTN, and BTS surveys areas during the mosquito season.....	45
Figure 26.	Response curves and permutation importance of the top 15 variables included in models to predict caribou suitability in the GMT, BTN, and BTS surveys areas during the oestrid fly season	46
Figure 27.	Response curves and permutation importance of the top 15 variables included in models to predict caribou suitability in the GMT, BTN, and BTS surveys areas during late summer...	47
Figure 28.	Response curves and permutation importance of the top 15 variables included in models to predict caribou suitability in the GMT, BTN, and BTS surveys areas during the fall migration season.	48
Figure 29.	Estimated selection for landcover classes by caribou of the Teshekpuk Herd based on an integrated step-selection analysis of winter movements	52
Figure 30.	Estimated selection for elevation, NDVI, and Topographic Position Index based on an integrated step-selection analysis by caribou of the Teshekpuk Herd based on an integrated step-selection analysis of winter movements	53
Figure 31.	Estimated selection for distance to ice roads by caribou of the Teshekpuk Herd based on an integrated step-selection analysis of winter movements.....	54
Figure 32.	Distribution of other large mammals observed during aerial and ground surveys in the Bear Tooth Unit Area during 2020 and 1991–2020	55

LIST OF TABLES

Table 1.	Number of TCH and CAH radio-collar deployments and total number of collared animals that provided movement data for the Bear Tooth Unit caribou study.....	8
Table 2.	Number and density of caribou in the Bear Tooth North and Bear Tooth South survey areas, February–October 2020.....	21
Table 3.	Proportion of GPS collared Teshekpuk Herd caribou that crossed the proposed Willow alignment at least once in each season, 2004–2020.	33
Table 4.	Sample sizes and performance metrics for the species distribution model analysis for the NPRA survey area, 2002–2020.	39

Table 5.	Permutation Importance of variables used in species distribution models of caribou suitability in the GMT, BTN, and BTS survey areas during 8 different seasons, 2002–2020	49
Table 6.	Model selection results for female GPS-collared TCH caribou winter movements in the study area, by year 2018–2020.	52

LIST OF APPENDICES

Appendix A.	Full methods for calculating remote sensing metrics.	73
Appendix B.	Cover-class descriptions of the NPRA earth-cover classification	76
Appendix C.	Snow depth and cumulative thawing degree-days at the Kuparuk airstrip, 1981–2019	78
Appendix D.	Timing of annual snowmelt, compared with median date of snowmelt, on the central North Slope of Alaska during 2000–2020, as estimated from MODIS imagery.....	81
Appendix E.	Differences between annual relative vegetative biomass values and the 2000–2020 median during the caribou calving season on the central North Slope of Alaska, as estimated from NDVI calculated from MODIS satellite imagery	82
Appendix F.	Differences between annual relative vegetative biomass values and the 2000–2020 median at estimated peak lactation for caribou on the central North Slope of Alaska, as estimated from NDVI calculated from MODIS satellite imagery.....	83
Appendix G.	Differences between annual relative vegetative biomass values and the 2000–2020 median at estimated peak biomass on the central North Slope of Alaska, as estimated from NDVI calculated from MODIS satellite imagery.....	84

ACKNOWLEDGMENTS

This study was funded by ConocoPhillips Alaska, Inc., (CPAI) and was administered by Christina Pohl, CPAI Environmental Studies Coordinator, with support from Robyn McGhee of CPAI and Jasmine Woodland from Weston Solutions Inc. for whose support we are grateful. Valuable assistance with field logistics was provided by Mike Hauser, Zac Hobbs, and Krista Kenny. Alaska Department of Fish and Game (ADFG) biologists played crucial collaborative roles in this study by capturing caribou, deploying radio collars, and providing telemetry data under a cooperative agreement among ADFG, CPAI, and ABR. We thank ADFG biologists Lincoln Parrett and Elizabeth Lenart for their professional cooperation and assistance. Brian Person of the North Slope Borough Department of Wildlife Management (NSB) provided GPS and satellite telemetry data, valuable information, and advice. Bob Gill of 70 North LLC and Bob Eubank of North River Air provided safe and efficient piloting of survey airplanes under flying conditions that often were less than optimal. Assistance in the field was provided by ABR employees Nick Moser, Tim Obritschkewitsch, Kelly Lawhead, Sam Vanderwaal, and Robert McNown. Support during data collection, analysis, and report production was provided by Christopher Swingley, Dorte Dissing, Will Lentz, Pamela Odom, and Tony LaCortiglia. Review by Adrian Gall of ABR and Robyn McGhee and Christina Pohl of CPAI improved this report.

INTRODUCTION

BACKGROUND

The caribou monitoring study for the Bear Tooth Unit (BTU) area is being conducted on the Arctic Coastal Plain of northern Alaska in the northeastern portion of the National Petroleum Reserve–Alaska (NPRA; Figure 1). This region is used primarily by one herd of barren-ground caribou (*Rangifer tarandus granti*)—the Teshekpuk Caribou Herd (TCH), although some animals from the Central Arctic Herd (CAH) may use the area in some years. The TCH generally ranges from the Colville River to the Chukchi Sea north of the Brooks Range (Person et al. 2007, Wilson et al. 2012, Parrett 2015a).

Most of the TCH remains on the coastal plain year-round. The primary calving area is around Teshekpuk Lake and the primary area of insect-relief habitat in midsummer is the swath of land between Teshekpuk Lake and the Beaufort Sea coast (Kelleyhouse 2001; Carroll et al. 2005; Parrett 2007, 2015a; Person et al. 2007; Yokel et al. 2009; Wilson et al. 2012). Since 2010, the calving distribution of the TCH appears to have expanded west, with some calving extending west of Atqasuk (Parrett 2015a; Prichard et al. 2019a).

The majority of TCH caribou winter on the coastal plain, generally west of the Colville River, although approximately one third of the herd, including a disproportionate number of males, winter in the central Brooks Range (Parrett 2015a, Prichard et al. 2019a, Prichard et al. 2020b). Similar to other herds, atypical herd movements sometimes occur. In a highly unusual movement, a large proportion of the TCH wintered far to the east in the Arctic National Wildlife Refuge (ANWR) in 2003–2004 following an October rain-on-snow event (Bieniek et al. 2019).

The TCH has experienced large cyclical population changes typical of barren-ground caribou herds. The herd increased substantially in size from the mid-1970s, when it consisted of only a few thousand animals, to the early 1990s (Figure 2; Parrett 2015a). The TCH experienced a dip in numbers in the early 1990s but increased steadily from 1995 to its peak estimated size of 68,932 animals in July 2008 (Parrett 2015a). The herd subsequently declined to 39,172 animals in 2013

but stabilized to 41,542 (SE = 3,486) by July 2015 and increased to a minimum of 56,255 by July 2017 (Klimstra 2018, Parrett 2015b). Although the new higher-resolution digital photography introduced in 2017 may have contributed to higher population counts since 2015, the increase in estimated herd size indicates that the TCH has remained stable or increased since 2015.

The summer range of the Central Arctic Herd (CAH) of caribou is generally between the Colville and Canning rivers. Individuals sometimes cross over to the west of the Colville River, particularly during late summer and mid-summer movements to the Canadian Border have occurred during some years. CAH caribou typically calve in two groups; between the Colville and Kuparuk Rivers; and between the Sagavanirktok and Canning rivers (Wolfe 2000, Arthur and Del Vecchio 2009, Lenart 2015a). They use the Beaufort Sea coast during periods of mosquito harassment (White et al. 1975, Dau 1986, Lawhead 1988), and generally winter in or near the Brooks Range, usually east of the Dalton Highway/Trans-Alaska Pipeline (TAPS) corridor (Arthur and Del Vecchio 2009, Lawhead et al. 2015, Lenart 2015a, Nicholson et al. 2016), although some animals have remained north of the Brooks Range on the coastal plain in recent years (Prichard and Welch 2020, 2021).

Population trends of the CAH have largely mirrored those of the TCH (Figure 2; Lenart 2009, 2015a, 2017, 2019, 2021). The herd grew rapidly from ~5,000 animals in the mid-1970s to a peak size of 68,442 caribou in 2010 (Lenart 2021). The herd subsequently declined rapidly to 22,630 caribou by July 2016 (Lenart 2017). The herd then increased to 30,069 caribou by July 2019 (Lenart 2019), although, similar to the TCH, some of the recent apparent increase in herd size may have been a result of higher-resolution digital photography for conducting the photocensus. The magnitude of the decline from 2010 to 2016 may have been affected by emigration of some CAH animals to the Porcupine Caribou Herd and TCH, with which the CAH often intermixes on winter range.

This monitoring study builds on prior research funded by ConocoPhillips Alaska, Inc. (CPAI; and its heritage companies Phillips Alaska, Inc., and ARCO Alaska, Inc.) that was conducted on the Colville River delta and adjacent coastal plain east

Introduction

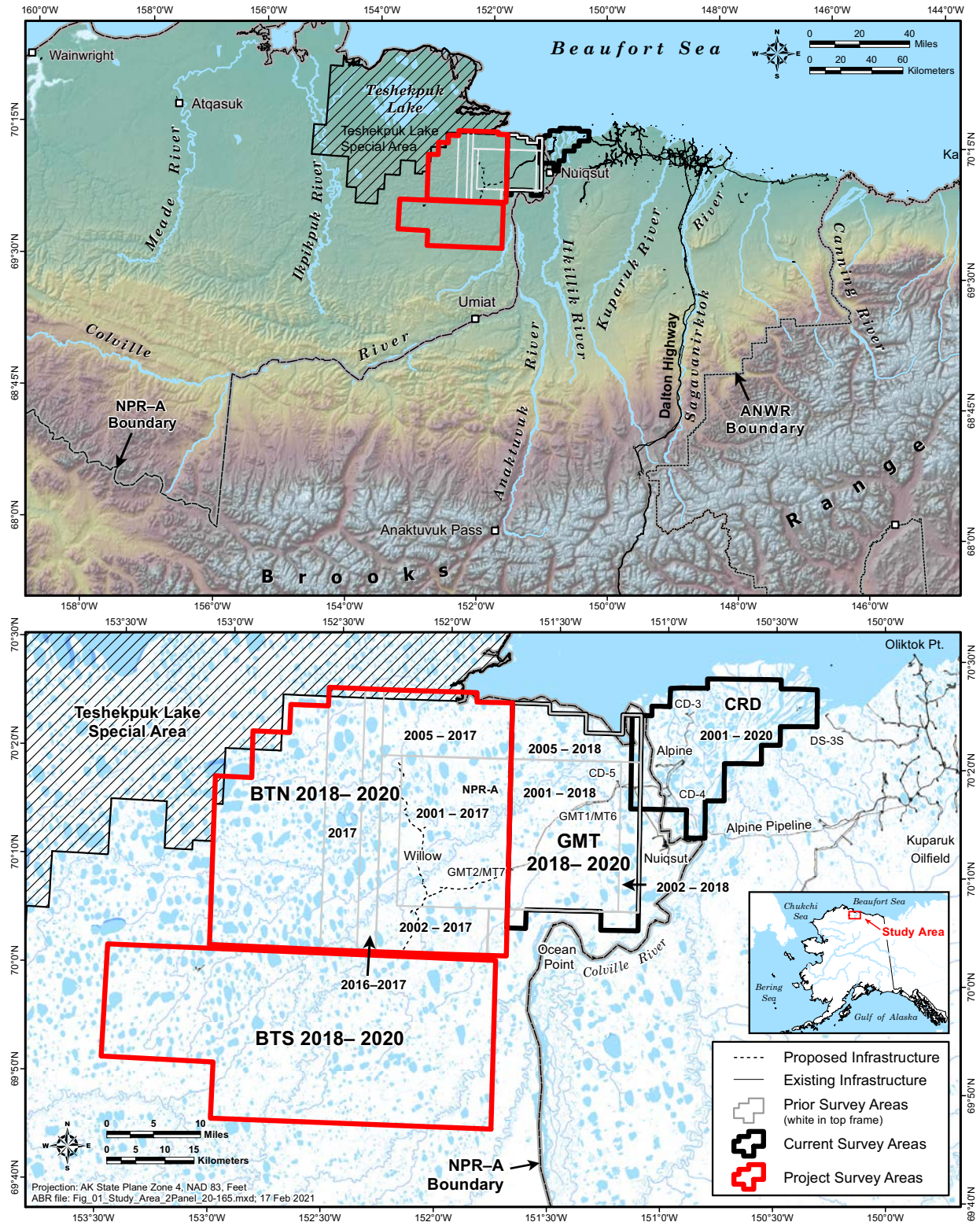


Figure 1. Location of the caribou monitoring study area on the central North Slope of Alaska and detailed view showing locations of the Bear Tooth North and Bear Tooth South survey areas, 2001–2020.

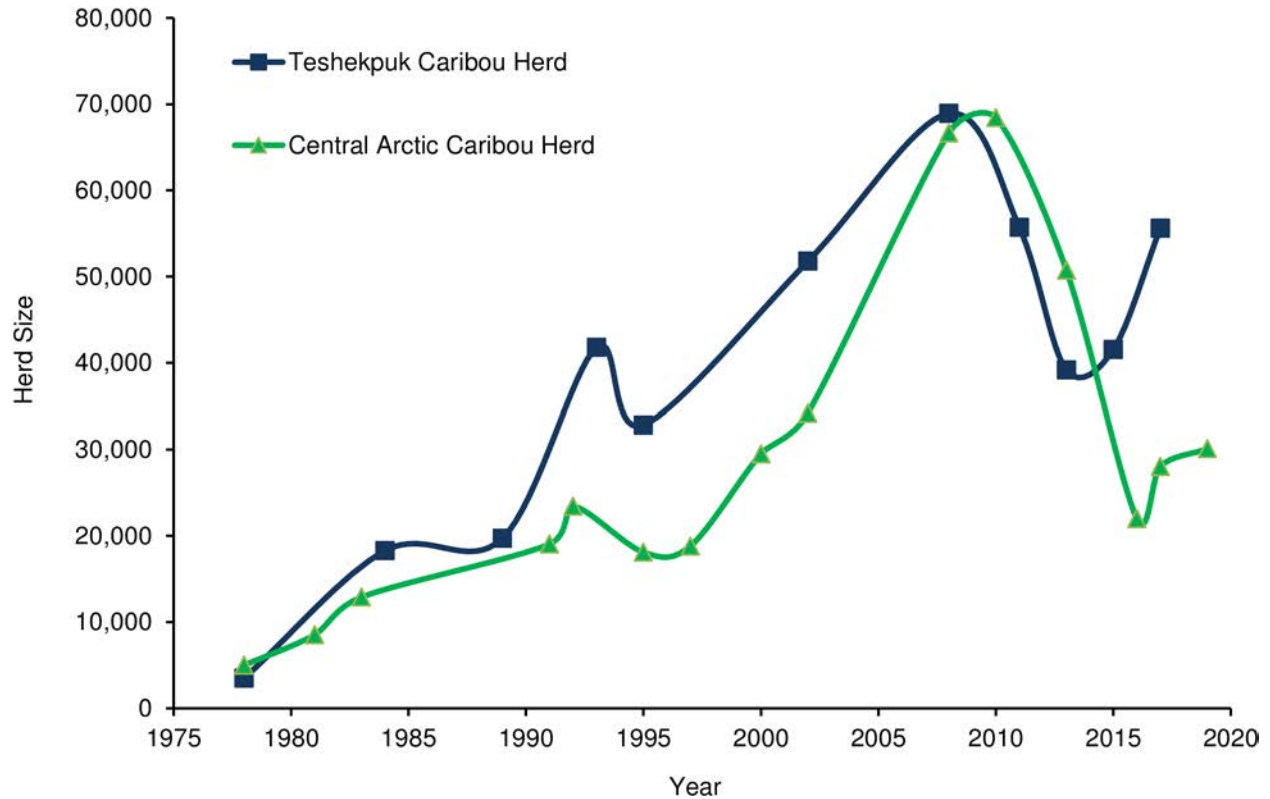


Figure 2. Population size of the Teshekpuk and Central Arctic caribou herds, 1975–2020, based on Alaska Department of Fish and Game census estimates.

of the delta (Alpine transportation corridor) beginning in 1992 and in the northeastern portion of the NPRA beginning in 1999 (Johnson et al. 2015; Jorgenson et al. 1997, 2003, 2004). Since 1990, contemporaneous, collaborative telemetry studies of caribou distribution and movements have been conducted in the region west of the Colville River by the Alaska Department of Fish and Game (ADFG), the North Slope Borough (NSB), and the Bureau of Land Management (BLM) (Philo et al. 1993, Carroll et al. 2005, Person et al. 2007, Wilson et al. 2012, Parrett 2015a, Prichard et al. 2017, 2018b, 2019c, 2020d). Consultants working for BP Exploration (Alaska), Inc., conducted aerial transect surveys over much of the TCH calving grounds during 1998–2001 (Noel 1999, 2000; Jensen and Noel 2002; Noel and George 2003) and the NSB conducted aerial survey areas of calving caribou between Wainwright and Atkasuk during 2013–2015 (Prichard et al. 2019a).

STUDY OBJECTIVES

Evaluation of the natural and anthropogenic factors affecting caribou distribution and movements in the study area fall into two broad categories: those affecting movements of individuals and those affecting distribution of herds. Clearly, these categories are linked and are not mutually exclusive, but the applicability of study methods differs between them. Information on the potential effects of development on caribou distribution can be collected using a variety of methods, including aerial transect surveys, radio telemetry, and other reported observations. Information about the potential effects on caribou movements, however, cannot be addressed adequately without employing methods such as radio telemetry that allow consistent tracking of individually identifiable animals.

Much of the research on caribou response to oilfield infrastructure has been conducted on the

CAH (Murphy and Lawhead 2000, Cameron et al. 2005, Prichard et al. 2020a), which has interacted with the Prudhoe Bay and Kuparuk oilfields for over 4 decades (Prichard et al. 2020a), but the herd winters in or near the Brooks Range (Nicholson et al. 2016, Prichard et al. 2020b) and provides few insights on caribou reactions to infrastructure during winter. Unlike the CAH, the majority of caribou in the TCH winter on the Coastal Plain (Person et al. 2007). As development expands west of the Colville River, wintering caribou are increasingly interacting with winter oilfield drilling and exploration activity. This provides an opportunity to examine how caribou react to ice roads built on the winter range of a caribou herd with only limited previous exposure to industrial development.

Several broad tasks were identified for study:

1. Evaluate the seasonal distribution, abundance, and movements of caribou in the study area, using a combination of historical and current data sets from aerial transect surveys and radio telemetry data obtained for this study and from ADFG/NSB/BLM under a cooperative agreement.
2. Characterize important habitat conditions, such as snow cover, spatial pattern and timing of snowmelt, seasonal flooding (if possible), and estimated biomass of new vegetative growth in the study area by applying remote-sensing techniques.
3. Compare caribou distribution with habitat distribution, remote-sensing data, and other landscape features to better understand factors influencing the seasonal distribution of caribou and evaluate potential impacts of future development.
4. Assess caribou movement patterns in relation to winter ice roads constructed in the area.
5. Record the distribution and abundance of other large mammals encountered incidentally during research conducted in the Bear Tooth Unit region.

STUDY AREA

CPAI began funding caribou surveys in the northeastern NPRA in 2001–2004. These studies continued during 2005–2014 under the North Slope Borough (NSB) Amended Development Permit 04-117 stipulation for the CD-4 drill site project (constructed during winter 2004–2005) which called for a 10-year study of the effects of development on caribou. The study area was specified as the area within a 48-km (30-mi) radius around the CD-4 drill site (Lawhead et al. 2015). Initially, aerial transect surveys were conducted in 3 survey areas which encompassed most of that 48-km radius (Lawhead et al. 2015): the NPRA survey area (expanded from 988 km² in 2001 to 1,310 km² in 2002; 1,720 km² in 2005); the Colville River Delta (CRD) survey area that encompasses CD-1 through CD-4 (494 km²); and the Colville East survey area (1,432–1,938 km², depending on the survey and year). Although 2014 was the tenth year of study, the Bureau of Land Management (BLM) required continued caribou studies in accordance with the Integrated Activity Plan (IAP) for the NPRA. In 2016, the study area was redefined to focus on the NPRA and CRD survey areas, so results for the final year of aerial surveys in the Colville East survey area were reported elsewhere (Prichard et al. 2018a). In 2016 and 2017, the NPRA survey area was expanded westward by 1 and 2 transects, respectively (1,818 km² in 2016; 2,119 km² in 2017). In November 2018, the North Slope Borough adopted Ordinance Serial No. 75-06-72, consolidating previous ordinances and rezoning lands for the GMT2/MT7 area as resource development districts. This ordinance required CPAI to fund a caribou study to use “a landscape analysis to investigate the distribution and movements of caribou around the Colville River Delta adjacent areas including all Alpine and associated developments to assess habitat relationships and possible impacts from development.”

In 2018, the NPRA survey area was therefore again redefined to focus on the three recently constructed drill sites: CD-5, constructed in winter 2013–2014, GMT1/MT6, constructed in winter 2016–2017, and GMT2/MT7, constructed in winter 2018–2019, as well as their connecting access roads) and pipelines (Figure 1, bottom). The

pipeline to GMT2/MT7 is scheduled to be completed in spring 2021. This newly defined Greater Moose's Tooth (GMT) survey area (776.6 km²) also includes the Nuiqsut Spur Road that was constructed by the Kuukpik Corporation in winter 2013–2014 to connect the village of Nuiqsut to the CD-5 access road. The results of research conducted in the CRD and GMT survey areas were reported separately (Welch et al. 2021).

The portion of the previous NPRA survey area west of GMT2/MT7 was expanded west and south to focus on the Willow prospect and other potential future developments within the Bear Tooth Unit (BTU). Results of studies within this new expanded study area are reported on here. For surveys and analysis, the BTU study area was split up into 2 survey areas, BTU North (BTN) and BTU South (BTS; Figure 1). To provide a wider context for analytical results and avoid duplication, some of the analyses in this report were conducted for all NPRA survey areas (GMT, BTN, and BTS; Figure 1) and those results are included in both this report and the CRD and GMT report (Welch et al. 2021). In 2021, continuation of caribou studies was stipulated by the North Slope Borough as part of the rezoning process for the Willow Project (NSB Ordinance 75-06-75).

The study area is located on the central Arctic Coastal Plain of northern Alaska (Figure 1, top). The climate in the region is arctic maritime (Walker and Morgan 1964). Winter lasts about eight months and is generally cold and windy. The summer thaw period lasts about three months (June–August) and the mean summer air temperatures in Nuiqsut during 1990–2020 range from 6.2–9.9°C (43.2–49.9°F; <http://climate.gi.alaska.edu/Climate/Normals>, accessed 27 January 2020) with a strong regional gradient of summer temperatures increasing with distance inland from the coast (Brown et al. 1975). Mean summer precipitation measured at Kuparuk and Colville Village is 9.7–12.5 cm (3.8–4.94 in), most of which falls as rain in July and August (<http://climate.gi.alaska.edu/Climate/Normals>, accessed 27 January 2020).

Spring is brief, lasting about 3 weeks from late May to mid-June, and is characterized by the flooding and break-up of rivers and smaller tundra streams. Summer weather is characterized by low precipitation, overcast skies, fog, and persistent northeasterly winds. The less common westerly

winds often bring storms that are accompanied by high wind-driven tides and rain (Walker and Morgan 1964). Summer fog occurs more commonly at the coast and on the delta than it does farther inland.

METHODS

To evaluate the distribution and movements of TCH caribou in the study area, ABR biologists conducted aerial transect surveys and analyzed existing telemetry data sets provided by ADFG, NSB, BLM, and the U.S. Geological Survey (USGS), and from GPS collars deployed specifically for this study in 2006–2010, 2013–2014, and 2016–2020. The majority of telemetry collars were scheduled to record one location every 2 hours during summer with less frequent locations during the winter; a typical collar deployment lasted 3 years.

Eight seasons per year were used for analysis of telemetry and aerial survey data, based on mean movement rates and observed timing of caribou life-history events (adapted from Russell et al. 1993 and Person et al. 2007): winter (1 December–30 April); spring migration (1–29 May); calving (30 May–15 June); postcalving (16–24 June); mosquito harassment (25 June–15 July); oestrid fly harassment (16 July–7 August, a period that also includes some mosquito harassment); late summer (8 August–15 September); and fall migration, a period that includes the breeding season, or rut (16 September–30 November).

WEATHER AND INSECT CONDITIONS

Temperature and wind data can be used to predict the occurrence of harassment by mosquitoes (at least five *Aedes* species) and oestrid flies (warble fly *Hypoderma tarandi* and nose bot fly *Cephenemyia trompe*) (White et al. 1975, Fancy 1983, Dau 1986, Russell et al. 1993, Mörschel 1999, Yokel et al. 2009). To estimate spring and summer weather conditions in the area during 2020, we used meteorological data from National Weather Service reporting stations at Kuparuk and Nuiqsut. Thawing degree-day sums (TDD; total daily degrees Celsius above zero) were calculated using average daily temperatures at the Kuparuk airstrip. Average index values of mosquito activity

were estimated based on hourly temperatures from Nuiqsut, using equations developed by Russell et al. (1993). The estimated probability of oestrid-fly activity was calculated from average hourly wind speeds and temperatures recorded at Nuiqsut, using equations developed by Mörschel (1999).

CARIBOU DISTRIBUTION AND MOVEMENTS

AERIAL TRANSECT SURVEYS

Transect surveys provided information on the seasonal distribution and density of caribou in the study area (ADFG permit number 20-094). Surveys of the BTN and BTS survey areas (Figure 1, bottom) were conducted periodically from February to October 2020 in a fixed-wing airplane (Cessna 185 or Cessna 207), following the same procedures used since 2001 in the NPRA survey area (Lawhead et al. 2015 and references therein).

In 2020, aerial transect surveys in the BTN and BTS survey areas were scheduled for mid-February (mid-winter), mid-April (late winter), mid-May (spring migration), early June (calving), late June (postcalving), late July (oestrid fly), late August (late summer), and mid-September to early October (fall migration). Due to the global coronavirus pandemic, April and May surveys were not conducted. Additionally, due to inclement weather, the BTN and BTS surveys during the postcalving season were only partially completed.

During aerial surveys, 2 observers looked out opposite sides of the airplane and recorded data independently. The pilot navigated the airplane along transect lines using a GPS receiver and maintained an altitude of ~150 m (500 ft) above ground level (agl) or ~90 m (300 ft) agl. Surveys were flown at 90 m agl only during the calving and postcalving surveys and only in the western portion of the BTN survey area. The lower flight altitude was chosen to increase the ability to detect calves due to the anticipated high levels of calving activity near Teshekpuk Lake.

Transect lines were spaced at intervals of 3.2 km (2 mi) in BTN and 4.8 km (3 mi) in BTU South, following section lines on USGS topographic maps (scale 1:63,360). Observers counted caribou within an 800-m-wide strip on each side of the airplane when flying at 150 m agl

or a 400-m-wide strip when flying at 90 m agl. Therefore, we sampled ~50% of the BTN survey area when flying 150 m agl, 25% of the western portion of BTN when flying at 90 m agl during the calving and postcalving survey, and 33% of the BTS survey area while flying 150 m agl. The number of caribou observed in the transect strips was therefore adjusted (e.g., multiplied by 2, 3, or 4) to estimate the total number of caribou in the survey area on each survey. The strip width was delimited visually for the observers by placing tape markers on the struts and windows of the aircraft, as recommended by Pennycuik and Western (1972), or by measuring distances to recognizable landscape features displayed on maps in GPS receivers.

When caribou were observed within the transect strip, a GPS location was recorded when the plane was perpendicular to the animal or herd, the numbers of “large” caribou (adults and yearlings) and calves were recorded, and the perpendicular distance from the transect centerline was assigned to one of four 100-m or 200-m intervals, depending on the strip width. For plotting locations on maps, the midpoint of the distance interval was used (e.g., 300 m for the 200–400-m interval). Thus, the maximal mapping error for distance was estimated to be ~100 m. Confidence intervals for estimates of total caribou and calves were calculated with a standard error formula modified from Gasaway et al. (1986), using 3.2-km segments of the transects as the sample units.

Observations of all other large mammals were recorded during aerial surveys. We also compiled observations of large mammals made by other ABR researchers working on other projects in the area.

DENSITY MAPPING

To map seasonal densities of caribou for the period 2002–2020, we used the inverse distance-weighted (IDW) interpolation technique of the *gstat* package (Pebesma 2004) in program *R* (R Core Team 2020) using all aerial survey data located within the current GMT and BTU survey areas, consistent with previous reports (Prichard et al. 2020c, 2020d). Each grid cell was 1.6 km wide by 1.6 or 3.2 km long, depending on the transect length, for a total of 208 cells and 114 cells in the BTN and BTS survey areas, respectively. We

calculated density in each grid cell by dividing the total number of caribou observed in a grid cell on each survey by the land area in the grid cell. The best power (from 1 to 1.2) and the best number of adjacent centroids (from 10 to 24) to use in the calculations were selected based on the values that minimized the residual mean square error. This analysis produced color maps showing surface models of the estimated density of all caribou (large caribou plus calves) observed over the entire analysis area for each season.

RADIO TELEMETRY

Satellite Collars

Satellite (Platform Transmitter Terminal; PTT) telemetry used the Argos system (operated by CLS America, Inc.; CLS 2016) and locations were transferred monthly to the NSB for data archiving. Satellite collar locations for the TCH were transmitted either at 6 h/day for a month after deployment and then 6 h every other day throughout the year, or once every 6 days in winter and every other day during summer (Lawhead et al. 2015). The CAH satellite collars were programmed to operate 6 h/day or 6 h every 2 days (Fancy et al. 1992, Lawhead et al. 2015).

Satellite-collar data were obtained from ADFG, NSB, and BLM for TCH animals during the period July 1990–November 2020 (Lawhead et al. 2006, 2007, 2008, 2009, 2010, 2011, 2012, 2013, 2014, 2015; Person et al. 2007; Prichard et al. 2017, 2018, 2019d, 2020c, this study) and for CAH caribou during the periods October 1986–July 1990 (from USGS), July 2001–September 2004, and April 2012–September 2016 (Cameron et al. 1989, Fancy et al. 1992, Lawhead et al. 2006, Lenart 2015a; Table 1). In the TCH sample (based on herd affiliation at capture), 186 collars deployed on 166 different caribou (86 females, 80 males) transmitted signals for a mean duration of 571 days per collar. The CAH 1986–1990 sample included 17 caribou (16 females, 1 male). The CAH 2001–2004 and 2012–2020 deployment samples included 24 collars deployed on 24 caribou (16 females, 8 males), transmitting for a mean duration of 641 days per collar. Only collars that transmitted for >14 d were included in analysis. Satellite telemetry locations are considered accurate to within 0.5–1.0

km of the true locations (CLS 2016), but the data require screening to remove spurious locations (Lawhead et al. 2015).

GPS Collars

GPS collars purchased by BLM, NSB, ADFG, and CPAI (TGW-3680 GEN-III or TGW-4680 GEN-IV store-on-board configurations with Argos satellite uplink, manufactured by Telonics, Inc., Mesa, AZ) were deployed 317 times by ADFG biologists on 223 different TCH caribou (208 females, 15 males; Table 1) during 2004 and 2006–2020, with a mean deployment duration of 668 days. GPS collars (purchased by CPAI and ADFG) were deployed 182 times on 127 different female CAH caribou during 2003–2020, with a mean duration of 600 days. Only collars that transmitted for >14 d were included in analysis. Collars were programmed to record locations at 2-, 3-, 5-, or 8-h intervals, depending on the desired longevity of the collar (Arthur and Del Vecchio 2009, Lawhead et al. 2015).

GPS collars were deployed on female caribou, with the exception of 15 collars deployed on TCH males. Females are preferred for GPS collar deployment because the collar models used are subject to antenna problems when using the expandable collars that are required to allow for increased neck size of males during the rut (Dick et al. 2013) and adult males have a shorter lifespan. Caribou were captured by ADFG personnel firing a handheld net-gun from a Robinson R-44 piston-engine helicopter. In keeping with ADFG procedures for the region, no immobilizing drugs were used (Parrett 2015a, Lenart 2021).

Data reports from Argos satellite uplinks were downloaded daily from CLS America, Inc. (Largo, MD), and the full dataset was downloaded after the collars were retrieved. Data were screened to remove spurious locations using methods described in Lawhead et al. (2015).

SEASONAL OCCURRENCE IN THE STUDY AREA

Seasonal use of the BTN and BTS survey areas was evaluated using several methods. We used Kernel Density Estimation (KDE) to calculate utilization distributions of caribou during different periods. We first calculated the mean location of each caribou for every 2-day period during the

Table 1. Number of TCH and CAH radio-collar deployments and total number of collared animals that provided movement data for the Bear Tooth Unit caribou study.

Herd ^a / Collar Type	Years	Female		Male		Total Deployments
		Deployments	Individuals	Deployments	Individuals	
Teshekpuk Herd						
VHF collars ^b	1980–2005	n/a		n/a		212
Satellite collars	1990–2020	97	86	89	80	186
GPS collars	2004–2020	299	208	18	15	317
Central Arctic Herd						
VHF collars ^b	1980–2005	n/a		n/a		412
Satellite collars	1986–1990	16	16	1	1	17
Satellite collars	2001–2004	10	10	2	2	12
Satellite collars	2012–2020	6	6	6	6	12
GPS collars	2003–2020	182	127	0	0	182

^a Herd affiliation at time of capture.

^b n/a = not available, but most collared animals were females.

year. We then used fixed-kernel density estimation in the *ks* package for *R* (Duong 2017) to create utilization distribution contours of caribou distribution for every 2-day period throughout the year (all years combined) based on these mean locations. We then calculated an average utilization distribution for each combination of season, herd, and sex by calculating the average pixel values for each two-day utilization distribution. By calculating the average of utilization distributions based on the mean location for each animal, we were able to account for movements within a season while not biasing the calculation due to autocorrelation among locations for a single caribou or due to unequal sample sizes among caribou. The plug-in method was used to calculate the bandwidth of the smoothing parameter. Because caribou are sexually segregated during some seasons, kernels were analyzed separately for females and males, although the sample size for male CAH caribou was insufficient to allow kernel density analysis. We also calculated a separate kernel for parturient TCH females during the calving season to delineate the calving range of the TCH.

We also calculated KDE by month (all years combined) for TCH males, TCH females, and CAH females. The proportion of each monthly utilization distribution from KDE within the survey areas was then calculated to determine the predicted monthly proportions of the herds expected to be using the study areas.

To visualize movements of caribou outfitted with GPS collars, we used dynamic Brownian Bridge Movement Models (dBBMM) to create utilization distribution maps of movements based on the locations of collared individuals (Kranstauber et al. 2014). These dBBMM models, a modification of earlier Brownian bridge models (Horne et al. 2007), use an animal's speed of movement and trajectory calculated from intermittent GPS locations to create a probability map describing relative use of the area traversed. We computed the 95% isopleth of movements for each individual TCH caribou outfitted with a GPS collar in the area and then overlaid the isopleth layers for each season to calculate the relative proportion of collared caribou using each 100-m pixel. This visualization displays the seasonal use of the area by TCH caribou as a function of both caribou distribution and movements. The dBBMM

models were computed using the *move* package in *R* (Kranstauber et al. 2017).

We examined GPS- and satellite-collar data to describe movements of individual caribou in the immediate vicinity of existing and proposed infrastructure. All GPS-collared TCH segments were mapped to visualize movements in the study area. We also calculated the proportion of collared TCH caribou that crossed the alignments at least once during a season for each year. We excluded animals that were present for less than half the season or with fewer than 30 locations per season. Locations within 30 days of collaring were removed. Additionally, we calculated the proportion of each monthly utilization distribution within 4 km of the proposed road and pad alignments (Proposed road alignment Alternative B, 1 Jan 2020).

REMOTE SENSING

The remote sensing methods are summarized here; a full description of remote sensing methods can be found in Appendix A. We analyzed 2020 snow cover and 2000–2020 vegetation greenness using gridded, daily reflectance and snow-cover products from MODIS Terra and Aqua sensors. The snow-cover data were added to the data compiled for 2000–2019 (see Lawhead et al. 2015 and Prichard et al. 2017 and 2018b for detailed description of methods). The entire vegetation index record, based on atmospherically corrected surface reflectance data, was processed to ensure comparability of greenness metrics.

SNOW COVER

Snow cover was estimated using the fractional snow algorithm developed by Salomonson and Appel (2004). A time series of images covering the April–June period was analyzed for each year during 2000–2020. Pixels with >50% water (or ice) cover were excluded from the analysis. For each pixel in each year, we identified:

- The first date with 50% or lower snow cover (i.e., “melted”)
- The closest prior date with >50% snow cover (i.e., “snow”)
- The midpoint between the last observed date with >50% snow cover and the first observed date with <50% snow cover,

which is an unbiased estimate of the actual snowmelt date (the first date with <50% snow cover)

- The duration between the dates of the two satellite images with the last observed “snow” date and the first observed “melted” date, providing information on the uncertainty in the estimate of snowmelt date. When the time elapsed between those two dates exceeded one week because of extensive cloud cover or satellite sensor malfunction, the pixel was assigned to the “unknown” category.

VEGETATIVE BIOMASS

The Normalized Difference Vegetation Index (NDVI; Rouse et al. 1973) is used to estimate the biomass of green vegetation within a pixel of satellite imagery at the time of image acquisition (Rouse et al. 1973). The rate of increase in NDVI between two images acquired on different days during green-up has been hypothesized to represent the amount of new growth occurring during that time interval (Wolfe 2000, Kelleyhouse 2001, Griffith et al. 2002). NDVI is calculated as follows (Rouse et al. 1973; <http://modis-atmos.gsfc.nasa.gov/NDVI/index.html>):

$$\text{NDVI} = (\text{NIR} - \text{VIS}) \div (\text{NIR} + \text{VIS})$$

where:

NIR = near-infrared reflectance (wavelength 0.841–0.876 μm for MODIS), and

VIS = visible light reflectance (wavelength 0.62–0.67 μm for MODIS).

NDVI during the calving period (NDVI_Calving) was calculated from a 10-day composite period (1–10 June) for each year during 2000–2020 (adequate cloud-free data were not available to calculate NDVI_Calving over the entire study area in some years). NDVI values near peak lactation (NDVI_621) were interpolated based on the linear change from two composite periods (15–21 June and 22–28 June) in each year. NDVI_Rate was calculated as the linear change in NDVI from NDVI_Calving to NDVI_621 for each year. Finally, NDVI_Peak was calculated from all

imagery obtained between 21 June and 31 August each year during 2000–2020. Due to the availability of new forage models, NDVI_Calving, NDVI_621, NDVI_Rate, and NDVI_Peak were not included in analyses of caribou distribution in 2020, but we included summaries of these metrics in this report for comparison with previous reports.

FORAGE MODELING

We applied forage models from Johnson et al. (2018) that incorporate daily NDVI values as well as habitat type, distance to coast, and days from peak NDVI to predict biomass, nitrogen, and digestible energy for a given location on a given day. These models may provide metrics that are more directly related to caribou forage needs than NDVI alone.

Johnson et al. (2018) calibrated the forage models for 4 broad vegetation classes (tussock tundra, dwarf shrub, herbaceous mesic, and herbaceous wet). Following their approach, we used the Alaska Center for Conservation Science (ACCS) land cover map for Northern, Western, and Interior Alaska (Boggs et al. 2016), aggregated on the “Coarse_LC” attribute. This map is based on the North Slope Science Initiative (NSSI 2013) with the addition of the aggregation field. We calculated the modal land cover class for each 500-m pixel.

Snow water equivalent (SWE) estimates were obtained from the Daymet Version 3 model output data (Thornton et al. 2016). This model provided gridded estimates of daily weather parameters for North America and Hawaii at 1 km resolution. SWE was extracted based on the location and date.

For each date from the start of the calving season through the end of the late summer season (30 May–15 September) and for each year with telemetry locations (2002–2020) we mapped NDVI, annual NDVIMax, and days to NDVIMax. Then, we applied the equations from Johnson et al. (2018) to calculate forage nitrogen content and forage biomass for the 4 broad vegetation classes.

HABITAT CLASSIFICATION

We used the NPRA earth-cover classification created by BLM and Ducks Unlimited (2002; Figure 3) to classify habitats for analyses. The NPRA survey area contained 15 cover classes from the NPRA earth-cover classification (Appendix B),

which we lumped into nine types to analyze caribou habitat use. The barren ground/other, dunes/dry sand, low shrub, and sparsely vegetated classes, which mostly occurred along Fish and Judy creeks, were combined into a single riverine habitat type. The two flooded-tundra classes were combined as flooded tundra and the clear-water, turbid-water, and *Arctophila fulva* classes were combined into a single water type; these largely aquatic types are used very little by caribou, so the water type was excluded from the analysis of habitat preference.

Some previous reports (e.g., Lawhead et al. 2015) used a land-cover map created by Ducks Unlimited for the North Slope Science Initiative (NSSI 2013); however, discontinuities in classification methodology and imagery bisected our survey area and potentially resulted in land-cover classification differences in different portions of the survey area, and so we reverted to the BLM and Ducks Unlimited (2002) classification instead.

SPECIES DISTRIBUTION MODELING

We fit a relationship between caribou group locations and a suite of environmental predictors that characterized weather, habitat, and topography. In previous years, we used resource selection function (RSF) models to evaluate relationships between caribou locations and explanatory variables. While still a highly valid method, RSFs are limited by the number of predictor variables and model complexity that can be incorporated into the model. Therefore, we decided to model relationships between environmental covariates and caribou distribution using the Maxent Java application (Phillips et al. 2020). Maxent is one of the most commonly used methods for computing species distribution models due to its ease of use and its predictive performance relative to other methods, especially with small sample sizes (Elith et al. 2006, Phillips et al. 2006, Warren and Seifert 2011, Merow et al. 2013). Maxent uses presence-only data and environmental variables to model a relative environmental probability distribution (suitability) across a landscape using a maximum entropy model framework (Phillips et al. 2006). Maxent is a commonly used data mining technique that

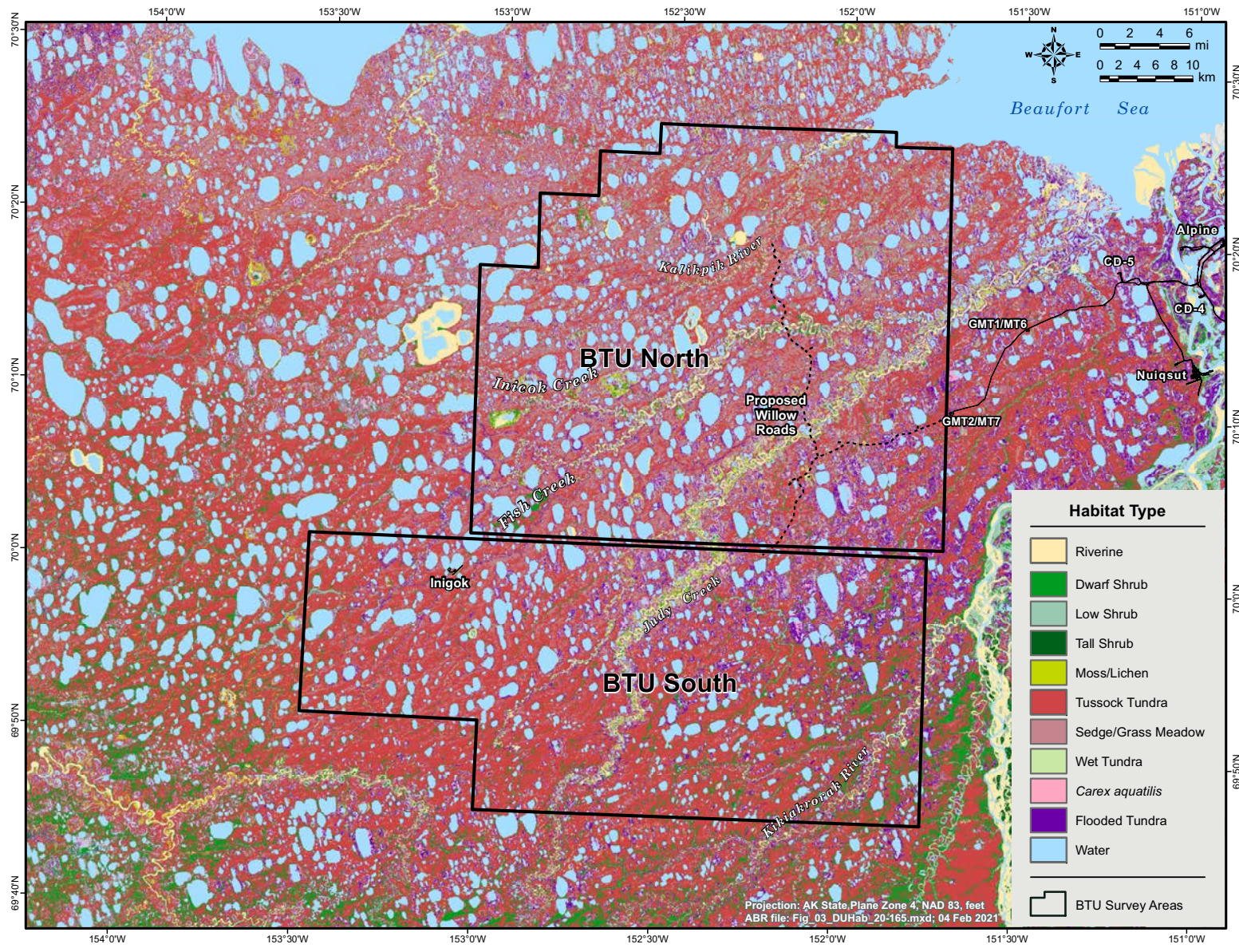


Figure 3. Habitat types used for caribou habitat-selection analysis in the Bear Tooth Unit study areas, National Petroleum Reserve-Alaska.

compares complex combinations of variables, variable transformations, and multiple variable interactions to find the best model for predicting the distribution of training and test data (Phillips et al. 2006, Elith et al. 2011, Merow et al. 2013, Phillips 2017). Because this is a data mining method, the emphasis is modeling predictions (mainly maps). As a result, the reported relationships between caribou distribution and environmental variables are more likely to be due to spatial correlation rather than causal relationships when compared to methods like RSF. However, Maxent provides tools for evaluating model performance and validity, variable contributions and relationships, and species distribution model (SDM) maps for investigation.

We used the same method for selecting caribou location data for Maxent as we did for the previously used RSF models (Prichard et al. 2020c, Prichard et al. 2020d). We included group locations from aerial surveys and locations from GPS-collared individuals. Locations from animals outfitted with satellite-collars (PTT) were not used in these analyses due to the lower accuracy of locations from those collars. We used caribou locations from aerial transect surveys conducted during 2002–2020 in the BTN, BTS, and GMT combined survey areas, but the seasonal sample sizes for the CRD survey area were too small to support analysis. The available GPS-collar data spanned the period 11 May 2003–30 December 2020 and were filtered to include only locations falling within the aerial survey area. We subsampled GPS locations at 48-h intervals in all seasons to standardize the time between GPS-collar locations, maintain an adequate sample size, and reduce the effect of autocorrelation on results (Lair 1987, McNay et al. 1994). We assumed that 48 h was enough time for a caribou to move across the entire study area, thereby minimizing autocorrelation. We excluded caribou locations in waterbodies on the habitat map and in areas that were excluded from the NDVI calculations because they were predominantly water-covered.

For each actual caribou or caribou group location, we generated 25 random locations in non-water habitats within the same survey area as the actual location. We were therefore testing for selection at the level of specific areas or attributes

for animals that were within the survey area. For this analysis we use the terms “selection” and “avoidance” to refer to attributes that are used more than expected or less than expected by caribou, when compared with random points.

We ran seasonal models to compare actual caribou locations to random locations using the following explanatory variables: habitat type (merged into the eight non-water categories; Figure 3), mean annual precipitation (MAP; Crookston and Rehfeldt 2010), degree-days greater than 5 °C (DD5; Crookston and Rehfeldt 2010), annual moisture index (AMI; Dunk et al. 2019), elevation, aspect (categorical variable with 8 directions and flat), slope, local elevational difference (LED; Dunk et al. 2019), topographic position index (TPI; Jenness et al. 2013), terrain ruggedness index (TRI; Wilson et al. 2007), topographic ruggedness index (TRI2; Riley et al. 1999), topographic wetness index (TWI; Theobald 2011) and flat and gentle sloping landforms (Theobald 2011).

AMI was calculated as the ratio of the square root of (DD5)/MAP, LED was calculated as the difference between the elevation of a pixel and the minimum elevation within a 27 pixel radius, TPI compares the elevation of each pixel to the mean elevation of cells within a defined radius. High TPI values indicate that a pixel has a high elevation relative to adjacent pixels (e.g., ridgetops), TRI was calculated as the mean of the absolute difference between the elevation of a pixel and the elevation of the 8 pixels surrounding it, TRI2 was calculated as the standard deviation of the elevation within a 3x3 rectangular window centered on a pixel, and TWI represents the relative water accumulation potential based on factors related to slope and hillshade. Because the spatial scale that caribou may select these features is unknown, we calculated these variables at 5 different spatial scales. Mean proportions of each variable were calculated at the 120 m scale using the Aggregate Tool and at the 0.5 km, 1.0 km, 2.0 km, and 3.2 km scales using the Focal Statistics Tool in ArcGIS Pro.

Additionally, we used daily NDVI, daily nitrogen, daily biomass, maximum NDVI, and daily snow water equivalent (SWE) at each location and time used in the analysis. These we calculated based on 500-m pixels. We calculated landscape ruggedness (Sappington et al. 2007)

over a 150-m by 150-m box centered at each 30-m pixel. The median snow-free date (date at which the pixel is typically snow-free [Macander et al. 2015]), distance to coast, and west-to-east distribution were calculated for each location used in the analysis. Because of the different seasonal importance of these variables, the median snow-free date was used only for the winter, spring migration, and calving seasons, SWE was only used for the winter and spring migration seasons, and daily NDVI, nitrogen, and biomass variables were used only for the snow-free seasons (calving, postcalving, mosquito, oestrid fly, and late summer seasons).

While Maxent is computationally capable of handling many model coefficients that may be highly correlated (Elith et al. 2011, Phillips et al. 2017), high levels of correlation among variables can limit the ability to interpret the influence of specific variables (Merow et al. 2013). We therefore used a two-step process to reduce the number of variables, simplify the model, and aid in interpretation. In the first step, we selected a single spatial scale for each variable. For each season, we first calculated the test-ratio, the ratio of the mean values of environmental variables at caribou group locations to the mean of the randomly generated background locations, at each of the 5 spatial scales. A large test ratio indicates that the values of that variable are more different at locations used by caribou compared to random locations and therefore, suggests some selection of that variable by caribou. For each variable, we only retained the spatial scale with the largest test ratio (Dunk et al. 2019). This produced the scale-defined variable dataset (one spatial scale for each variable). For the second stage of variable selection, we removed highly correlated variables. We categorized variables into three groups: weather, habitat, and topography. We then calculated the Variance Inflation Factor (VIF) for all variables within each of these categories and removed variables with VIF values >5 . Once inter-category VIFs were <5 , we calculated the VIFs for all remaining variables combined and used a relaxed threshold. We removed variables if the $VIF > 10$. The relaxed VIF threshold was a compromise to retain variables while still minimizing the amount of correlation among variables. All calculations were performed in R (R version 4.0.2, R Core Team

2020) using the ‘usdm’ and ‘raster’ packages (Hijmans 2020, Naimi et al. 2014).

After determining the set of explanatory variables to be used, we ran the Maxent models for each season individually. By default, Maxent automatically generates background points from within a single study area, which does not work for this analysis because our random locations are drawn from within the bounds of multiple survey areas. Therefore, we used the samples-with-data (SWD) method in Maxent where the user supplies datasets with environmental data already extracted for both used and random points (Phillips 2017). We allowed Maxent to automatically choose among linear, quadratic, product (interactions), hinge (similar to splines), and categorical forms of variables and allowed Maxent to use locations with some missing values of explanatory variables. Hinges can be applied multiple times to the same function, providing for a very flexible framework to model relationships in the data (Elith et al. 2011). We used 1,000 maximum iterations and allowed samples with some NULL values to be included. All other settings were left at default.

Ideally, the Maxent model will fit the training data well but also generalize outside of sampled locations (Phillips et al. 2006). To avoid overfitting the training data, Maxent employs L1 regularization to constrain modeled distributions to lie within a certain interval around the empirical mean rather than matching it exactly (Phillips et al. 2006, Warren and Seifert 2011, Merow et al. 2013). Maxent allows users to vary the constant regularization multiplier (RM) that penalizes all parameters to reduce over-fitting and shrinks coefficients towards or to zero, thus reducing the number of parameters in the model. Lower values of the RM can lead to overly complicated models, overparameterization, and overfitting, while values that are too high can lead to overly simplified models that overpredict suitability (Cao et al. 2013). The Maxent default value of 1 has been optimized to best balance between overfitting and overgeneralizing the data and was based on a dataset from 226 species from 6 regions around the world (Phillips and Dudik 2008, Elith et al. 2006). However, models using this default value sometimes overfit the training data or can be overly simplistic (Anderson and Gonzalez 2011, Warren and Seifert 2011, Cao et al. 2013, Merow et al.

2013, Radosavljevic and Anderson 2014). Many different researchers have investigated the best method for optimizing the RM (Warren and Seifert 2011, Cao et al. 2013, Radosavljevic and Anderson 2014, Galante et al. 2018).

For all models, Maxent provides receiver operating characteristic (ROC) curves with an associated area under the curve (AUC) that can be used to assess model performance (Phillips 2017). We chose to use the AUC value of withheld test data (AUCtest) as a metric to optimize the RM value as described in Warren and Seifert (2011) because this metric performed very well when sample sizes are large (>1,000 locations), which was often the case with our analyses. We therefore ran our models with RMs of 0.75, 1, 2, 3, 4, 5, and 6 and chose the model with the highest AUCtest. We ran the initial models on a random selection of 80% of the data (training data) and used the remaining 20% of locations to independently assess the model performance (test data). Once the top model based on AUCtest was identified, the Maxent model was re-run with the best RM and 100% of the data for training.

To assess variable importance, Maxent calculates a permutation importance value for each variable in the model. The permutation importance value is calculated as the drop in the AUC value from the training data (AUCtrain) after Maxent randomly reassigns the values of each variable in turn and re-runs the model. A large drop in AUCtrain indicates that the variable was important to overall performance, while a small drop in AUCtrain indicates a random permutation of the variable has similar predictive power to the actual data. Maxent also provides response curves to show the relationship between each explanatory variable and the predicted suitability. These curves represent the effect of changing the values of one variable while holding all other variables in the model constant. AUC values from 0.7-0.8 are generally considered to acceptable model performance, 0.8-0.9 indicate excellent model performance, and >0.9 indicate outstanding model performance (Hosmer and Lemeshow 2000). Results of the model were mapped using the cloglog function (complimentary log-log), which is currently the best transformation for estimating the probability of presence (Fithian et al. 2015, Phillips et al. 2017).

In order to map the suitability results, we needed to use a consistent set of rasters for each season. Because some variables varied over time, we used the median values of daily NDVI, nitrogen, biomass, and SWE calculated at the midpoint of each season, median yearly maxNDVI, and the median date of snowmelt since 2002 as input variables for the suitability maps.

DISTRIBUTION RELATIVE TO ICE ROADS

We used integrated Step-Selection Analysis (iSSA) to test for differences in space use and movement characteristics of caribou using methods similar to Prichard et al. (2020a). This analysis allowed us to model caribou movement patterns in relation to variables thought to be important to caribou distribution (landcover, TPI, elevation, distance to ice road or gravel road, and peak NDVI). We could then examine the pattern of movements in relation to distance to ice roads while accounting for the effect of other important covariates. iSSA uses random locations generated at each step along an animal's path to compare where an animal goes with the other choices available to that individual at that step (Fortin et al. 2005, Thurfjell et al. 2014). The iSSA extends typical step-selection models by selecting random points from analytical distributions and allowing movement-related covariates (step length and turn angle) to be included in the model (Avgar et al. 2016). This procedure makes it possible to simultaneously examine which factors influence locations selected by caribou and how movement metrics change.

For landcover classes, we combined the BLM and Ducks Unlimited (2002) landcover classes into six classes (including water) to analyze caribou habitat use. We combined four classes (clear water, turbid water, Ice, and *Arctophyla fulva*) into a water class; we combined four classes (*Carex aquatilis*, two flooded tundra types, and wet tundra) into a wet tundra class, we combined 6 classes that occur rarely and usually in riverine areas (moss/lichen, tall shrub, dunes/dry sand, sparsely vegetated, barren ground, and *Dryas*) into a riverine class, and we combined dwarf shrub tundra and low shrub tundra into a dwarf/low shrub tundra class. We retained the sedge/grass meadow

and tussock tundra classes. We included the water class in this analysis because the lakes would have been frozen in these months and thus, more likely to be used by caribou. Most of the area consisted of the landcover classes dwarf/low shrub tundra (29%), tussock tundra (24%), water (20%), or wet tundra (15%). Landcover class is likely to influence caribou distribution through various factors such as ease of walking, forage quality or quantity, or amount of snow or water.

We also used TPI (calculated using a cell radius of 4), the median peak NDVI value from 2000–2017, and elevation as variables to help explain caribou movements. A high TPI may be related to snow depth as a result of wind scouring of ridgetops and snow deposition in low lying areas, and median peak NDVI should provide a measure of how much vegetation is present on the pixel during summer, although the vegetation would be senesced and covered by snow during the winter. We also calculated the distance from caribou locations to the nearest ice road or gravel road. We combined ice roads and gravel roads because they both had vehicle traffic and therefore likely to have similar potential impacts on caribou movements. In addition, because ice roads were connected to gravel roads, any potential differences in impacts would be confounded and difficult to separate.

We used the R package *amt* (Signer et al. 2018) to run the iSSA models. For each caribou location, we generated 15 new random locations inside the study area. Location data was subset to 12 hr intervals, the maximum interval used during the study. TCH caribou move less during the winter than during other times of year (Person et al. 2007, Prichard et al. 2014), therefore 12-hour fix rates are likely to provide adequate temporal resolution to examine movement in relation to ice roads. Because we were interested in movements near ice roads, we restricted the data set to TCH locations from December through April when ice roads were likely to be under construction or in use. There were limited numbers of collared caribou in the area from 2012–2013, 2013–2014, 2015–2016, and 2017–2018, and only short sections of ice roads were constructed in 2014–2015 and 2016–2017. Hence, the best data to examine caribou movements near ice roads came from 2018–2019 and 2019–2020 when there

were both extensive ice roads and many collared caribou in the analysis area. Package *amt* selects random locations from a Gamma distribution for step length and a von Mises distribution for turn angle (Signer et al. 2018). Random locations were selected separately for each animal in each year and therefore were sampled from distributions estimated from movement characteristics specific to each individual and year. Used and random locations were compared using a conditional logistic regression model that treated each movement step as a stratum. For each starting location and the 16 ending locations (1 used and 15 random), we calculated the landcover class, distance to the nearest road or pad, TPI, elevation, peak NDVI, and the distance to the nearest ice road.

Continuous variables, except distance to ice road, were scaled by subtracting the mean and dividing by the standard deviation before running the model to aid in interpretation. We first found the best model using all combinations of 4 variables: (1) landcover class; (2) TPI; (3) elevation; and (4) peak NDVI. We did not include interaction terms in the model selection. We included individual caribou ID as a cluster variable to adjust standard errors for autocorrelation by calculating a robust standard error using a Huber sandwich estimator (Therneau 2015). The step-length (log-transformed), turn-angle (cosine of turn angle), and an interaction between step-length and turn angle variables were included in all models (Forester et al. 2009).

We selected the model with the lowest Akaike Information Criterion (AIC) score as the best model (Burnham and Anderson 2002) using a 2-stage model selection process for each year. In the first stage, we found the best model using all combinations of the initial variables (landcover class, TPI, elevation, and peak NDVI). In the second stage, we added a distance-to-ice-roads variable to the best first stage model. We used the natural cubic spline of distance-to-roads-or -pads to allow for a more flexible model. Cubic splines fit a series of cubic equations to sections of the data but constrain the different lines to meet at pre-defined locations (knots) on the x-axis. Adding more knots adds additional flexibility to the model. We ran the best model from the first stage of model selection with the addition of the

distance-to-ice-roads variable with 3 different series of knot locations (4 km; 4 and 8 km; or 4, 8, and 16 km) and chose the final model with the lowest AIC score as the best model.

We used bootstrap resampling of individual caribou to calculate 95% confidence intervals of the model coefficients from the best model (Prichard et al. 2020a). We ran the model once, and then took a random sample of individual caribou (with replacement) equal to the original number of caribou in the dataset for that year and reran the model. We ran each model with 999 resampled data sets to produce 1000 total model runs. We then calculated the 95% confidence intervals as the 25th and 975th highest values of each model coefficient.

RESULTS

WEATHER CONDITIONS

Air temperatures in spring 2020 were near the 30-year average (1983–2020) and snow melted slightly earlier than usual at the Kuparuk airport (Figure 4, Appendix C–D). Approximately half of the snowpack melted during 9–10 May when temperatures reached 1.7 °C (35.0 °F). Snow depths of approximately 10 cm (3.9 in) persisted at the Kuparuk airstrip from 10–20 May but then declined to zero or trace level by 29 May when temperatures were again above freezing. Temperatures were variable during early and mid-June but were generally below average.

Other weather stations are located closer to the study area (CD5, Nuiqsut, Alpine, Colville Village), but those datasets cover a shorter period of time and they do not all measure snow depth. While specific temperature and snow depth values may differ by station, the seasonal trends are generally similar among stations. Survey crews flying 8–10 June confirmed that almost all areas were snow free except for in snow accumulation zones such as along streams, and even small ponds were ice-free.

Mosquitos in the study area usually emerge from the middle of June through early July, whereas oestrid flies do not generally emerge until mid-July. Daily air temperatures in mid-June were near average but predicted mosquito harassment did not exceed 50% in late June or early July

(Figure 5) and only approached 50% on two days during this period. ABR biologists conducting ground-based surveys for other projects near the Colville River delta reported moderate mosquito activity starting around 25 June.

Weather conditions were generally not conducive to high insect activity during the remainder of the 2020 insect season. From June through early August strong winds (>10 mph) occurred frequently, and temperatures were often below average. Temperatures were generally above average for the remainder of August (Figure 4, Appendix C). This resulted in zero days with a high probability of oestrid fly harassment (>50% probability) and only 4 days with a high probability of mosquito harassment, although 3 of those days occurred in August when the severity of mosquito harassment is generally lower (Figures 5).

CARIBOU DISTRIBUTION AND MOVEMENTS

AERIAL TRANSECT SURVEYS

BTN Survey Area

Eight aerial surveys of the BTN survey area were attempted between 25 February and 6 October 2020 (Figure 6). The late winter and spring migration surveys were cancelled due to health concerns stemming from the emerging COVID-19 pandemic. The postcalving survey was conducted with only one observer due to an illness with the second observer. The estimated density ranged from a high of 3.22 caribou/km² during the 18 June postcalving survey in the western portion of the survey area to a low of 0.12 caribou/km² during the 6 October survey (Table 2). The calving survey had the second-highest estimated density. During the calving survey, we estimated 2,634 caribou were in the study area. Assuming a TCH population size of 56,255, ~4.7% of the herd was estimated to be in the BTN survey area during the calving survey. We observed 13 calves in the BTN survey area during the calving survey whereas we observed 21 calves during the postcalving survey with only one observer (Table 2).

BTS Survey Area

Eight aerial surveys of the BTS survey area were attempted between 26 February and 7 October (Figure 6). The late winter and spring

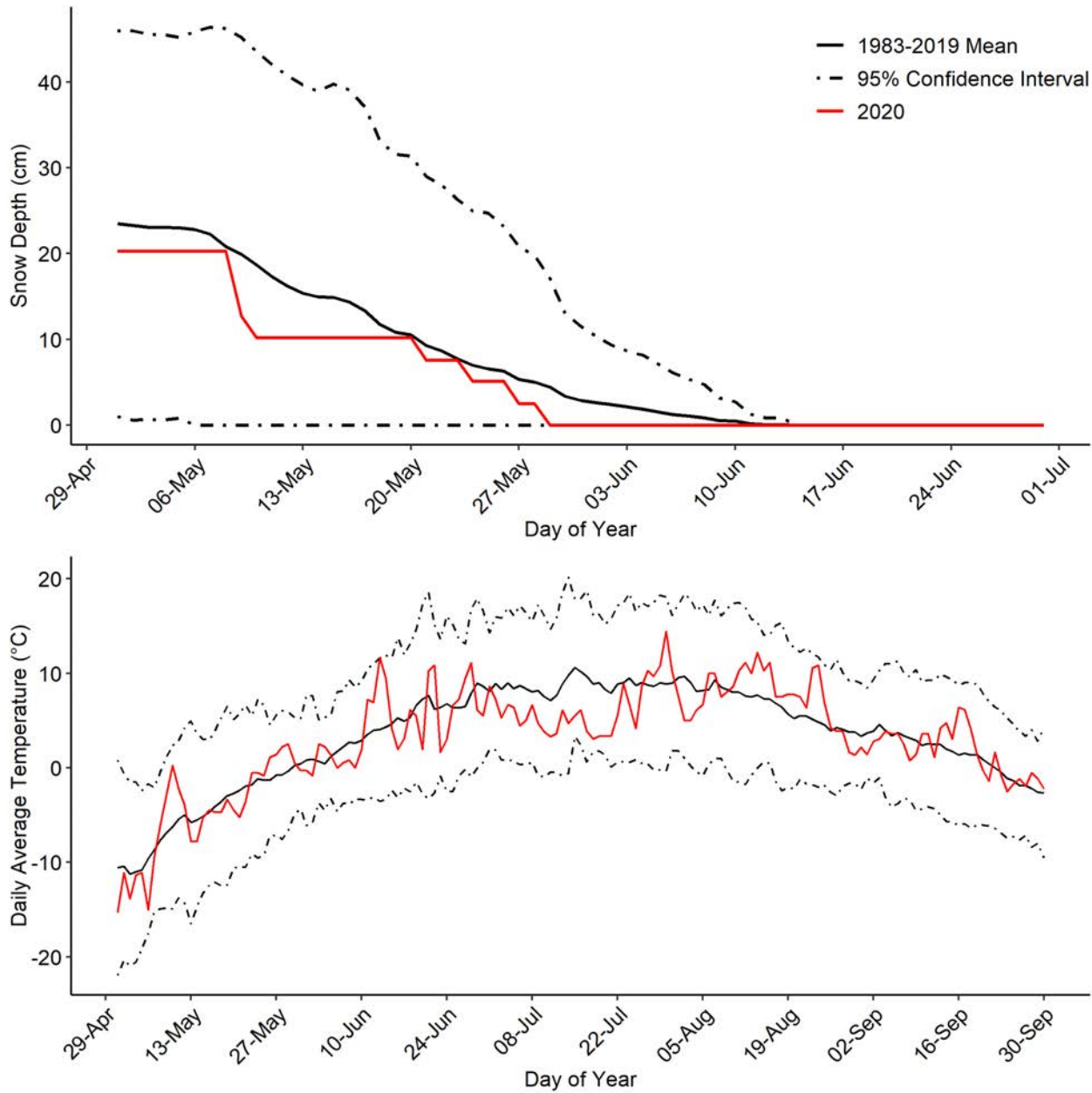


Figure 4. Snow depth, long-term mean (1983–2019), and 95% confidence interval at the Kugaruk airstrip, May–June 2020 (top) and daily average air temperature, long-term mean, and 95% confidence interval at Kugaruk, May–September 2020 (bottom).

Results

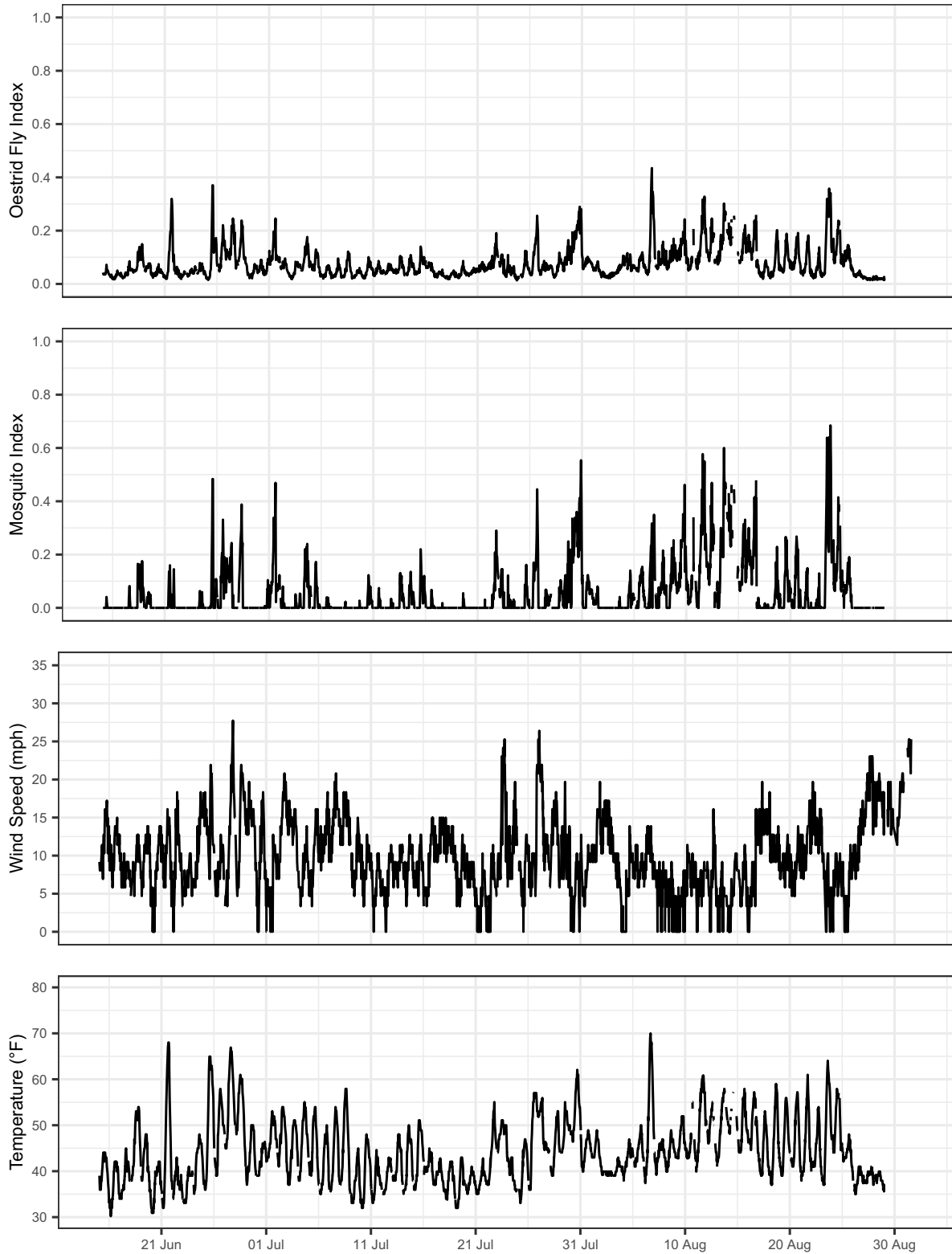


Figure 5. Hourly air temperature, wind speed, mosquito probability index, and oestrid fly probability index at Nuiqsut, 15 June–1 September 2020.

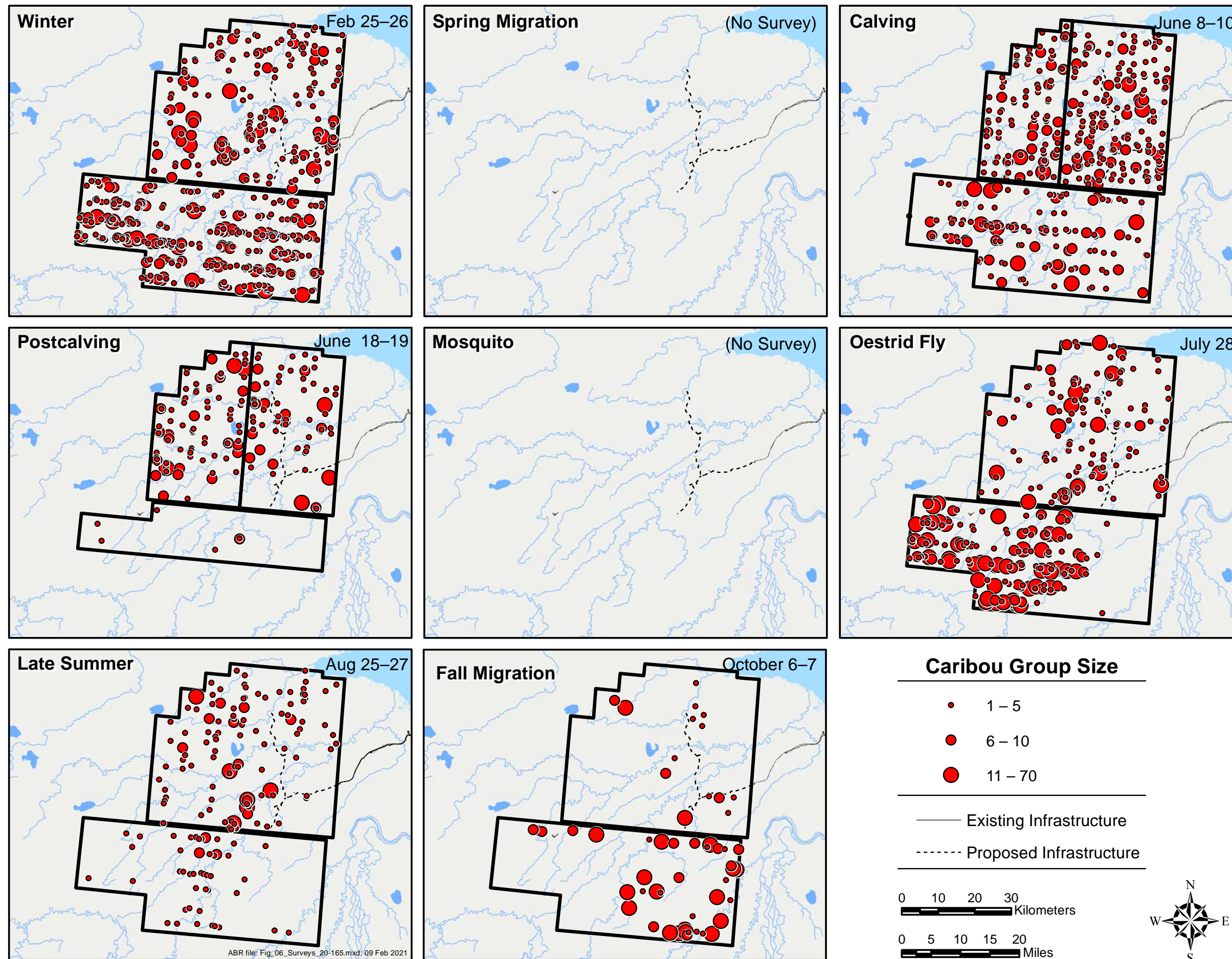


Figure 6. Distribution and size of caribou groups observed during aerial surveys in seven seasons in the Bear Tooth North and Bear Tooth South survey areas, February–October 2020.

Page intentionally left blank.

Table 2. Number and density of caribou in the Bear Tooth North and Bear Tooth South survey areas, February–October 2020.

Survey Area and Date	Total Area (km ²) ^a	Observed Large Caribou ^b	Observed Calves ^c	Observed Total Caribou	Mean Group Size ^d	Estimated Total Caribou ^e	SE ^f	Density (caribou/km ²) ^g
BTN								
Feb 25	2,122	794	nr	794	4.3	1,588	150.6	0.75
June 8–9 (East) ^h	1,288	583	6	589	3.3	1,178	42.9	0.91
June 8 (West) ^h	834	357	7	364	3.4	1,456	176.0	1.75
June 18–19 (East) ^h	1,143	275	6	281	4.2	1,124	149.7	0.93
June 18 (West) ^h	979	379	15	394	4.4	3,152	629.2	3.22
July 28	2,122	633	nr	633	5.1	1,266	165.5	0.60
Aug 25–27	2,122	467	nr	467	2.9	934	203.5	0.44
Oct 6 ⁱ	2,122	70	nr	70	5.0	263	55.3	0.12
BTS								
Feb 26	1,747	1,402	nr	1,402	4.1	4,206	595.3	2.41
June 8–10	1,747	512	11	523	4.3	1,569	263.0	0.90
June 18 ^h	870	16	2	14	2.7	96	46.8	0.11
July 28	1,747	1,234	nr	1,234	8.3	3,702	430.8	2.12
August 25	1,747	180	nr	180	2.2	540	261.2	0.31
October 7 ⁱ	1,747	435	nr	435	11.2	2,453	534.8	1.40

^a Survey coverage was 50% of this area in BTN and 33% in BTS unless otherwise noted.

^b Adults + yearlings.

^c nr = not recorded; calves not differentiated reliably due to larger size.

^d Mean Group Size = Observed Total Caribou ÷ number of caribou groups observed.

^e Estimated Total Caribou = Observed Total Caribou adjusted for survey coverage.

^f SE = Standard Error of Estimated Total Caribou, calculated following Gasaway et al. (1986), using transects as sample units.

^g Density = Estimated Total Caribou ÷ Area.

^h Survey was conducted with a single observer reducing survey coverage to 25% in BTN West on 8 June and BTN East on 18–19 June, 16.5% in BTS on 18 June, and 12.5% in BTN West on 18 June.

ⁱ Applied a Sightability Correction Factor of 1.88 (Lawhead et al. 1994) to correct for low sightability due to patchy snow.

migration surveys were cancelled due to health concerns stemming from the emerging COVID-19 pandemic, and the BTS postcalving survey was only partially conducted due to persistent fog. The postcalving survey was conducted with only one observer due to illness with the second observer. The estimated density of caribou in BTS ranged from a high of 2.41 caribou/km² on 26 February to a low of 0.11 caribou/km² on 18 June (Table 2). During the winter survey, we estimated 4,206 caribou were in the study area, which would account for ~7.5% of the TCH. We observed 11 calves during the calving survey and 2 calves during the postcalving survey.

Results from the seasonal density mapping of caribou recorded on aerial surveys of the

NPRA/BTN & BTS survey areas during 2002–2020 also showed large differences among seasons (Figure 7). Densities of caribou have been highest in the western BTN and northern BTS survey areas. Caribou are most widely distributed across the area during fall migration. The highest mean density was observed during the oestrid fly season but results from that season were highly influenced by several very large groups that were observed in 2005.

RADIO TELEMETRY

Radio collars provide detailed location and movement data throughout the year for a small number of individual caribou. The telemetry data also provide valuable insight into herd affiliation

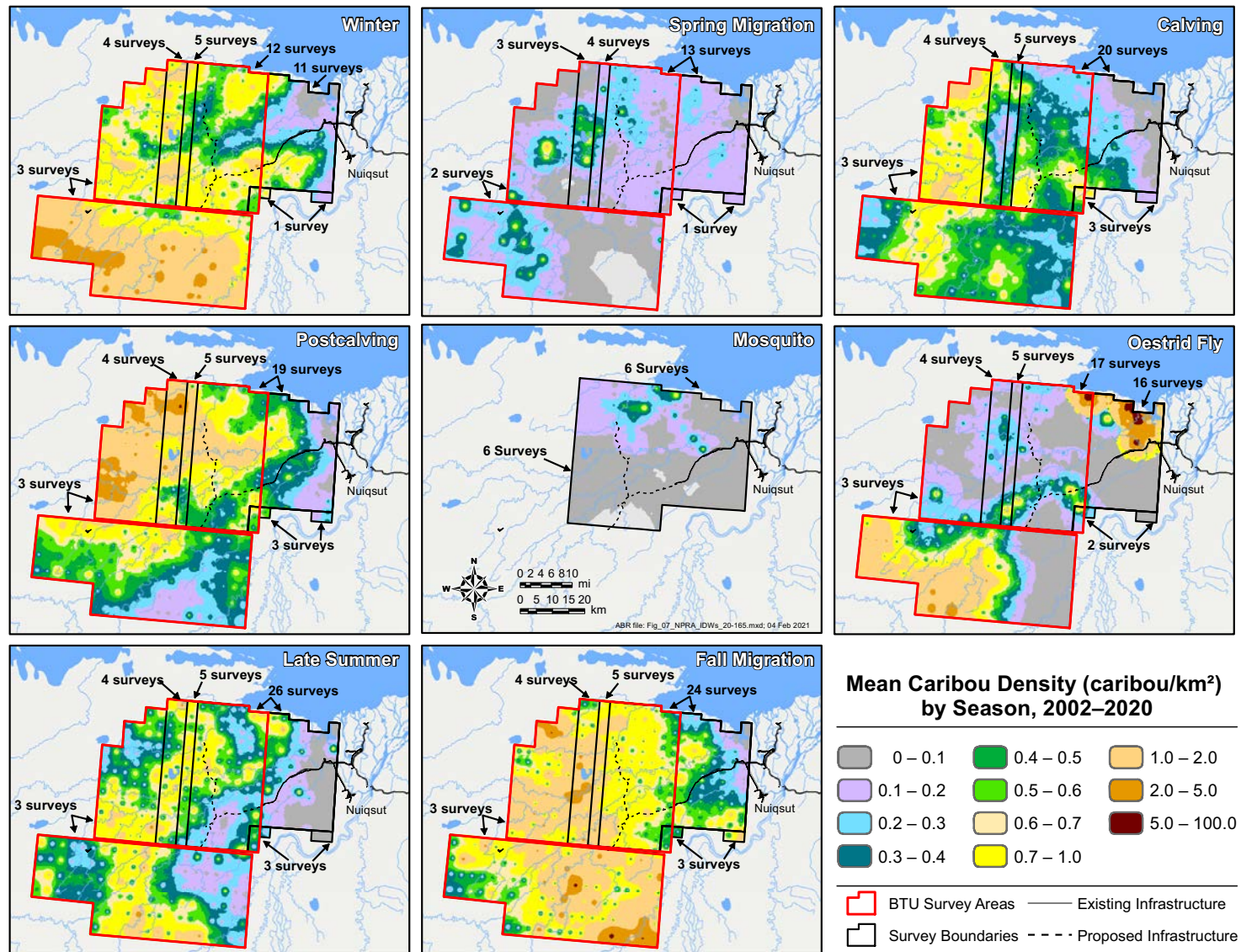


Figure 7. Mean seasonal densities of caribou in the NPRA caribou survey areas based on inverse distance-weighting interpolation of aerial survey results, 2002–2020.

and distribution, which is not available from transect surveys. Mapping of the telemetry data from PTT and GPS collars clearly shows that the study area is located at the eastern side of the annual range of the TCH and west of the annual range of the CAH (see below).

Kernel Density Analysis

Seasonal concentration areas were analyzed using fixed-kernel density estimation, based on locations from satellite and GPS collars deployed on 273 TCH females and 90 TCH males during 1990–2020 and on 138 CAH females and 8 CAH males during 2001–2020. These numbers differ from the number of collar deployments listed earlier (Table 1) because some individuals switched herds after collaring. Kernels were used to produce 50%, 75%, and 95% utilization distribution contours (isopleths), which were assumed to correspond to density classes (high, medium, and low density) for female CAH caribou and for male and female TCH caribou (Figures 8–10); the sample size of CAH males was too small to conduct this analysis for males separately. Although these analyses use data covering 20–30 years, the results are more heavily weighted for more recent years when more collars were deployed.

Female CAH caribou generally wintered between the Dalton Highway/TAPS corridor and Arctic Village, although in more recent years more wintering has occurred on the north side of the Brooks Range. They then migrated north in the spring to calve in two areas on either side of the Sagavanirktok River, spent the mosquito season near the coast (mostly east of Deadhorse), and dispersed across the coastal plain on both sides of the Sagavanirktok River and Dalton Highway/TAPS corridor during the oestrid fly and late summer seasons (Figure 8).

TCH caribou generally wintered on the Arctic Coastal Plain between Nuiqsut and Wainwright or in the central Brooks Range near Anaktuvuk Pass, migrated to their calving grounds near Teshekpuk Lake, and spent the rest of the summer on the coastal plain, primarily between Nuiqsut and Atqasuk (Figures 9–10). Compared with females, males were more likely to overwinter in the central Brooks Range instead of on the coastal plain. Males migrated to the summer range later in the

year during the calving and postcalving seasons and were not distributed as far west during summer (Figures 10). The distribution of parturient TCH females during calving (Figure 11) was similar to the distribution of all TCH females during calving (Figure 9) but was more concentrated around Teshekpuk Lake.

The BTN survey area was squarely within the 95% utilization distribution of female TCH caribou from fall migration through spring migration and within at least the 50% utilization distribution in all other seasons (Figures 9). As a result, 4.1–12.4% of female TCH caribou (based on the proportion of the utilization distribution) are expected to be in the survey area at any time during the year, with the highest levels of use expected during September (Figure 12). Use of the BTN survey area by TCH males increased sharply from May to a peak in July (13.8% of the utilization distribution) during the oestrid fly season. Use by males dipped in August (5.4%) but then rose again in September (10.3%) during the onset of the fall migration before dropping below 1% by November as males migrated into the foothills and mountains of the Brooks Range or toward Atqasuk during the winter (Figure 12). In contrast, there was almost no use (0.0%–0.8%) of the BTN survey area by collared CAH females throughout the year (Figure 12). The BTN survey area is far to the west of the typical CAH summer range, so little use of the area was expected.

TCH females used the BTS survey area to a similar or lesser extent than the BTN survey area in all months (0.5–7.1% of the population based on the proportion of the utilization distribution; Figure 12). The main differences were apparent in May, June, and July when utilization of the BTS dropped off dramatically. Caribou were located closer to Teshekpuk Lake from pre-calving through the mosquito season. The difference was also apparent in September when more female caribou were located in the BTN survey area. Use of the survey area by males followed a similar pattern to their use of the BTN survey area with little use from November through May (0.4%–1.7%) when males are in their winter ranges, and moderate use (4.4%–12.6%) from June through October. When compared to the BTN survey area, use of the BTS by males was similar in June as males were still migrating north from their winter range, lower in

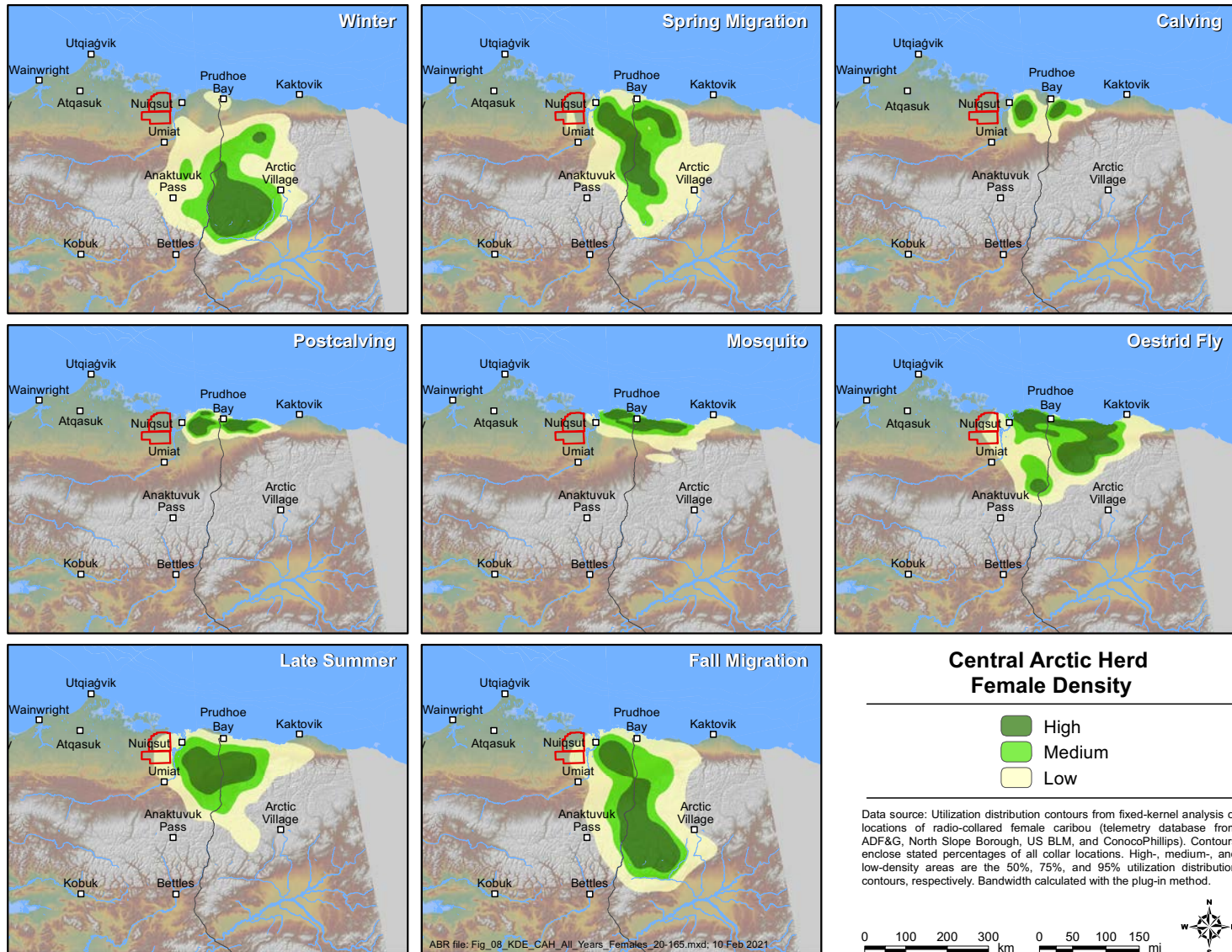


Figure 8. Seasonal distribution of Central Arctic Herd female caribou based on fixed-kernel density estimation of telemetry locations, 2001–2020.

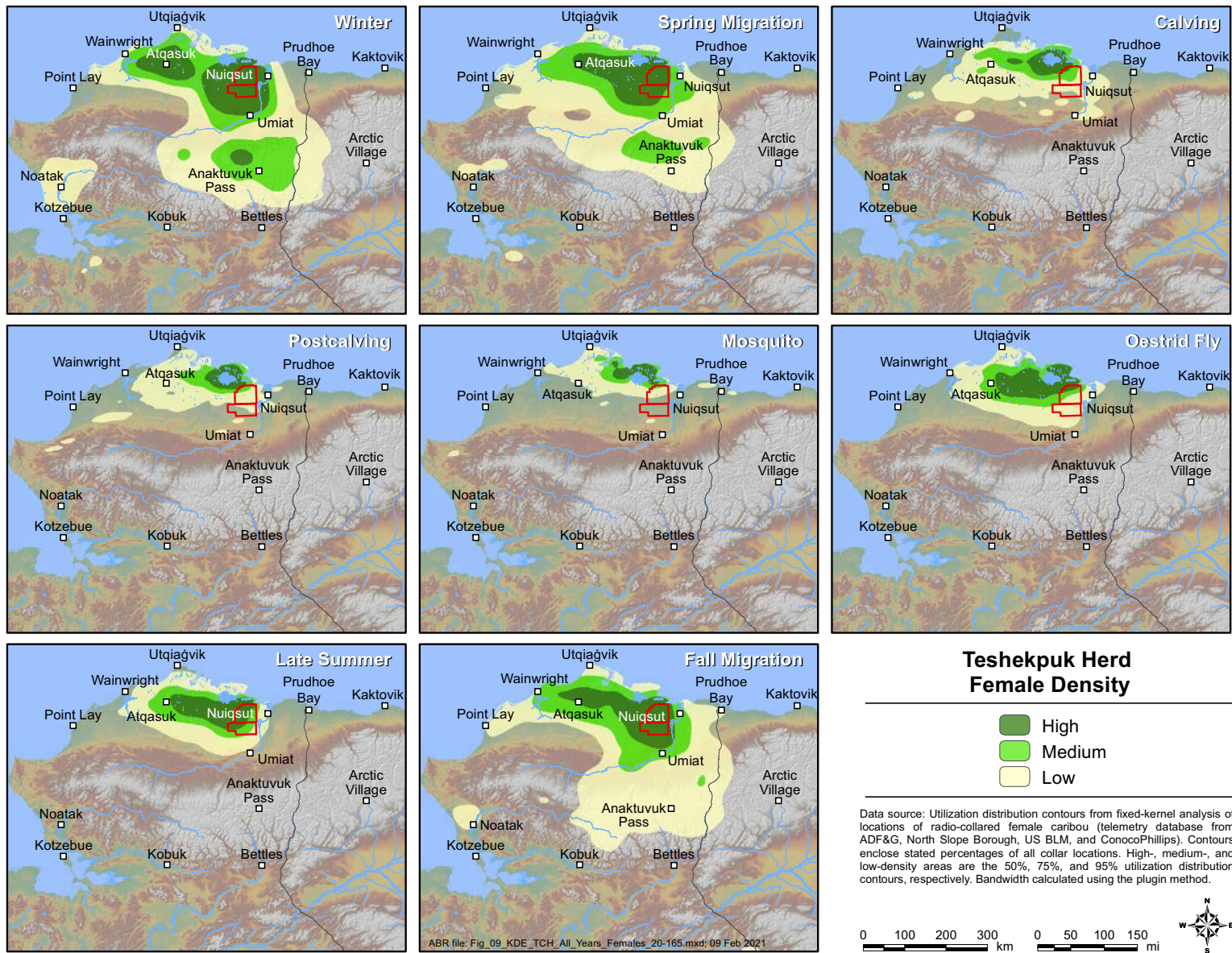


Figure 9. Seasonal distribution of Teshekpuk Caribou Herd females based on fixed-kernel density estimation of telemetry locations, 1990–2020.

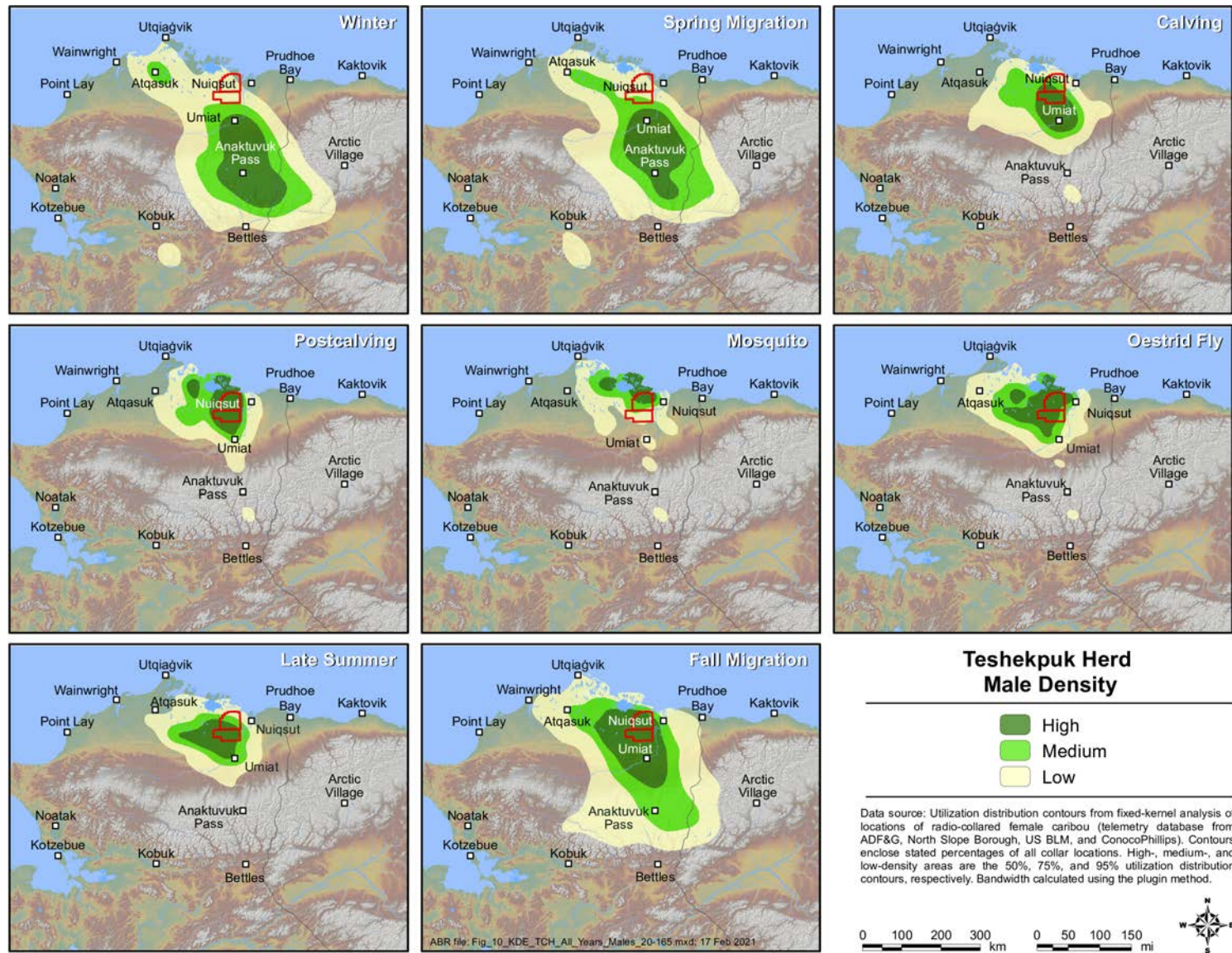


Figure 10. Seasonal distribution of Teshekpuk Caribou Herd males based on fixed-kernel density estimation of telemetry locations, 1997–2020.

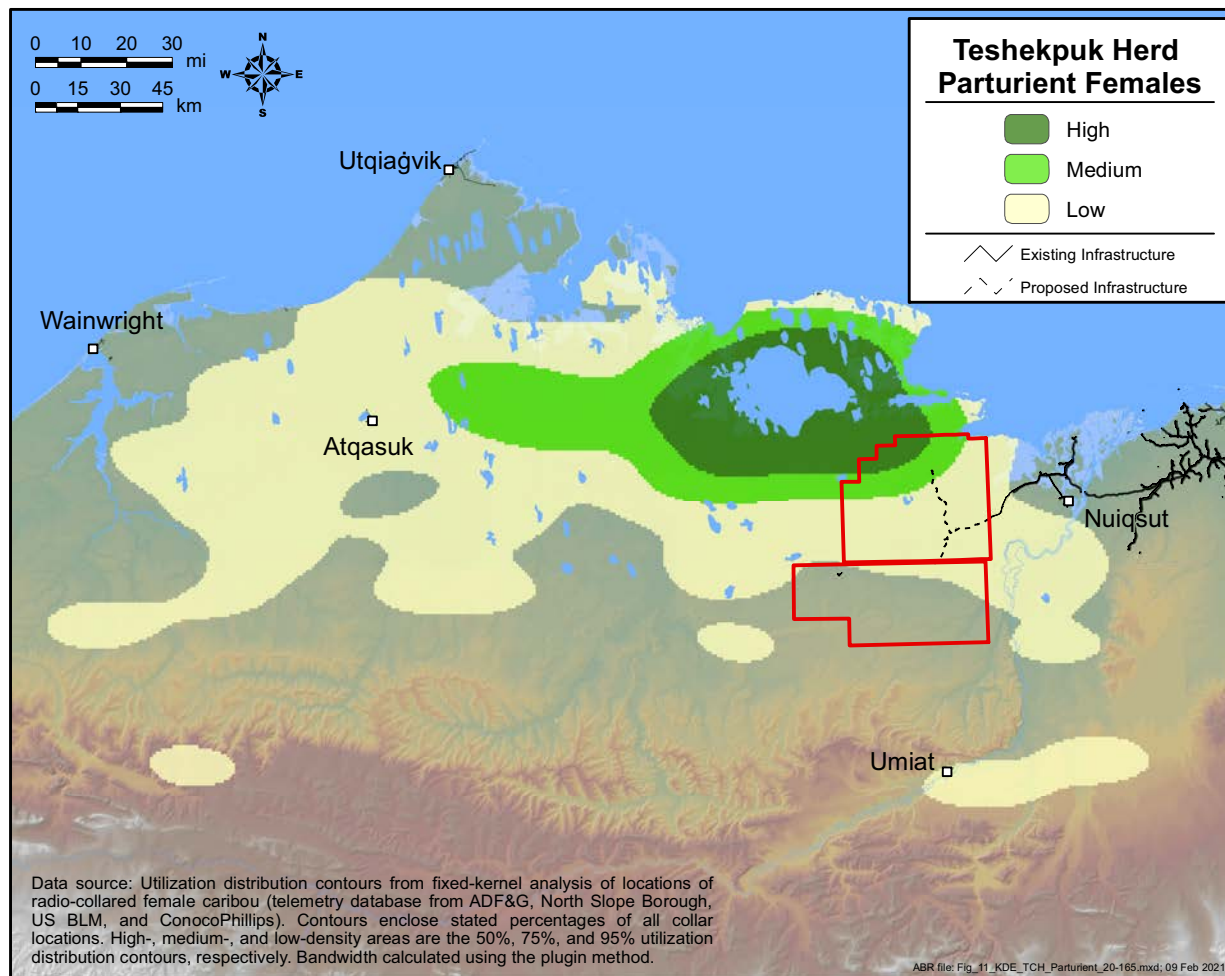


Figure 11. Distribution of parturient females of the Teshekpuk Caribou Herd during calving based on fixed-kernel density estimation of telemetry locations, 1990–2020.

July when caribou were closer to the coast for mosquito relief, and higher in August and September when caribou dispersed inland as insect harassment abated. There was almost no expected use (0.1%–0.8%) of the BTS survey area by collared CAH females throughout the year (Figures 8 and 12).

Mapping Movements

Mapping of movements by TCH caribou in the study area derived from the dBBMMs corroborated the results from the KDE analysis, but provided more high-resolution details. The models showed that TCH females used the BTU survey areas during all seasons, although their use

of the area and movement rates varied widely among seasons (Figure 13). During winter, female caribou exhibited low rates of movement and were distributed widely but concentrated in and around the BTS survey area. During the spring migration and calving seasons, TCH females moved across the study area from the south and southeast to the northwest as they migrated toward the core calving area bordering Teshekpuk Lake. During the postcalving and mosquito seasons, caribou largely remained west and north of the study area, often traversing the narrow corridors between Teshekpuk Lake and the Beaufort Sea (Yokel et al. 2009). During the oestrid fly season, TCH females were still more concentrated near the coast, but moved

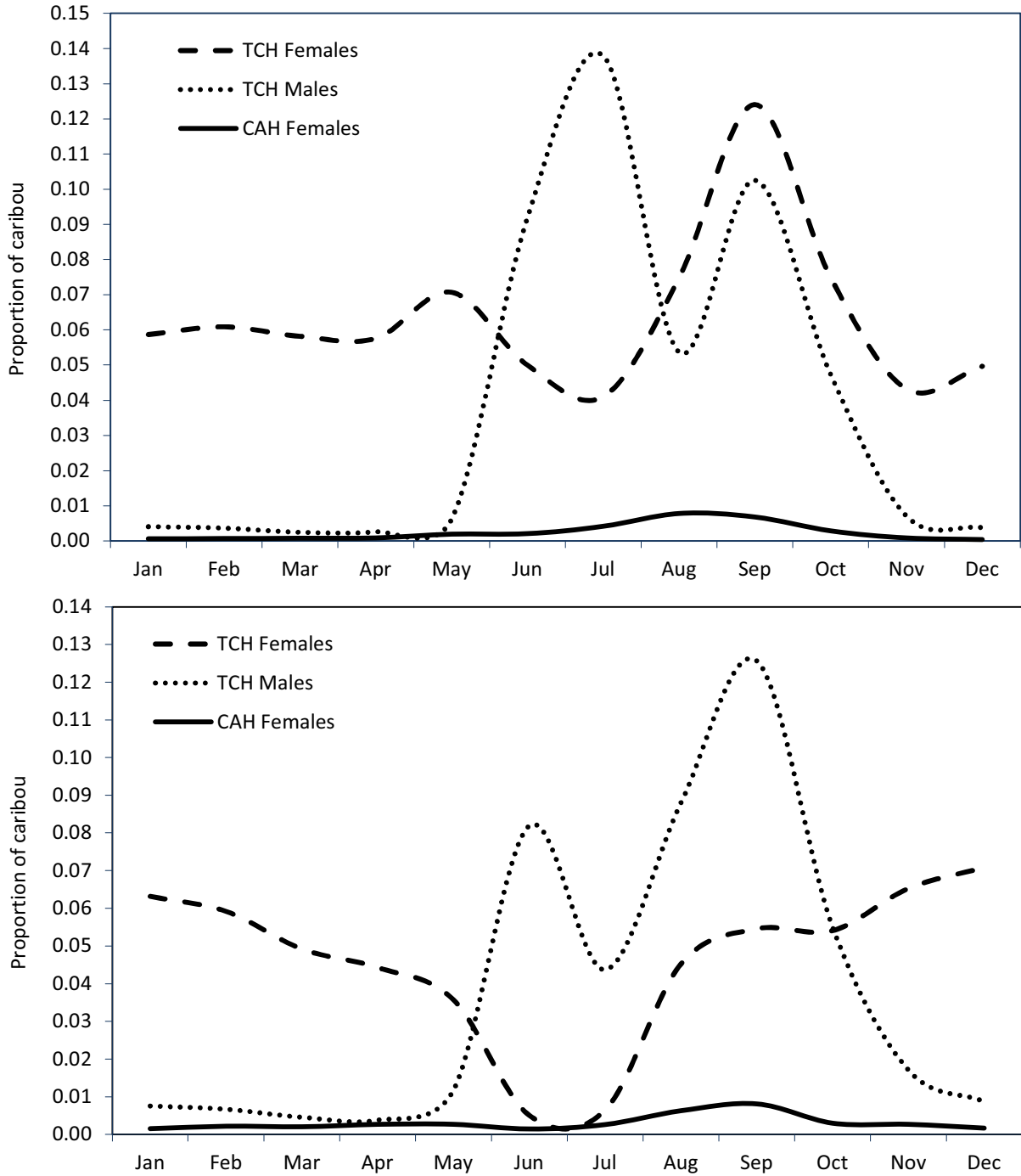


Figure 12. Proportion of CAH and TCH caribou within the Bear Tooth Unit North (top) and Bear Tooth Unit South (bottom) survey areas, based on fixed-kernel density estimation, 1990–2020.

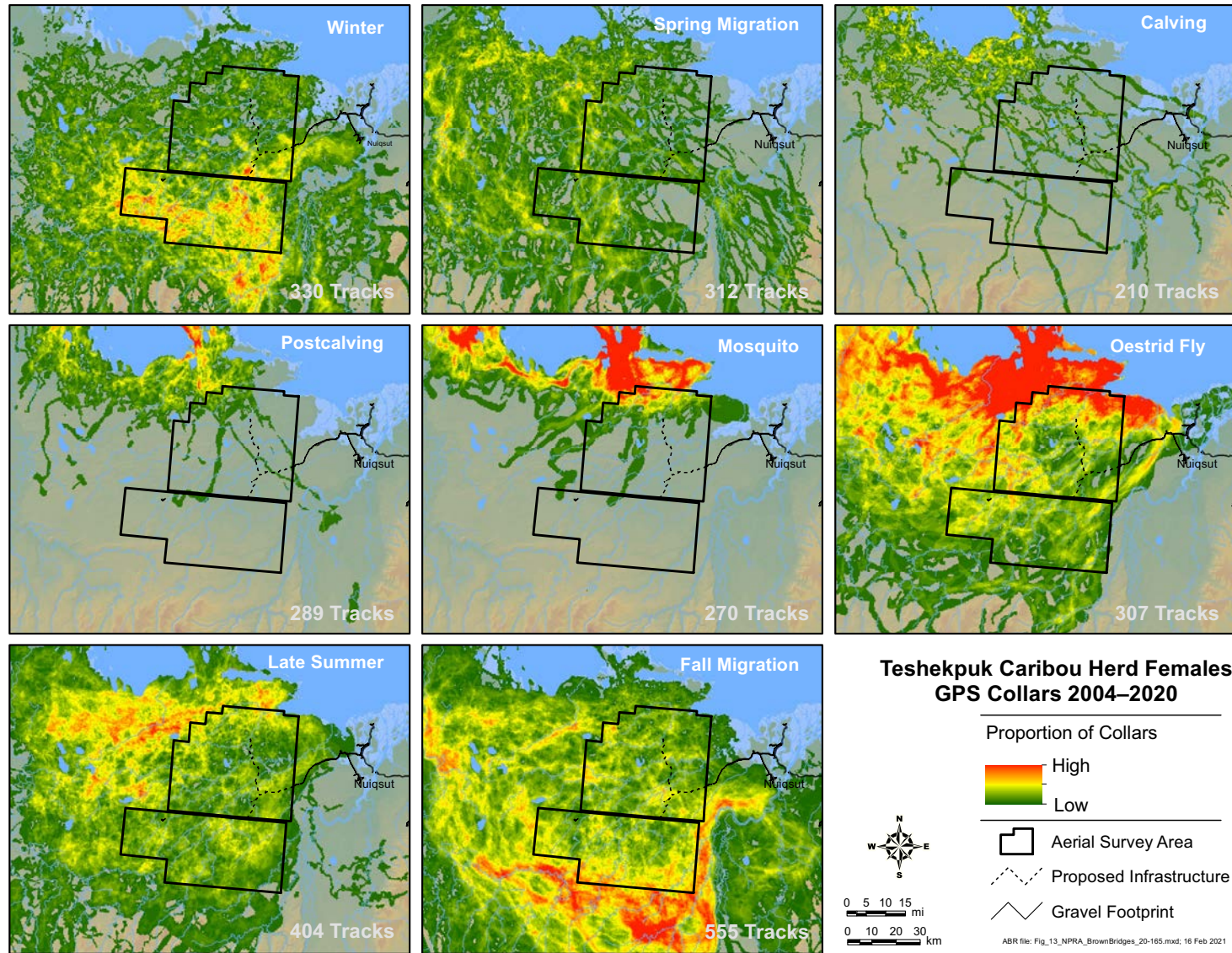


Figure 13. Movements of GPS-collared female caribou of the Teshekpuk Herd in the vicinity of the proposed Willow development during each of 8 seasons based on 95% isopleths of dynamic Brownian Bridge movement models.

rapidly and often dispersed inland away from Teshekpuk Lake, with occasional large movements through the survey areas. During late summer, caribou were usually found dispersed inland throughout much of both survey areas. During the fall migration season, female TCH caribou dispersed even more widely and moved towards wintering grounds. Approximately 30 percent of the herd typically overwinters in the Brooks Range and some of those animals moved through the BTS survey area during migration.

MOVEMENTS NEAR PROPOSED WILLOW INFRASTRUCTURE

Consistent with the location of existing infrastructure on the eastern edge of the TCH range, movements by collared TCH and CAH caribou near proposed Willow infrastructure have occurred more frequently than movements near existing infrastructure in the GMT and CRD survey areas to the east (Figures 13, 14). The percentages of the utilization distributions within 4 km of roads and pads ranged from 0.0%–2.6% with notable differences by sex (Figure 15). Males were most likely to be within 4 km of proposed roads and pads from June through October and almost no use of this area occurred after the fall migration, whereas females maintained a constant presence for most of the winter months, decreased occurrence in June and July, and increased occurrence in August, September, and October.

Analysis of GPS collars from 2004 through 2020 indicates that there were 923 crossings of the proposed Willow road alignments (Figure 14) and up to 14% of collared caribou cross the proposed Willow road alignment in a given season (Table 3). The highest proportion of collared caribou crossings was during the fall migration season (mean = 14%; annual range = 7–46%), followed by the oestrid fly season (mean = 8%; annual range = 0–36%), and winter (mean = 8%; annual range = 1–29%). The lowest proportion of collared TCH caribou crossings the Willow alignments was during the postcalving (mean = 2%; annual range = 0–4%) and mosquito seasons (mean = 1%; annual range = 0–3%).

REMOTE SENSING

Because MODIS imagery covers large areas at a relatively coarse resolution (250- to 500-m

pixels), it was possible to evaluate snow cover and vegetation indices over a much larger region extending beyond the study area with no additional effort or cost. The region evaluated extends from the western edge of Teshekpuk Lake east to the Canada border and from the Beaufort Sea inland to the northern foothills of the Brooks Range. The ability to examine this large region allowed us to place the study area into a larger geographic context in terms of the chronology of snow melt and vegetation green-up, both of which are environmental variables that have been reported to be important factors affecting caribou distribution in northern Alaska (Kuropat 1984, Johnson et al. 2018).

SNOW COVER

Based on observations from survey crews and records from weather stations in the area (Figure 4; Appendix C), the timing of snowmelt was approximately average for most of the region in 2020. Estimated snow cover from MODIS data indicated active snowmelt was widespread in the BTN and BTS survey areas on 29 May and the entire region was generally snow-free by 4 June (Figure 16). For the BTN and BTS survey areas, this timing was similar to or slightly earlier than the median date of snowmelt computed for the past 20 years (Figures 17–18, Appendix D).

The median dates of snow melt for each pixel computed using 2000–2020 data (where the date of melt was known within one week) indicated that nearly all of the snow on the coastal plain typically melted over a period of three weeks between 25 May and 11 June (Figure 17; Appendix D). Snowmelt progressed northward from the foothills of the Brooks Range to the outer coastal plain, occurred earlier in the “dust shadows” of river bars and gravel roads, and occurred later in the uplands and numerous small drainage gullies. The southern coastal plain, wind-scoured areas, and dust shadows typically melted during the last week of May (Figure 17). The central coastal plain and most of the Colville River delta usually melted in the first week of June, leaving snow on the northernmost coastal plain, in uplands, and in terrain features that trap snow, such as stream gullies. During the second week in June, most of the remaining snow melted, although some deep snow-drift remnants, lake ice, and *aufeis* persisted

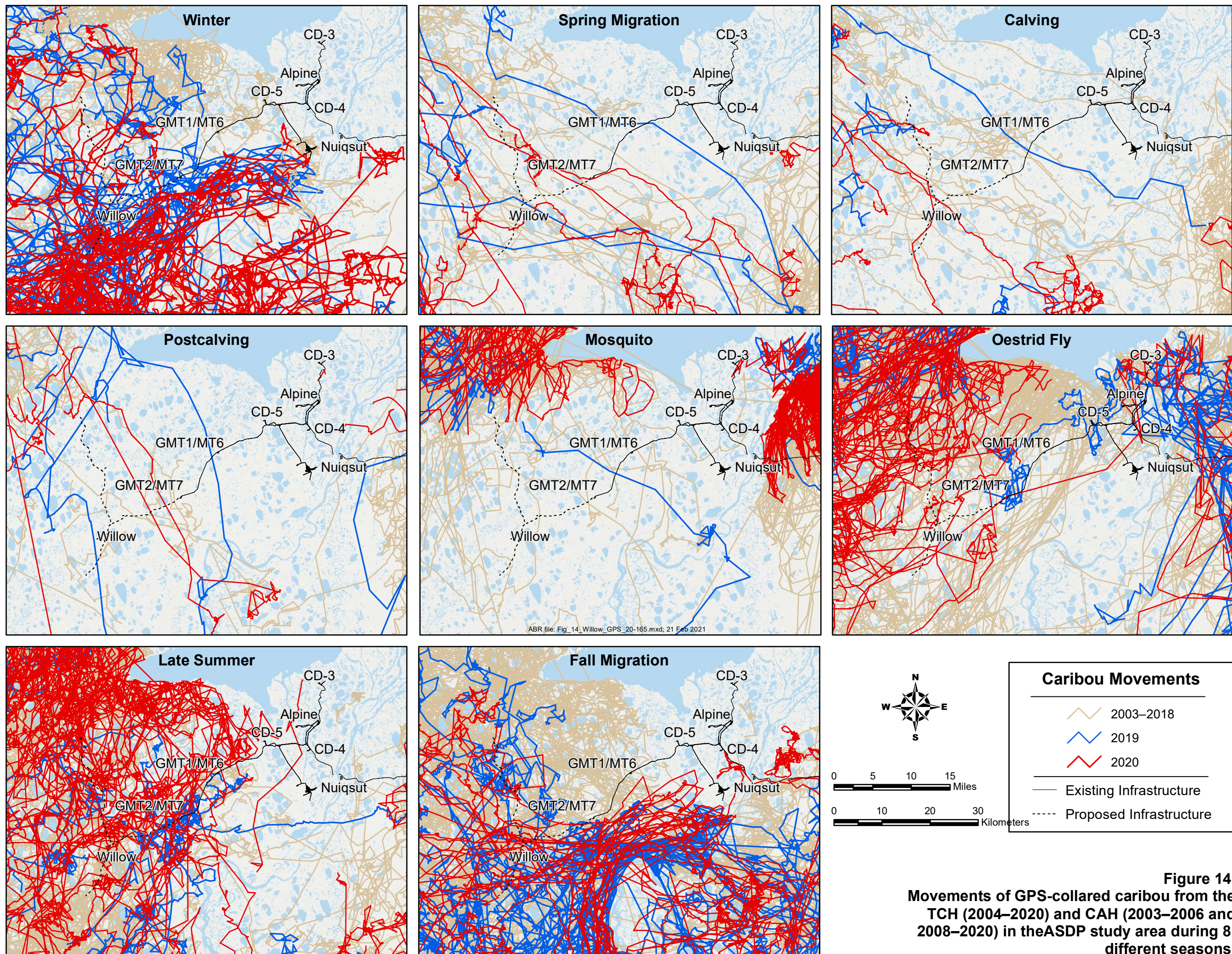


Figure 14. Movements of GPS-collared caribou from the TCH (2004–2020) and CAH (2003–2006 and 2008–2020) in the ASDP study area during 8 different seasons.

Page intentionally left blank.

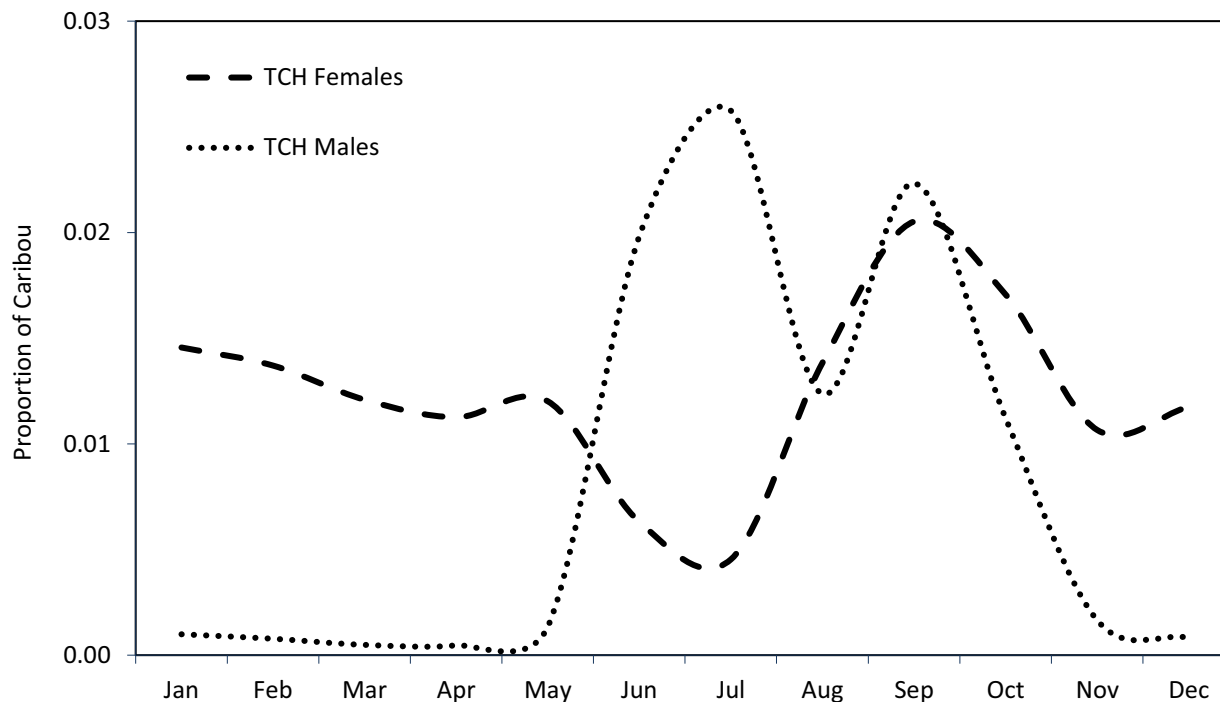


Figure 15. Proportion of caribou from the Teshekpuk Herd within 4 km of the proposed Willow development alignments, based on fixed-kernel density estimation, 1990–2020.

Table 3. Proportion of GPS collared Teshekpuk Herd caribou that crossed the proposed Willow alignment at least once in each season, 2004–2020. Numbers in parenthesis indicate the number of collared caribou used in the analysis. Locations within 30 days of collaring were removed and then animals with fewer than 50 locations or active less than half the season were removed from the analysis.

Year	Spring Migration	Calving	Postcalving	Mosquito	Oestrud Fly	Late Summer	Fall Migration	Winter
2004						0.00 (10)	0.40 (10)	0.20 (10)
2005–2009	0.02 (49)	0.10 (49)	0.00 (49)	0.00 (39)	0.36 (45)	0.09 (76)	0.12 (75)	0.01 (70)
2010–2014	0.06 (88)	0.04 (84)	0.02 (81)	0.01 (83)	0.08 (108)	0.02 (122)	0.09 (116)	0.03 (101)
2015	0.05 (20)	0.06 (18)	0.00 (15)	0.00 (16)	0.04 (26)	0.08 (26)	0.46 (26)	0.04 (23)
2016	0.22 (23)	0.05 (22)	0.00 (22)	0.00 (22)	0.02 (47)	0.02 (52)	0.16 (51)	0.02 (49)
2017	0.02 (46)	0.02 (46)	0.00 (29)	0.00 (44)	0.02 (60)	0.01 (76)	0.07 (74)	0.01 (70)
2018	0.06 (65)	0.02 (64)	0.04 (27)	0.03 (64)	0.00 (66)	0.07 (84)	0.15 (80)	0.29 (77)
2019	0.03 (70)	0.01 (69)	0.03 (35)	0.00 (75)	0.00 (98)	0.03 (106)	0.10 (105)	0.10 (100)
2020	0.04 (98)	0.02 (97)	0.04 (50)	0.00 (100)	0.14 (108)	0.21 (118)	0.16 (117)	
All Years	0.05 (459)	0.03 (449)	0.02 (308)	0.01 (343)	0.08 (558)	0.07 (670)	0.14 (654)	0.08 (500)

into early July (Figure 17). In the GMT survey area, snow melt occurred earliest near stream channels and a south-to-north gradient was apparent, with snow typically melting several days later near the coast. Previous comparisons of the performance of the MODIS subpixel-scale snow-cover algorithm with aggregated Landsat imagery suggest that the overall performance of the subpixel algorithm is acceptable, but that accuracy degrades near the end of the period of snow melt (Lawhead et al. 2006).

VEGETATIVE BIOMASS

Compared with the median NDVI since 2000 (Figure 17), the estimated vegetative biomass during calving (NDVI_Calving) and during peak lactation (NDVI_621) in 2020 was above normal across much of the study area (Figures 17–19; Appendices E–F). Those values were consistent with the average or slightly early snow melt in 2020. Peak NDVI was near normal in 2020 (Figure 18; Appendix G), indicating that, despite cool summer temperatures, 2020 was an average growing season overall. Therefore, the early gains in growth largely compensated for the below average temperatures in July (Figure 4). In 2020, NDVI_Rate was low in inland areas with earlier snowmelt, but high in more coastal areas where snowmelt occurred later (Figure 19). This is consistent with a rapid increase in NDVI values soon after snowmelt, as standing dead biomass is exposed and rapid new growth of vegetation occurs.

SPECIES DISTRIBUTION MODELING

GENERAL SUITABILITY

Sample sizes for the seasonal location data used in the Maxent models ranged from 314 to 6,648 use locations for the years 2002–2020 combined (Table 4). The best performing RM based on AUCtest varied by season from 0.75 to 5.0 (Table 4). All models were able to predict caribou locations better than expected by random chance (Training AUC > 0.5). After re-running the models with the best performing RM and 100% of the data, the best performing model was the model for the mosquito season (AUC = 0.805) and the worst performing model was the model for the fall migration season (AUC = 0.619). Test AUC was

similar to training AUC in the top models, indicating that the models developed with the training data performed almost as well with separate test data. Clear distributional patterns and localized areas of high suitability were evident in all seasons (Figure 20).

In general, the variables with the highest relative permutation importance (>5) to the seasonal models included distance to coast, east-to-west distribution, the mean habitat proportion variables, and different measures of topography depending on the season (elevation, LED, TPI, gentle slopes, flat landforms, or ruggedness; Figures 21–28, Table 5). The geographic variables (distance to coast and/or east-to-west) were consistently in the top 3 for permutation importance. Median snowmelt date had a contribution >5% only during winter and SWE had a contribution >5% only during spring. Daily NDVI, maxNDVI, biomass, nitrogen, and TWI did not contribute more than 5% to any model.

SUITABILITY BY SEASON

The training AUC in the winter season was moderate at 0.685. Based on the suitability map for the winter season, suitability was lowest in the GMT survey area, higher in the northeastern BTN survey area, and highest in the BTS survey area (Figure 20). Suitability was relatively high throughout most of the BTS survey area and moderately high throughout much of the BTN survey area with lower suitability along drainages in both study areas. The variables with the largest permutation importance to the model included elevation (30.7), distance to coast (12.1), flat landforms (11.3), west-to-east distribution (10.2), the mean proportion of tussock tundra (7.7), and the mean proportion of riverine habitat (5.3; Figure 21, Table 4). Based on the response curves, suitability increased with higher elevations, farther from the coast, with lower proportions of flat landforms, and farther west. Caribou avoided wet habitats and preferred tussock tundra (Figure 21). Suitability was also higher in regions with moderate median SWE levels, and low at low maxNDVI values.

The training AUC for the spring migration model had the second highest value of all seasonal models at 0.746. Based on the suitability map, the

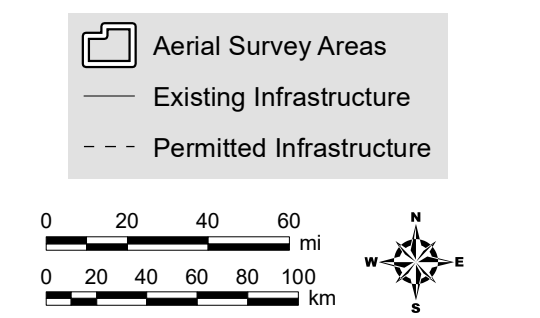
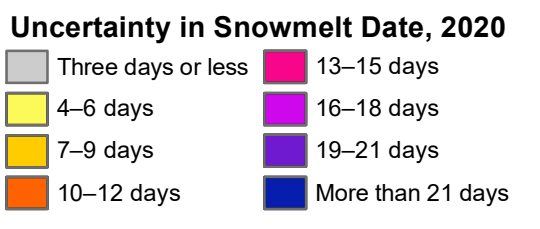
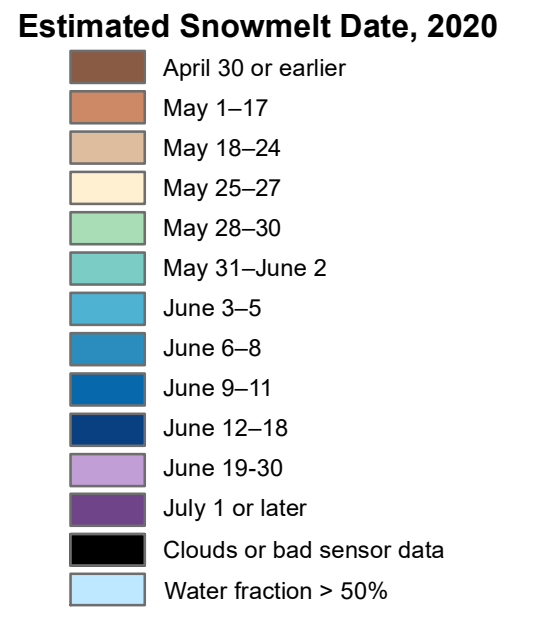
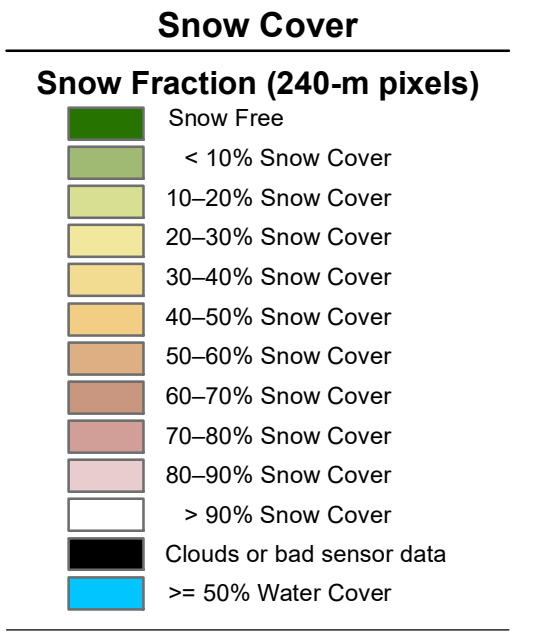
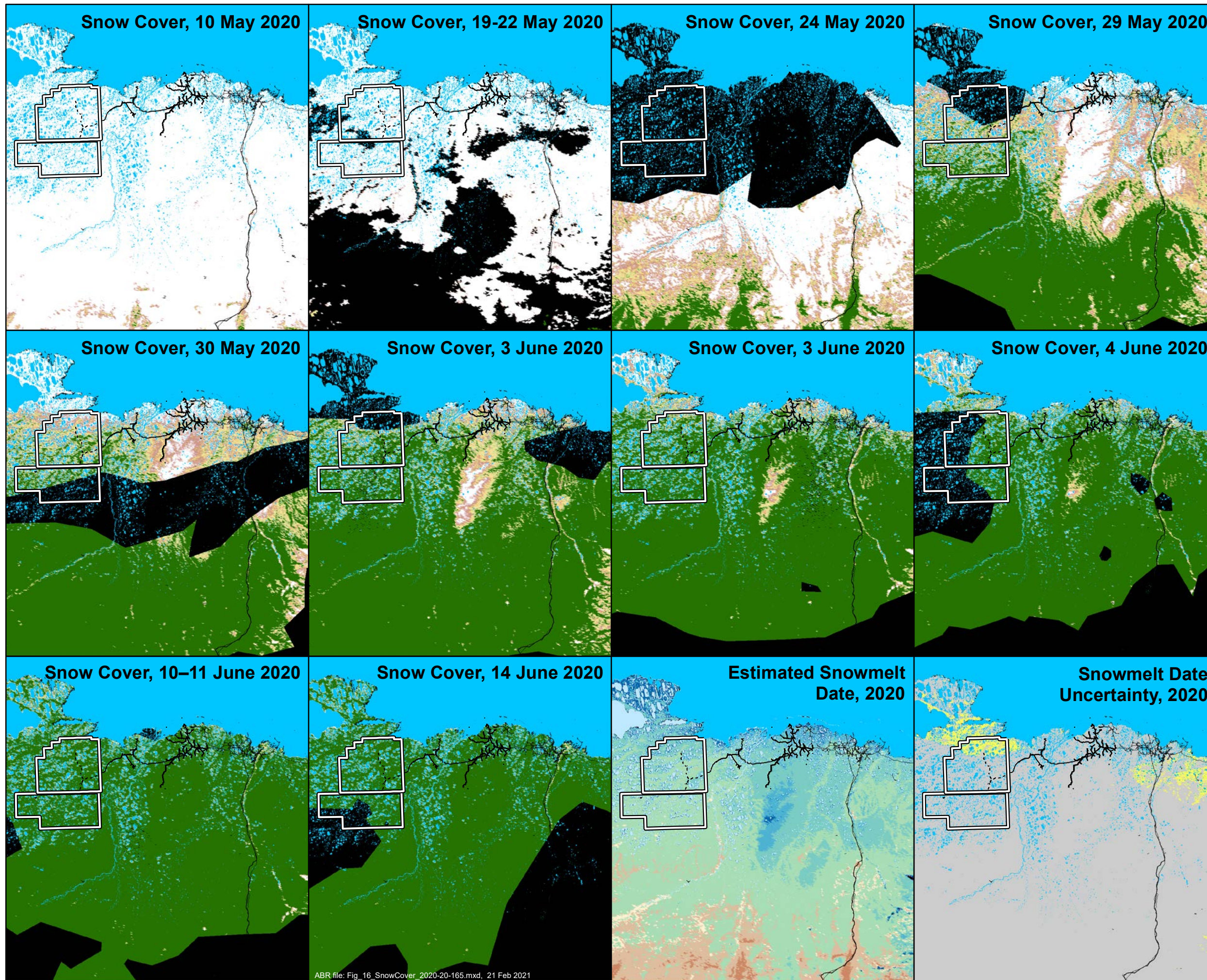
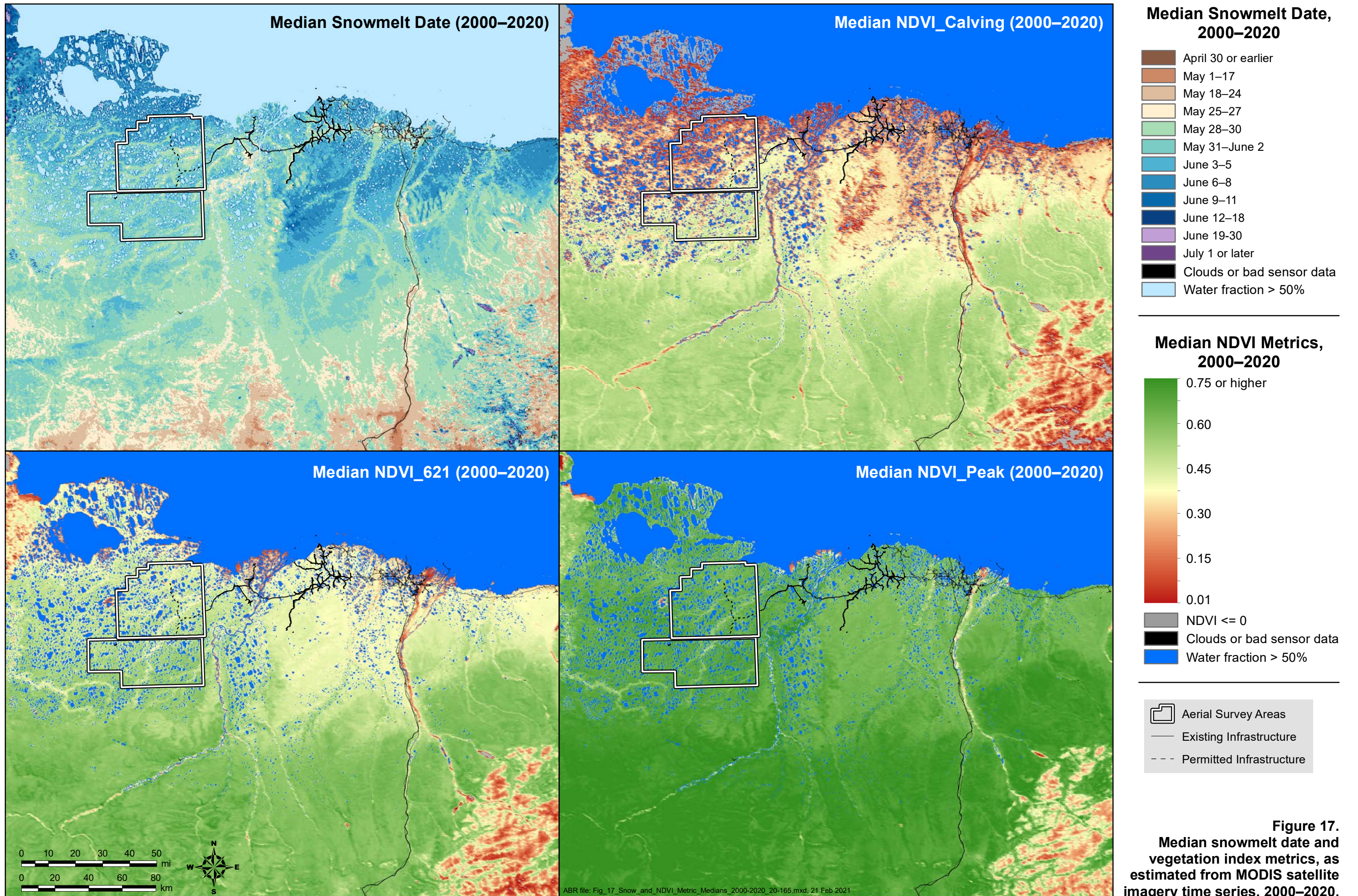


Figure 16. Extent of snow cover between early May and mid-June on the central North Slope of Alaska in 2020, as estimated from MODIS satellite imagery.



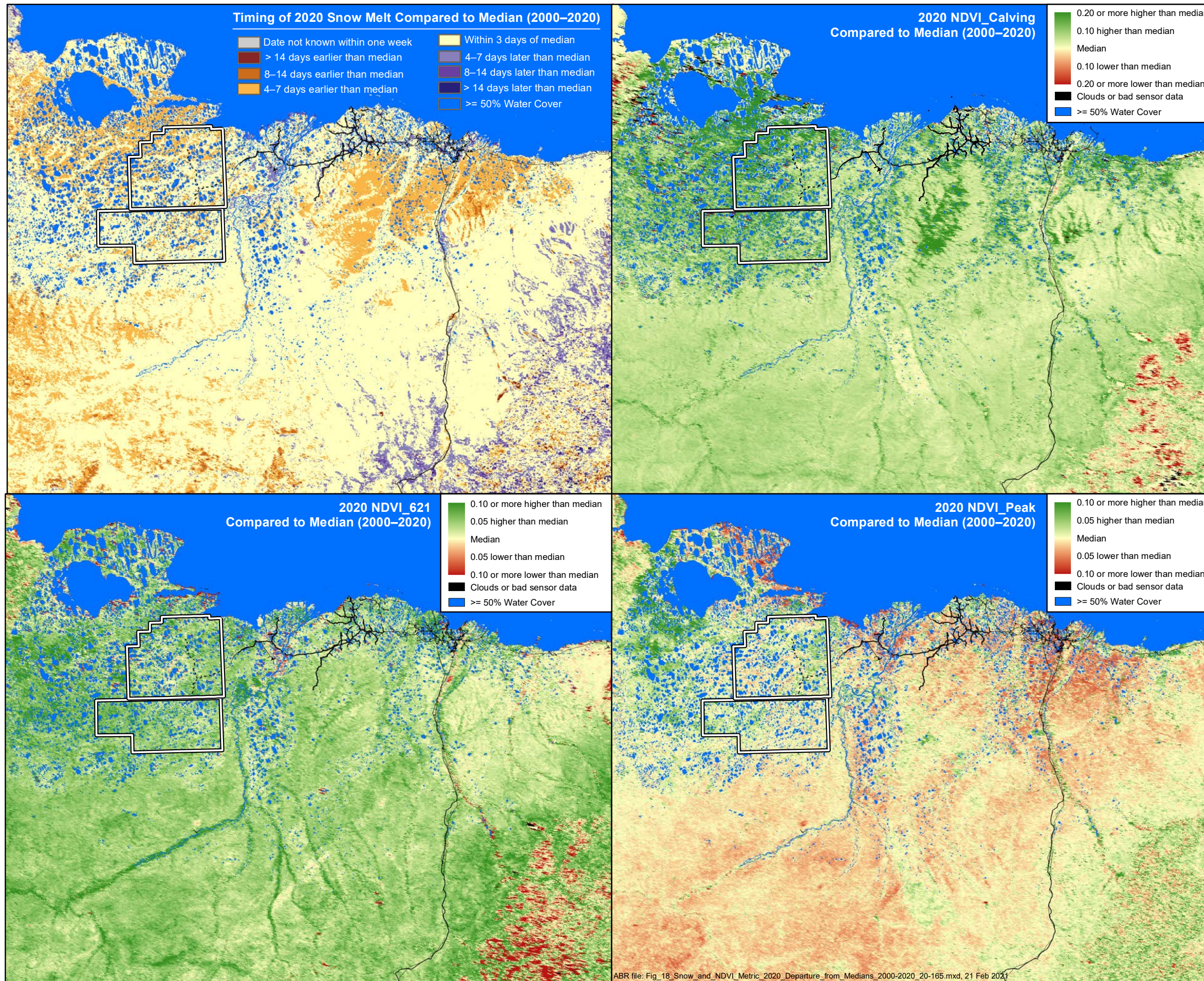


Figure 18.
 Departure of 2020 values
 from median snowmelt
 date and vegetation index
 metrics (2000–2020), as
 estimated from MODIS
 satellite imagery time series.

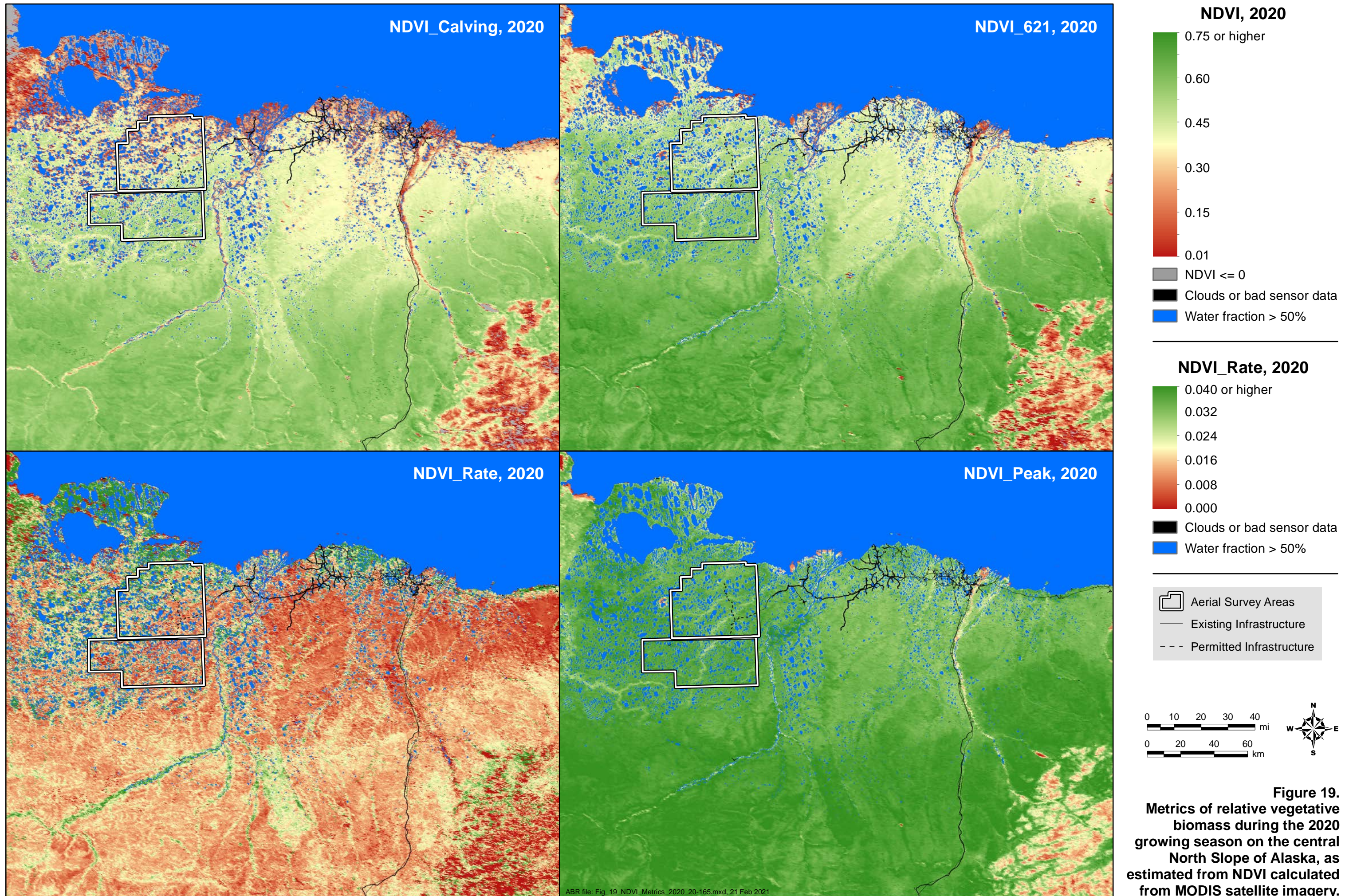


Table 4. Sample sizes and performance metrics for the species distribution model analysis for the NPRA survey area, 2002–2020. The regularization multiplier (RM) of 0.75, 1, 2, 3, 4, 5, 6, and 7 were compared and the RM and Area under the curve (AUC) values for training sample and test sample of the best model based on the highest test AUC is provided. The final AUC was calculated from the model when 100% of samples were run with the top RM value.

Season	Aerial Locations	Telemetry Locations	Total Locations	Regularization Multiplier	Training AUC	Test AUC	Final AUC
Winter	1,535	5,113	6,648	0.75	0.689	0.652	0.685
Spring	458	627	1,085	0.75	0.745	0.703	0.746
Migration							
Calving	1,704	202	1,906	2.00	0.657	0.635	0.653
Postcalving	1,789	92	1,881	1.00	0.672	0.668	0.671
Mosquito	88	226	314	5.00	0.809	0.774	0.805
Oestrid Fly	602	568	1,170	0.75	0.735	0.664	0.727
Late Summer	1,651	1,948	3,599	0.75	0.645	0.621	0.644
Fall Migration	2,239	3,574	5,813	2.00	0.623	0.614	0.619
Total	10,066	12,350	22,416				

model predicted the highest suitability farther to the west, with higher suitability in drainages or around lakes (Figure 20). The eastern BTS had relatively low suitability during spring. The variables with the largest permutation importance to the model included west-to-east (33.1), distance to coast (15.9), elevation (13.8), SWE (6.1), and the proportion of gentle slopes (5.8; Figure 22, Table 4). Based on the response curves, suitability increased in the west, further from the coast, and as the mean proportion of gentle slopes increased (Figure 22). Suitability was very low at the highest SWE values, indicating they are avoiding the deepest or densest snow and was also lower at lower elevations.

The training AUC for the calving season indicated moderate predictive power at 0.653. Based on the suitability map, suitability for all survey regions was generally lowest in the eastern portions of GMT, lower along creeks and streams, and highest in the BTN survey area (Figure 20). Suitability in the BTS survey area increased from the southwest to the northeast. The variables with the largest permutation importance to the model included west-to-east (38.0) and distance to coast (29.9 Figure 23, Table 4). The variables with the next highest permutation importance were the

proportion of flooded tundra (4.8) and tussock tundra (4.2) habitats, aspect (3.8), and elevation (3.2). Based on the response curves, suitability was highest at mid-longitudes and moderate distances to coast (Figure 23). Suitability was lower as the proportion of flooded tundra increased, and very low at low proportions of tussock tundra and at lower elevations. The daily biomass variable had a permutation importance of 2.7 and suitability generally increased with increasing biomass on the landscape. The daily nitrogen and NDVI variables contributed 0.3 and 2.0, respectively. Median snowmelt date only had a permutation importance of 1.1 but had a slight positive relationship with suitability, suggesting that caribou tend to be distributed in regions with slightly later melting snow, but other variables are more powerful at predicting suitability.

The training AUC for the postcalving season indicated moderate predictive power at 0.671. Based on the suitability map, suitability across all survey areas was highest along streams and increased to the northwest. Most of the BTN survey area was predicted to have high suitability (Figure 20). The variables with the largest permutation importance to the model included west-to-east (41.1), distance to coast (12.0), gentle

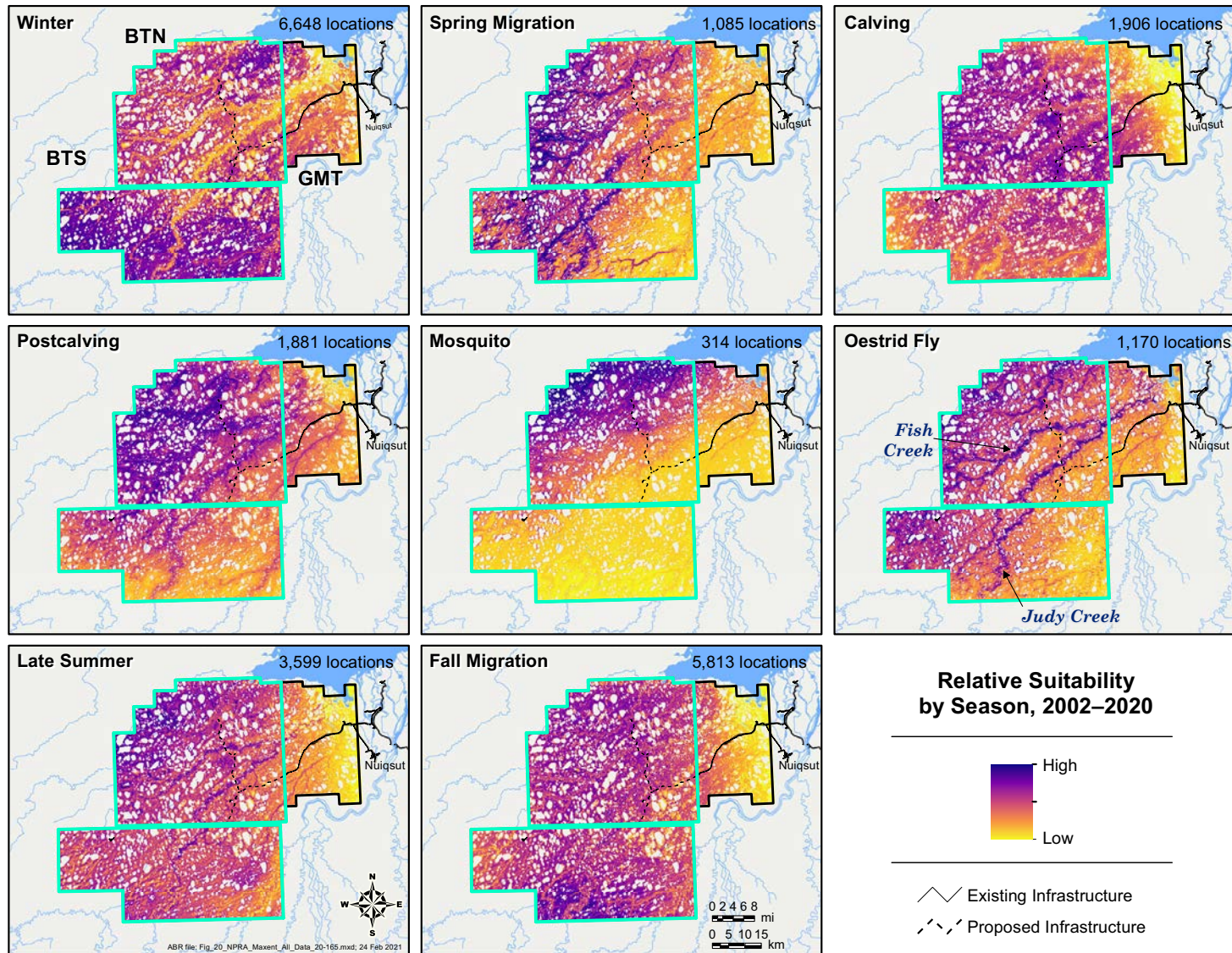


Figure 20. Predicted relative suitability for use of the GMT, BTN, and BTS survey areas by caribou during 8 different seasons, 2002–2020, based on Maxent analysis. Relative probabilities calculated using the 2020 values for daily NDVI, biomass, and nitrogen.

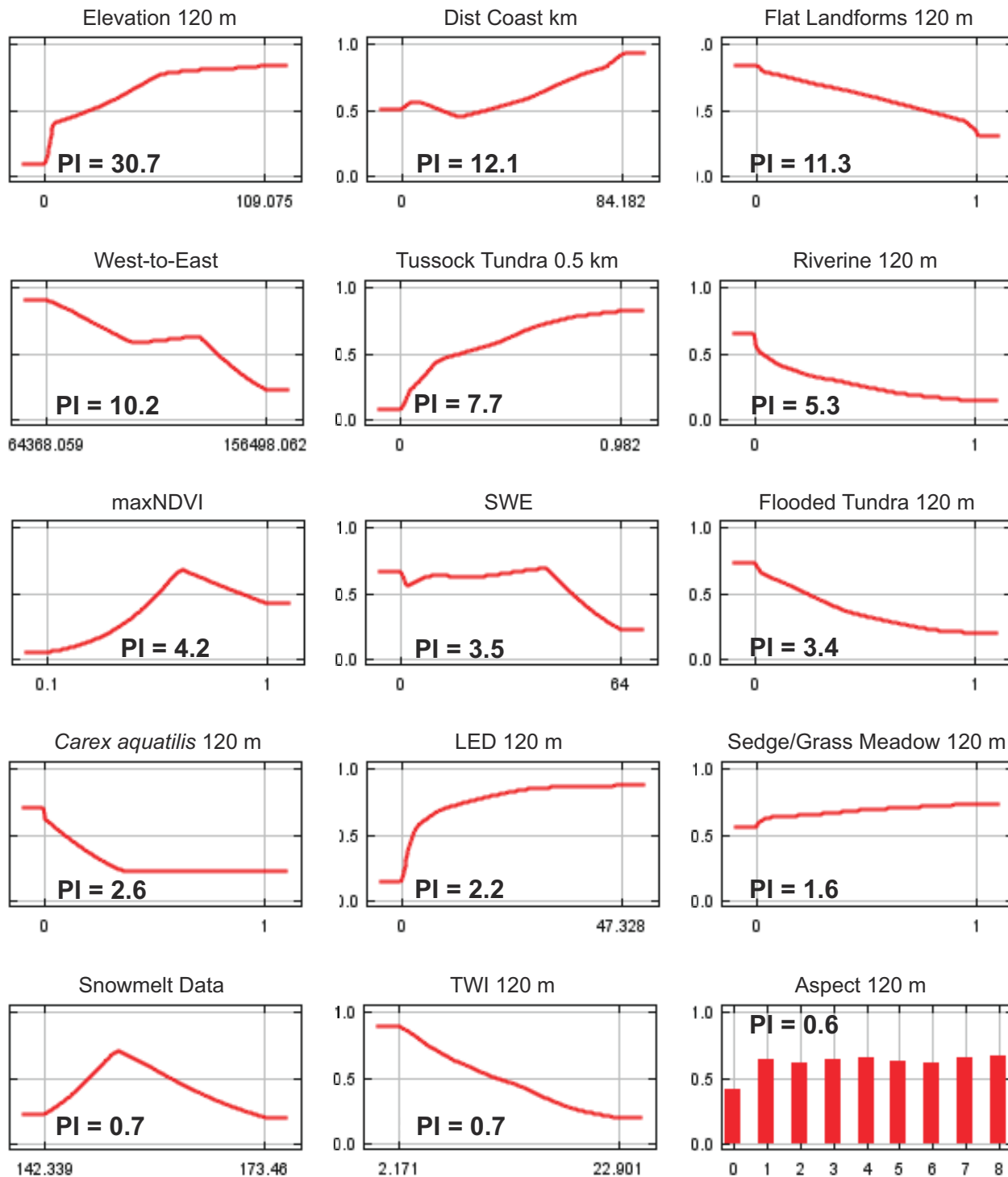


Figure 21. Response curves and permutation importance of the top 15 variables (based on permutation importance) included in models to predict caribou suitability in the GMT, BTN, and BTS surveys areas during the winter season. These plots reflect the dependence of predicted suitability both on the selected variable and on dependencies induced by correlations between the selected variable and other variables.

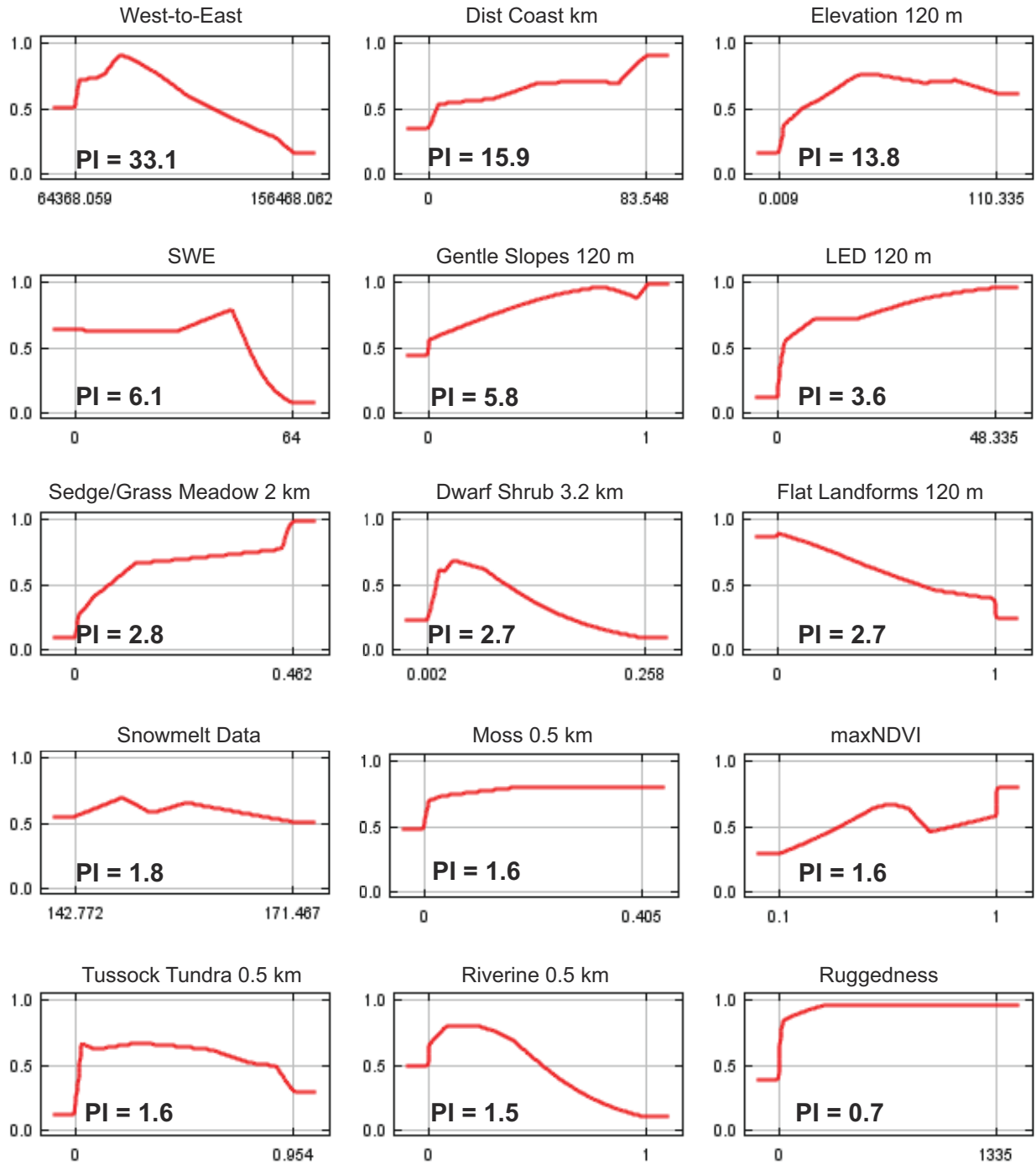


Figure 22. Response curves and permutation importance of the top 15 variables (based on permutation importance) included in models to predict caribou suitability in the GMT, BTN, and BTS surveys areas during the spring migration season. These plots reflect the dependence of predicted suitability both on the selected variable and on dependencies induced by correlations between the selected variable and other variables.

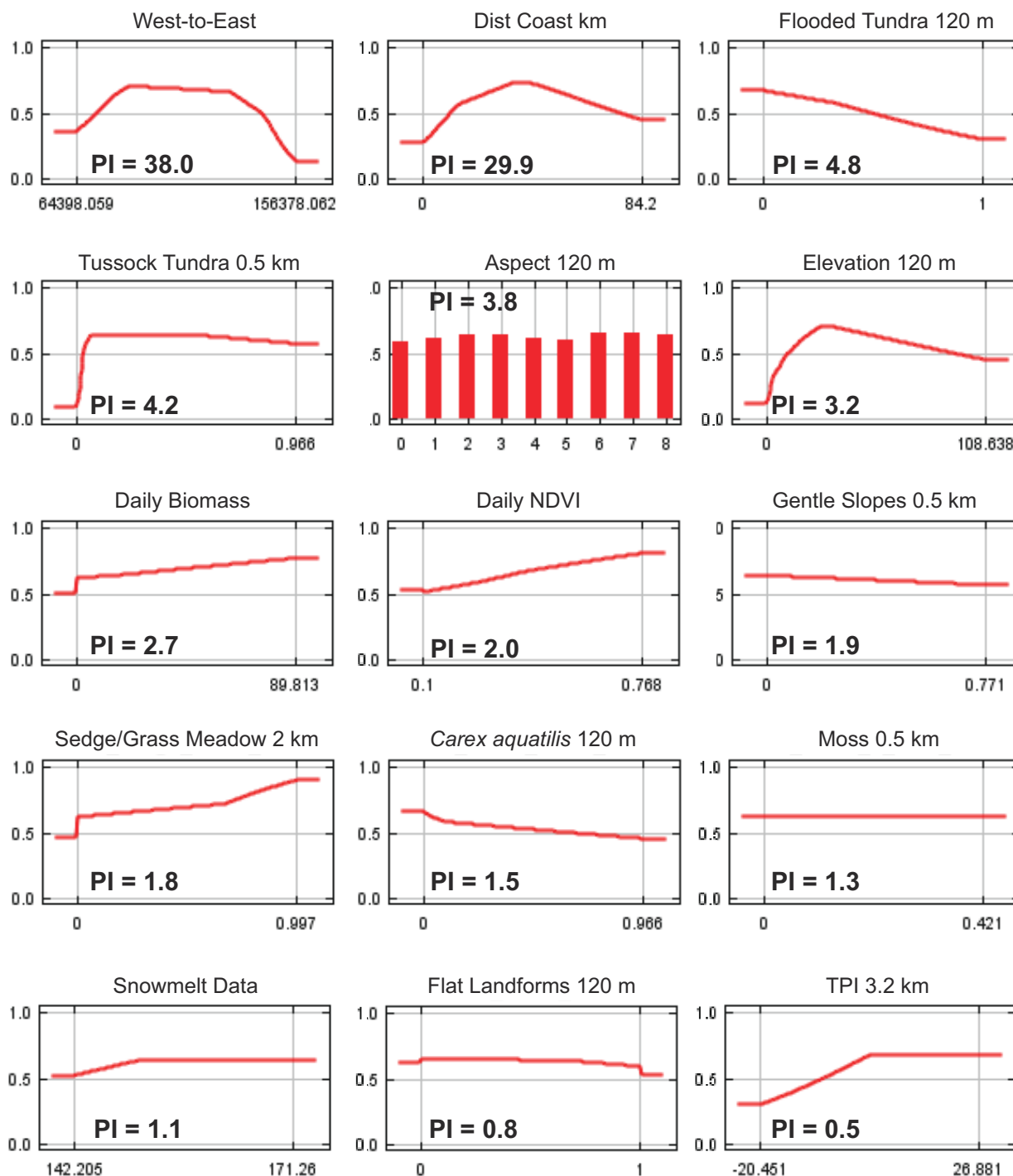


Figure 23. Response curves and permutation importance of the top 15 variables (based on permutation importance) included in models to predict caribou suitability in the GMT, BTN, and BTS surveys areas during the calving season. These plots reflect the dependence of predicted suitability both on the selected variable and on dependencies induced by correlations between the selected variable and other variables.

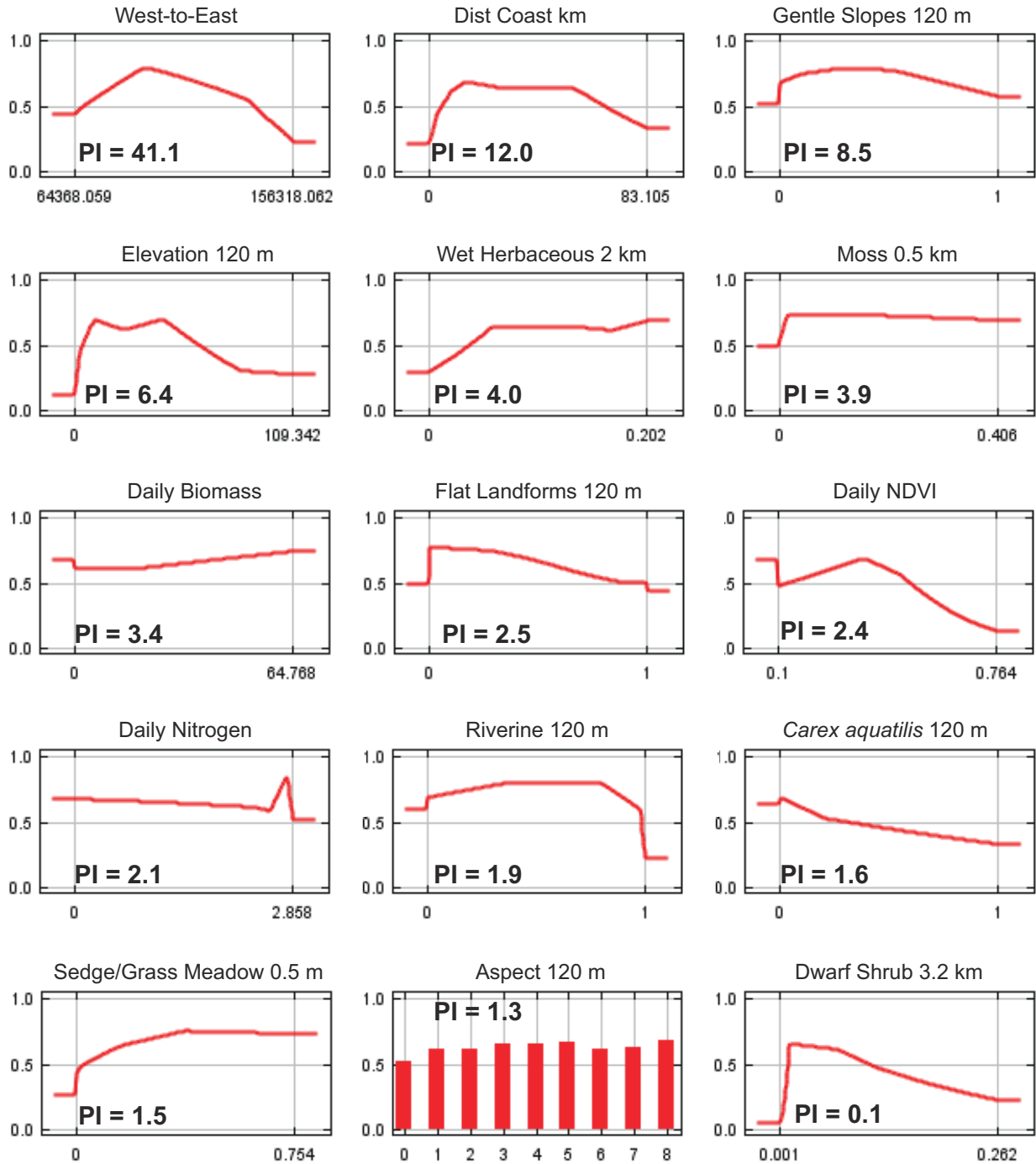


Figure 24. Response curves and permutation importance of the top 15 variables (based on permutation importance) included in models to predict caribou suitability in the GMT, BTN, and BTS surveys areas during the postcalving season. These plots reflect the dependence of predicted suitability both on the selected variable and on dependencies induced by correlations between the selected variable and other variables.

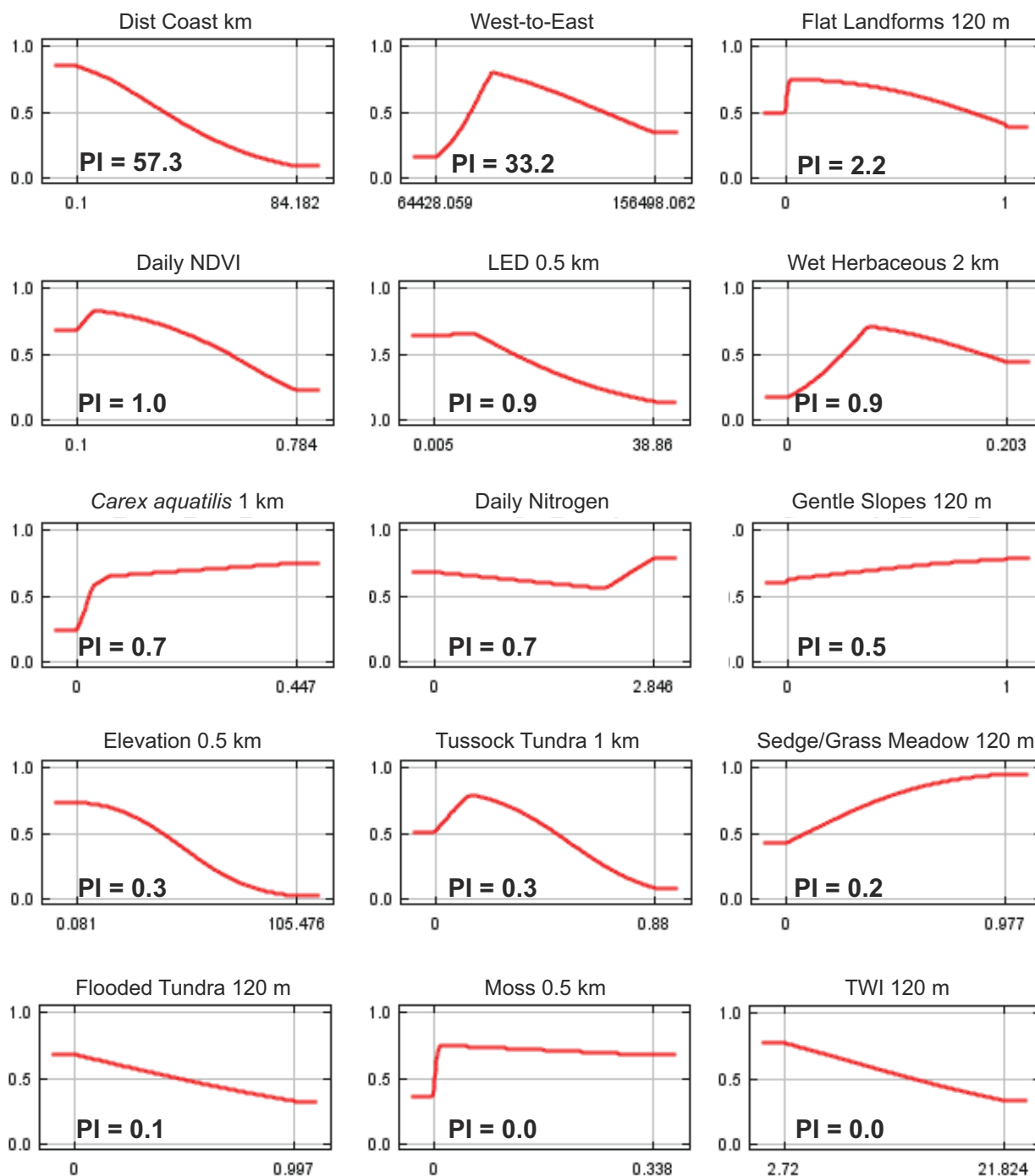


Figure 25. Response curves and permutation importance of the top 15 variables (based on permutation importance) included in models to predict caribou suitability in the GMT, BTN, and BTS surveys areas during the mosquito season. These plots reflect the dependence of predicted suitability both on the selected variable and on dependencies induced by correlations between the selected variable and other variables.

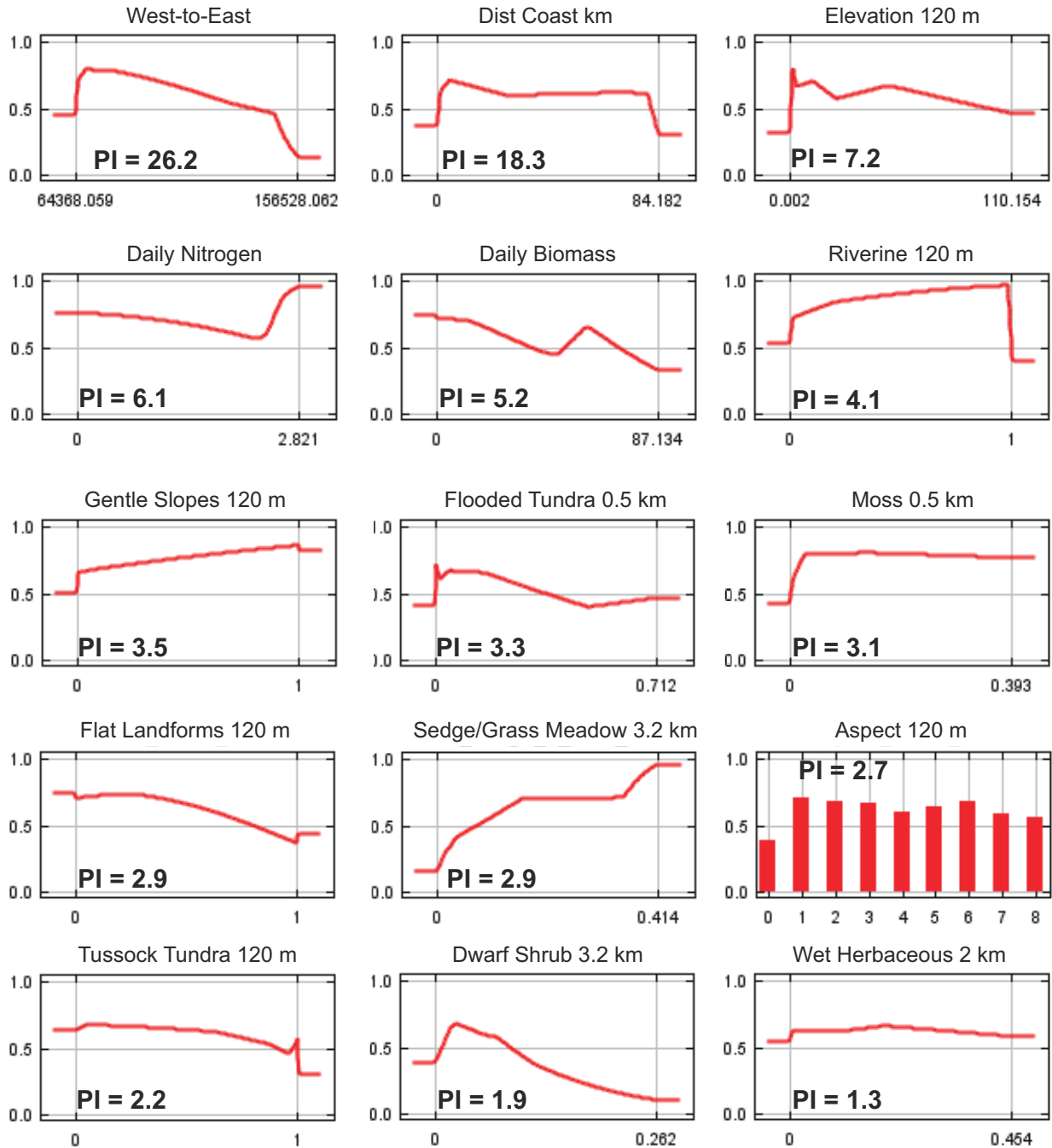


Figure 26. Response curves and permutation importance of the top 15 variables (based on permutation importance) included in models to predict caribou suitability in the GMT, BTN, and BTS surveys areas during the oestrid fly season. These plots reflect the dependence of predicted suitability both on the selected variable and on dependencies induced by correlations between the selected variable and other variables.

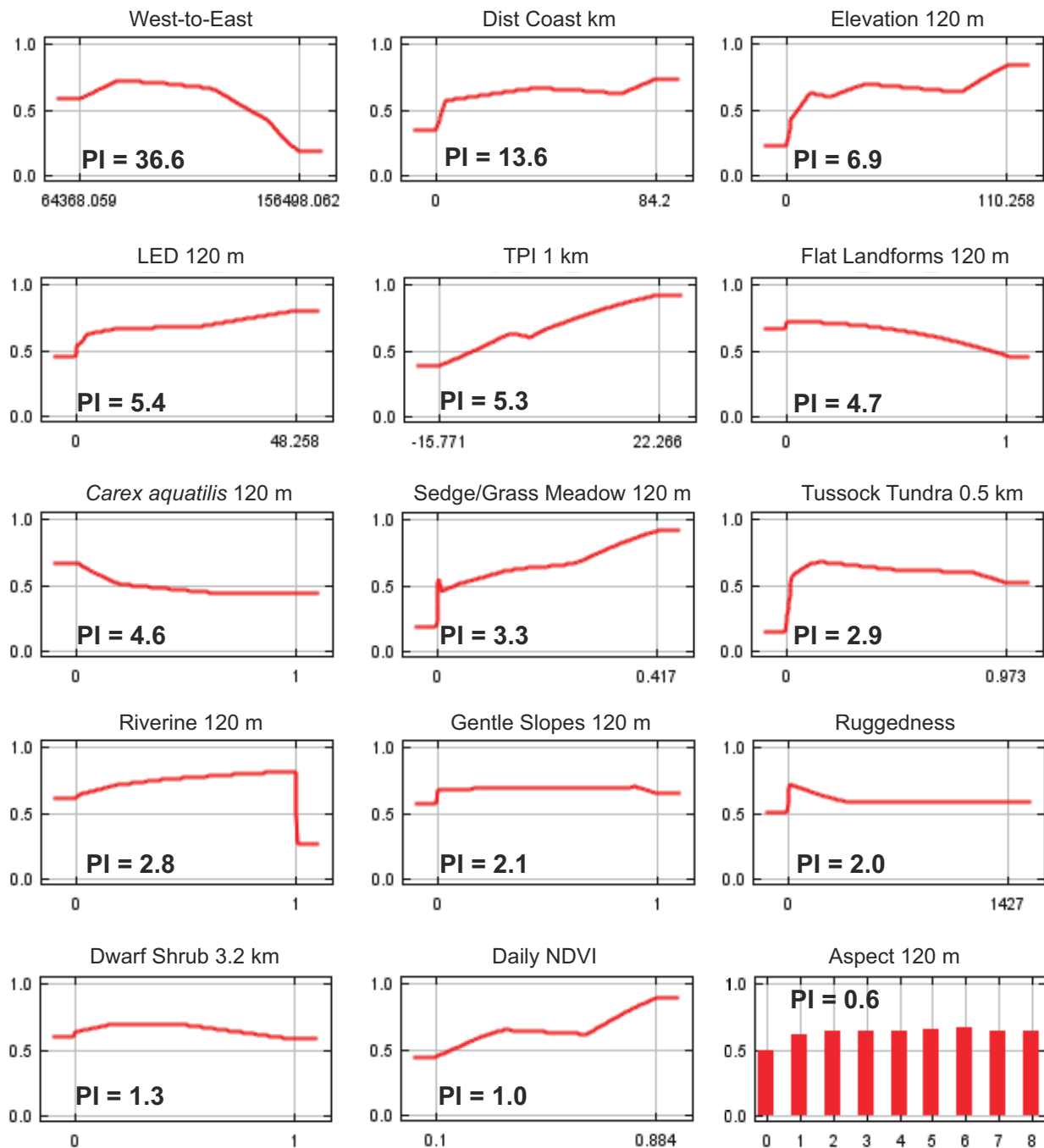


Figure 27. Response curves and permutation importance of the top 15 variables (based on permutation importance) included in models to predict caribou suitability in the GMT, BTN, and BTS surveys areas during late summer. These plots reflect the dependence of predicted suitability both on the selected variable and on dependencies induced by correlations between the selected variable and other variables.

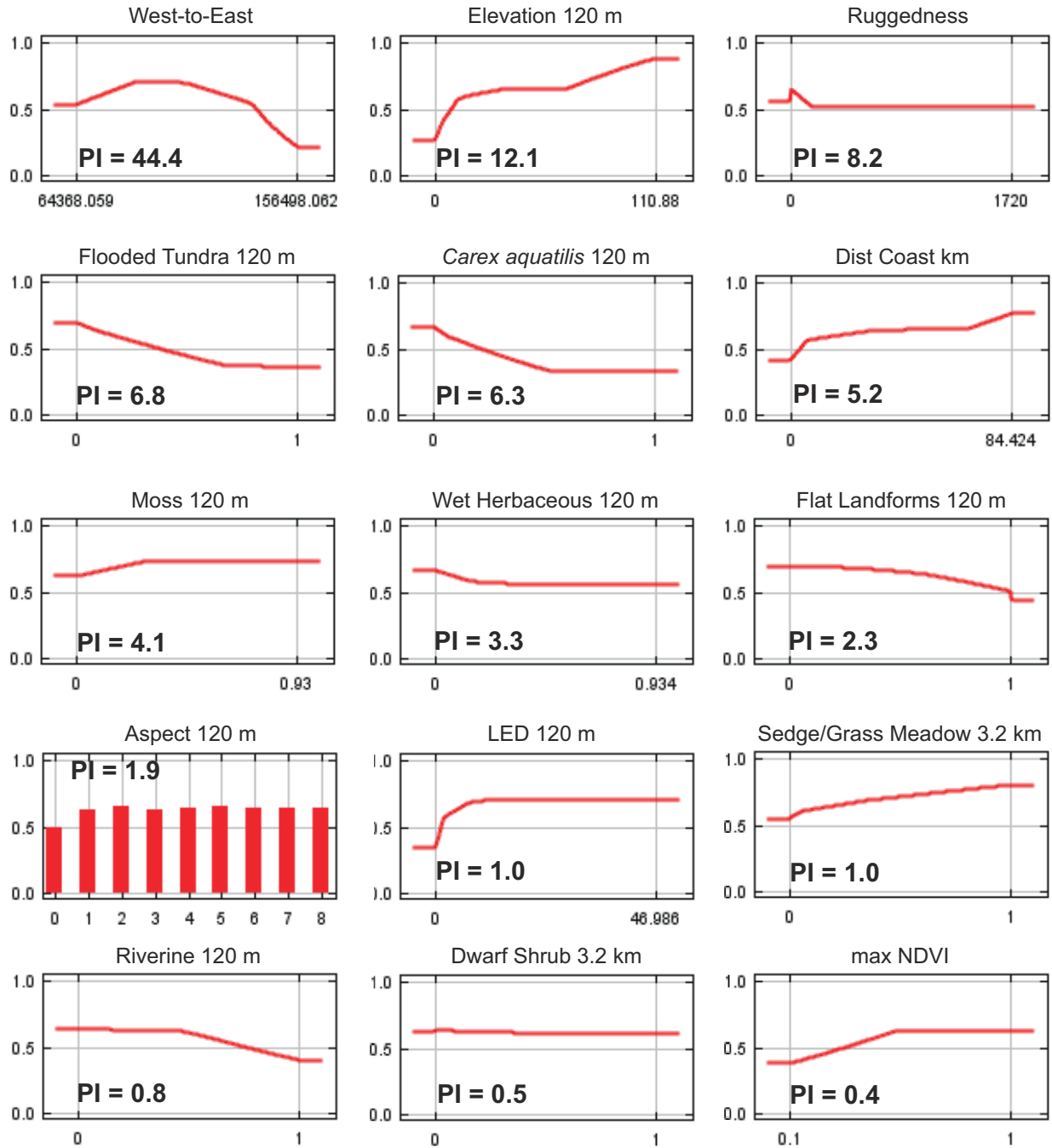


Figure 28. Response curves and permutation importance of the top 15 variables (based on permutation importance) included in models to predict caribou suitability in the GMT, BTN, and BTS surveys areas during the fall migration season. These plots reflect the dependence of predicted suitability both on the selected variable and on dependencies induced by correlations between the selected variable and other variables.

Table 5. Permutation Importance of variables used in species distribution models of caribou suitability in the GMT, BTN, and BTS survey areas during 8 different seasons, 2002–2020. Bold font indicates a permutation importance >5. Distance values represent the scale at which the variable was calculated.

Variable	Winter	Spring Migration	Calving	Postcalving	Mosquito	Oestrid Fly	Late Summer	Fall Migration
Aspect 120 m	0.6	0.0	3.8	1.3	0.1	2.7	0.6	1.9
Daily Biomass			2.7	3.4	0.5	5.2	0.9	
Distance Coast km	12.1	15.9	29.9	12.0	57.3	18.3	13.6	5.2
<i>Carex aquatilis</i> 1 km					0.7			
<i>Carex aquatilis</i> 120 m	2.6	1.2	1.5	1.6		0.2	4.6	6.3
Dwarf Shrub 3.2 km		2.7		0.1	0.9	1.9		
Dwarf Shrub 2.0 km	0.5							
Dwarf Shrub 120 m			0.2				1.3	0.5
Flooded Tundra 0.5 km		1.0				3.3		
Flooded Tundra 120 m	3.4		4.8	3.1	0.1		0.5	6.8
Moss 0.5 km		1.6	1.3	3.9	0.0	3.1		
Moss 120 m	0.7						1.0	4.1
Riverine 1 km			0.3					
Riverine 0.5 km		1.5						
Riverine 120 m	5.3			1.9	0.0	4.1	2.8	0.8
Sedge/Grass Meadow 3.2 km							3.3	
Sedge/Grass Meadow 2 km		2.0						
Sedge/Grass Meadow 0.5 km				1.5				
Sedge/Grass Meadow 120 m	1.6		1.8		0.2	2.9		1.0
Tussock Tundra 3.2 km				1.1				
Tussock Tundra 1 km					0.3			
Tussock Tundra 0.5 km	7.7	1.6	4.2				2.9	0.2
Tussock Tundra 120 m						2.2		

Table 5. Continued.

Variable	Winter	Spring migration	Calving	Postcalving	Mosquito	Oestrud Fly	Late Summer	Fall Migration
Wet Herbaceous 0.5 m						1.3		
Wet Herbaceous 2 km				4.0	0.9			
Wet Herbaceous 120 m	0.3	0.3	0.7				0.4	3.3
West-to-East	10.2	33.1	38.0	41.1	33.2	26.2	36.6	44.4
Elevation 0.5 km					0.3			
Elevation 120 m	30.7	13.8	3.2	6.4		7.2	6.9	12.0
Flat Landforms 120 m	11.3	2.7	0.8	2.5	2.2	2.9	4.7	2.3
Gentle Slopes 0.5 km			1.9			-		
Gentle Slopes 1 km								0.3
Gentle Slopes 120 m	0.5	5.8		8.5	0.5	3.5	2.1	
LED 0.5 km				0.9	0.9			
LED 2 km						0.9		
LED 120 m	2.2	3.6	0.4				5.4	1.0
maxNDVI	4.2	1.6	0.5	0.3	0.1	1.9	2.5	0.4
Daily NDVI			2.0	2.4	1.0	0.5	1.0	
Daily Nitrogen			0.3	2.1	0.7	6.1	0.7	
Ruggedness	0.9	0.7	0.2	1.8	0.0	1.7	2.0	8.2
Snowmelt Date	0.7	1.8	1.1			-		
SWE, spring		6.1						
SWE, winter	3.5							
TPI 1 km							5.3	
TPI 3.2 km	0.3		0.5	0.1	0.2	1.7		0.0
TPI 0.5 km		0.3						
TWI 120 m	0.7	1.9	0.1	0.0	0.0	2.2	0.9	1.2

slopes (8.5), and elevation (6.4; Figure 24, Table 4). Based on the response curves, suitability was higher at mid-longitudes, at small to mid-distances from coast (but not right along the coast), in areas with a low or moderate proportion of gentle slopes, and at low to moderate elevations (Figure 24).

The training AUC value for the mosquito season was the highest of all the seasonal models at 0.805. Based on the suitability map, high suitability during this season was generally confined to the coast, the northwest portion of BTN, and lake margins (Figure 20). The variables with the largest permutation importance to the model included distance to coast (57.3), west-to-east (33.2), flat landforms (2.2) and daily NDVI (1.0). No other variable had a contribution >1.0. Figure 25, Table 4). The response curve and the high permutation importance of the distance to coast variable indicates a strong selection for coastal areas (Figure 25). Suitability was higher close to the coast and at intermediate longitudes, with some evidence that lower proportions of flat landforms and lower NDVI values (like in coastal mudflats) were selected for.

The training AUC for the oestrid fly season was the third highest for the seasonal models at 0.727. Based on the suitability map, suitability for all survey areas generally increased from southeast to northwest and was highest along rivers and lake margins, especially near Fish and Judy creeks (Figure 20). The variables with the largest permutation importance to the model included west-to-east distribution (26.2), distance to coast (18.3), elevation (7.2), daily nitrogen (6.1), and daily biomass (5.2; Figure 26, Table 4). Based on the response curves, suitability increased to the west, was lowest in the extreme east and west of the study area, was higher at lower elevations, and was highest at the highest nitrogen levels.

The training AUC for the late summer season was low compared to other seasonal models at 0.644. Based on the suitability map, suitability was predicted to be relatively high throughout all of BTN and BTS, but lower along streams and some lake margins (Figure 20). The variables with the largest permutation importance to the model included west-to-east (36.6), distance to coast (13.6), elevation (6.9), LED (5.4), and TPI (5.3; Figure 27, Table 4). Based on the response curves, suitability was higher to the west, closer to the

coast, in areas with higher TPI values, and where mean LED was near zero.

The training AUC during the fall migration season was the lowest of all seasonal models at 0.619. Based on the suitability map, the lowest suitability was predicted to be in the eastern portion of GMT, highest in the southwest portion of BTS and generally moderate in other areas (Figure 20). The variables with the largest permutation importance to the model included west-to-east (44.4), elevation (12.0), ruggedness (8.2), the proportion of flooded tundra (6.8), the proportion of *Carex aquatilis* (6.3), and distance to coast (5.2; Figure 28, Table 4). Based on the response curves, suitability was highest at mid-longitudes, at higher elevations, and slightly higher when ruggedness was near zero (Figure 28). Suitability decreased with increasing proportions of flooded tundra and *Carex aquatilis*.

DISTRIBUTION NEAR ICE ROADS

The best model without distance to ice roads included all four variables (landcover, TPI, elevation, and NDVI) for both years. The addition of distance to ice roads resulted in a better model for both years as well as for both years combined (Table 6). Caribou generally selected for sedge/grass meadow and tussock tundra landcover classes relative to the reference category of dwarf/low shrub and avoided the riverine, wet tundra, and water landcover classes (Figure 29). Selection against water was the strongest of the landcover types. Caribou selected for areas with higher elevation, with higher peak NDVI, and higher TPI (Figure 30). The selection for different distances from the ice roads indicated some avoidance of areas within approximately 5 km of ice roads in 2018–2019, but there was no apparent avoidance in 2019–2020 (Figure 31).

OTHER MAMMALS

Observations of other large mammals were recorded by ABR biologists at widely scattered locations during wildlife surveys in 2020. These observations were compared to observations of large mammals observed during previous years (Figure 32).

In 2020, we observed 9 brown bears (*Ursus arctos*; hereafter grizzly bears) in 5 groups in the

Table 6. Model selection results (top 3 models) for female GPS-collared TCH caribou winter movements in the study area, by year 2018–2020. The best model for each year is in bold font.

Winter	Model	AIC	First Stage Δ AIC	Second Stage Δ AIC
2018–2019	Best Plus Dist. from Ice Roads (2 knots)	63,215.4	–	0
	Landcover, TPI, Elevation, NDVI	63,237.6	0	22.2
	Landcover, TPI, Elevation	63,269.6	31.9	54.2
2019–2020	Best Plus Dist. from Ice Roads (1 knot)	103,712.7	–	0
	Landcover, TPI, Elevation, NDVI	103,717.6	0	4.9
	Landcover, TPI, NDVI	103,806.5	88.9	93.8
All Years	Best Plus Dist. from Ice Roads (2 knots)	167,085.9	–	0
	Landcover, TPI, Elevation, NDVI	167,102.9	0	17.0
	Landcover, TPI, Elevation	167,239.1	136.2	153.2

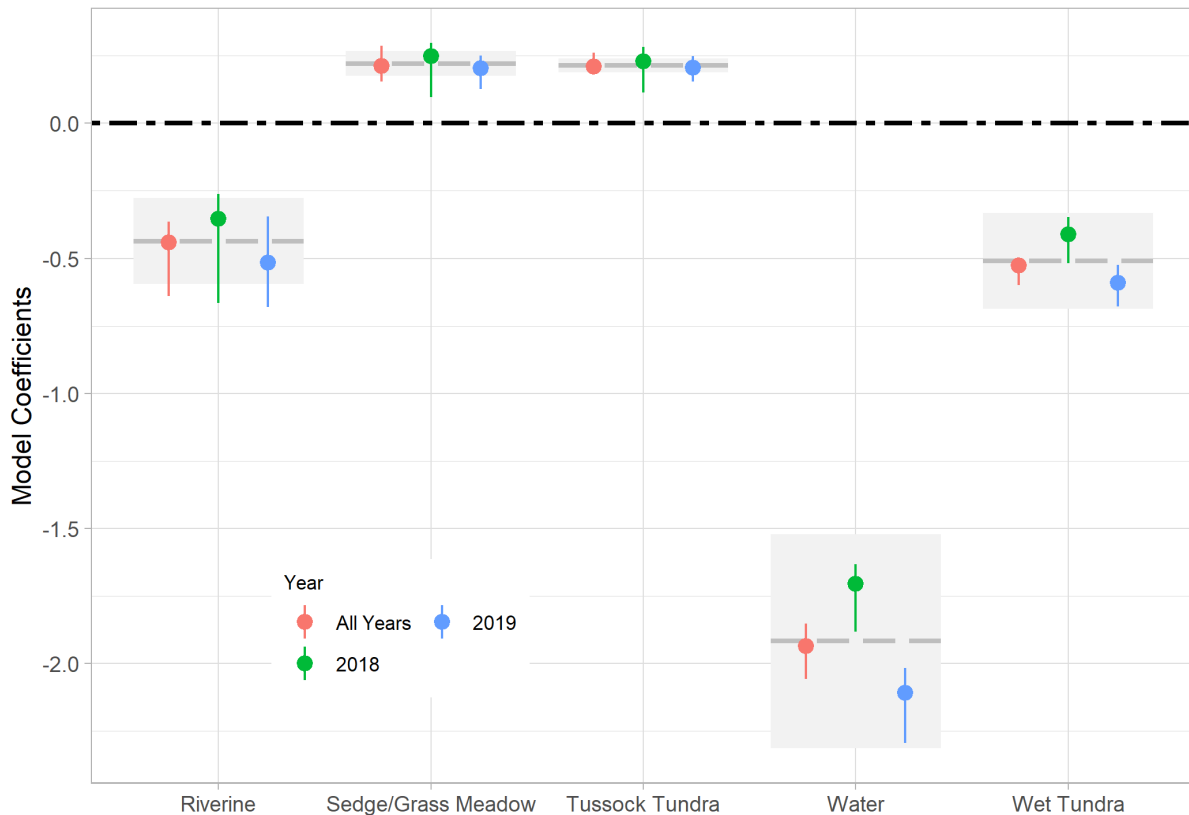


Figure 29. Estimated selection for landcover classes by caribou of the Teshekpuk Herd based on an integrated step-selection analysis of winter movements (December–April). Selection is relative to the reference class dwarf/low shrub tundra.

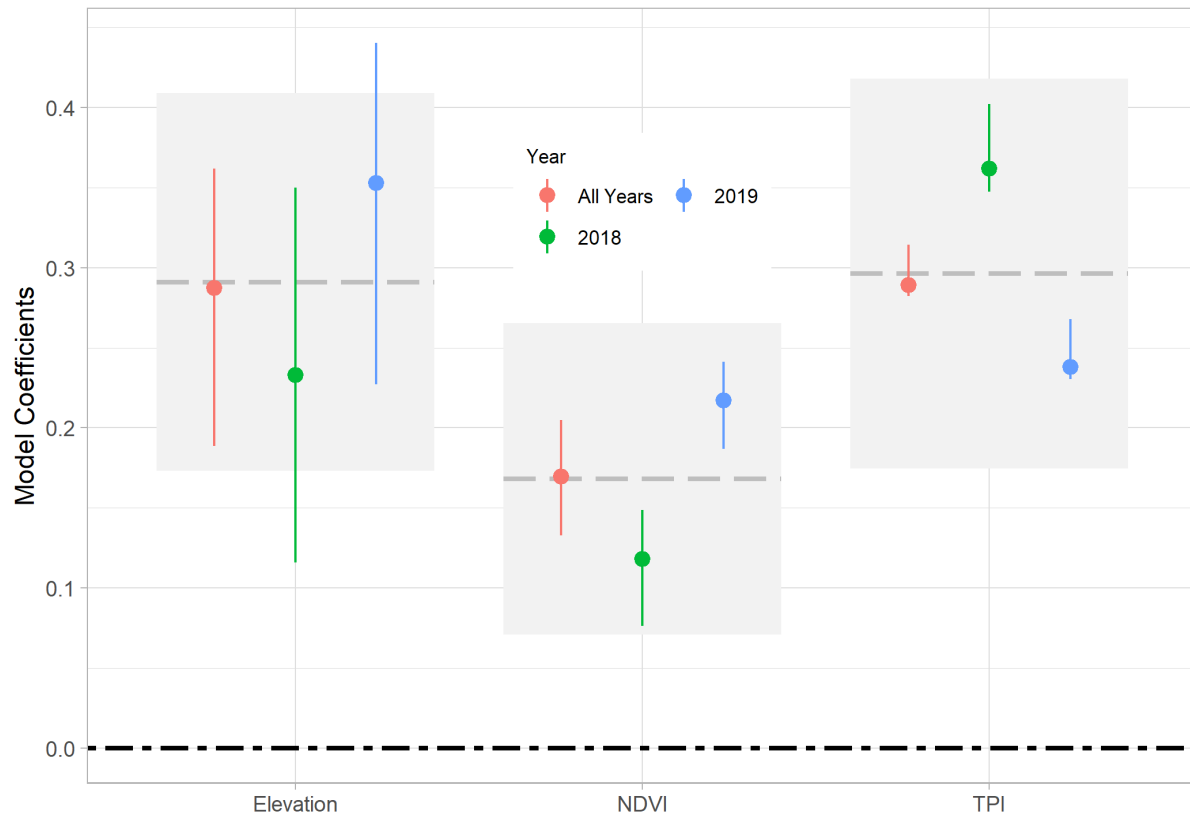


Figure 30. Estimated selection for elevation, NDVI, and Topographic Position Index (TPI) based on an integrated step-selection analysis by caribou of the Teshekpuk Herd based on an integrated step-selection analysis of winter movements (December–April).

BTN survey area, primarily along Fish or Judy creek and 5 grizzly bears in 2 groups in the BTS survey area (Figure 32). Three grizzly bear observations were in June, 2 were in August, and 2 were in October. A sow with 3 cubs was observed once in June in the BTS survey area and once in October in the BTN survey area. A single wolverine (*Gulo gulo*) was observed on 19 June southwest of GMT2/MT7 (Figure 32).

DISCUSSION

WEATHER, SNOW, AND INSECT CONDITIONS

Weather conditions exert strong effects on caribou populations throughout the year in arctic Alaska. Deep winter snow and icing events increase the difficulty of travel, decrease forage availability, and increase susceptibility to predation

(Fancy and White 1985, Griffith et al. 2002). Severe cold and wind events can cause direct mortality of caribou (Dau 2005). Late snowmelt can delay spring migration, cause lower calf survival, and decrease future reproductive success (Finstad and Prichard 2000, Griffith et al. 2002, Carroll et al. 2005). In contrast, hot summer weather can depress weight gain and subsequent reproductive success by increasing insect harassment at an energetically stressful time of year, especially for lactating females (Fancy 1986, Cameron et al. 1993, Russell et al. 1993, Weladji et al. 2003).

Weather condition variability results in large fluctuations in caribou density during the insect season as caribou aggregate and move rapidly through the study area in response to fluctuating insect activity. On the central Arctic Coastal Plain (including the study area), caribou typically move

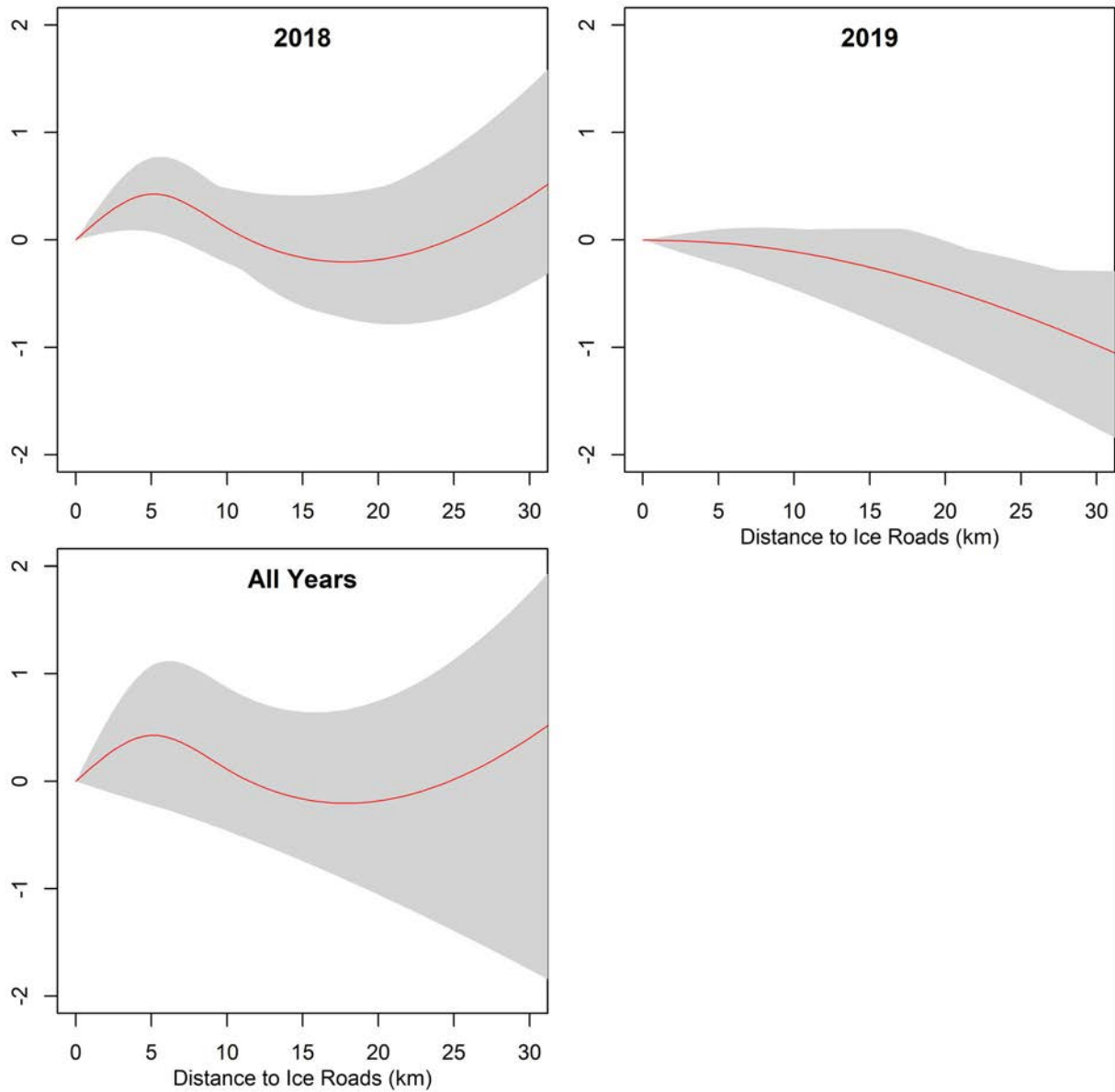


Figure 31. Estimated selection for distance to ice roads by caribou of the Teshekpuk Herd based on an integrated step-selection analysis of winter movements (December–April). Positive slopes indicate movement away from ice roads and negative slopes indicate movement towards ice roads.

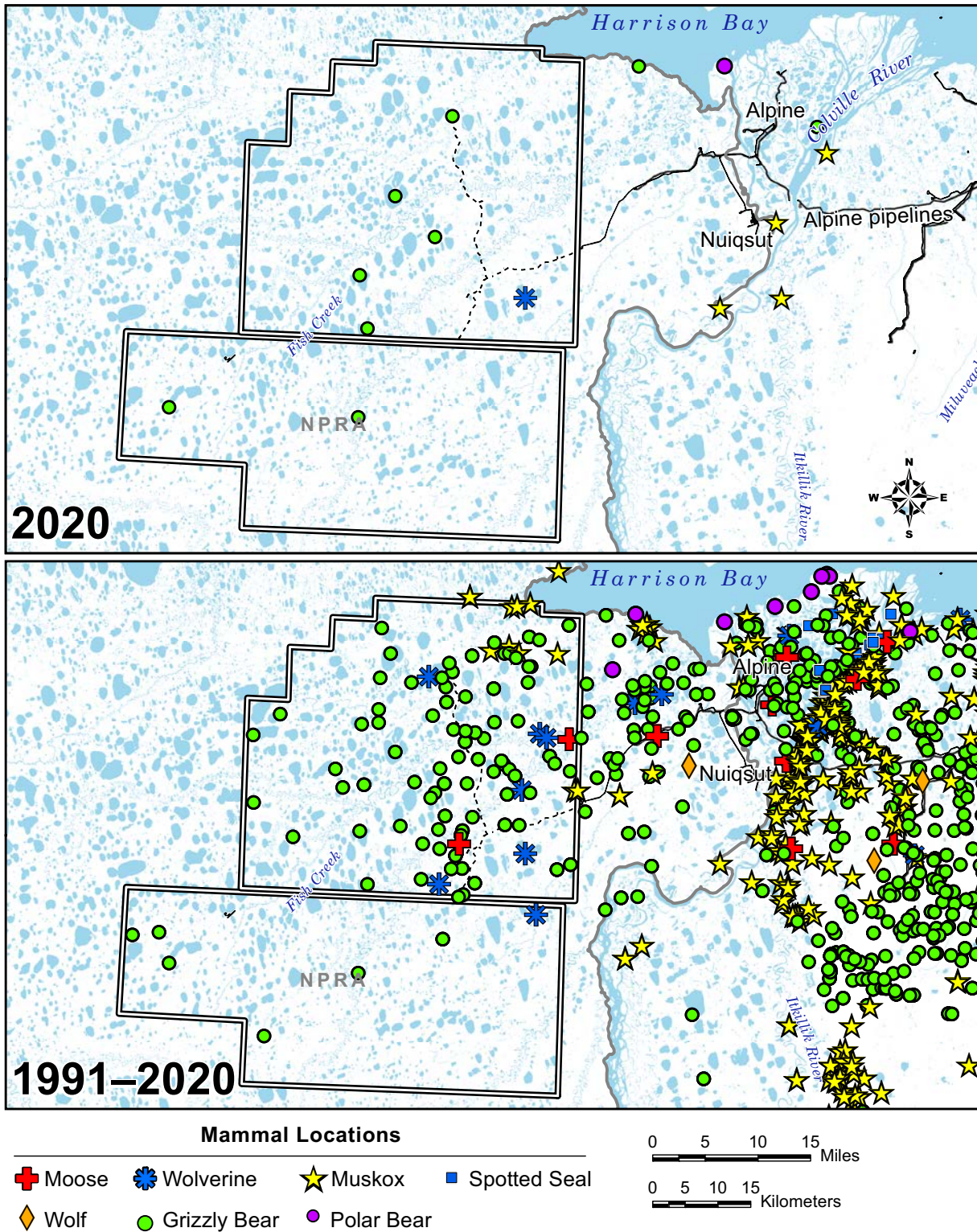


Figure 32. Distribution of other large mammals observed during aerial and ground surveys in the Bear Tooth Unit Area during 2020 and 1991–2020.

upwind and toward the coast in response to mosquito harassment and then disperse inland when mosquito activity abates in response to cooler temperatures and increased winds (Murphy and Lawhead 2000, Yokel et al. 2009, Wilson et al. 2012).

The absence of mosquitoes during mid-to late June likely led to improved caribou body condition after calving. The low number of days expected to have high insect harassment in mid-summer, were also likely to lead to good foraging conditions, and low energetic costs. Cool conditions in late summer and delayed onset of seasonal snow cover due to high temperatures in September (typical of recent years on the coastal plain; Cox et al. 2017) may have allowed caribou to increase their forage rate and improve their body condition prior to the onset of winter, although forage quality is greatly diminished in the fall compared to the summer (Gustine et al. 2017, Johnson et al. 2018).

CARIBOU DISTRIBUTION AND MOVEMENTS

Analysis of GPS, satellite, and VHF telemetry data sets spanning nearly three decades clearly demonstrates that the study area is in the eastern portion of the annual range of the TCH, and west of the annual range of the CAH. Use of the BTN and BTS survey areas by CAH caribou is usually very low, although several notable incursions have been recorded sporadically over the years. A few collared CAH females have switched to the TCH or calved west of the Colville River in isolated years (notably 2001), but it is a rare occurrence (Arthur and Del Vecchio 2009; Lenart 2009, 2015a; Prichard 2020b).

The TCH consistently uses the BTN and BTS survey areas to some extent during all seasons of the year. Most females overwinter primarily on the coastal plain whereas a disproportionately high number of males migrate south into the foothills and mountains of the Brooks Range to winter. Most TCH females calve near Teshekpuk Lake, northwest of the BTN and BTS survey areas (Kelleyhouse 2001, Carroll et al. 2005, Person et al. 2007, Wilson et al. 2012, Parrett 2015a, Prichard et al. 2019a). Males that wintered in the Brooks Range usually arrive on the coastal plain in June. When mosquito harassment begins in late

June or early July, caribou move toward the coast where lower temperatures and higher wind speeds prevail (Murphy and Lawhead 2000, Parrett 2007, Yokel et al. 2009, Wilson et al. 2012). The TCH uses the area between Teshekpuk Lake and the Beaufort Sea for their primary mosquito-relief habitat. After oestrid fly harassment begins in mid-July, the large groups that formed in response to mosquito harassment begin to break up and caribou disperse inland, seeking elevated or barren habitats such as sand dunes, mudflats, and river bars, with some using gravel roads and shaded locations in the oilfields under elevated pipelines and buildings (Lawhead 1988, Murphy and Lawhead 2000, Wilson et al. 2012, Prichard et al. 2020a).

In 2020, caribou density was moderate to high during the mid-winter survey on 25–26 February, with significantly more caribou located further inland in the BTS survey area. This was the first time that we have attempted an aerial survey in February, and we observed over 2,000 caribou in both survey areas combined, the highest total number for any survey in 2020. During winter, most of the TCH animals that remain on the coastal plain are widely distributed between Nuiqsut and Wainwright with high annual variation in distribution in and near the survey areas. These mid-winter surveys will provide valuable information about mid-winter caribou distributions in relation to exploration activities, ice roads, and existing infrastructure as development progresses west into areas that are more heavily used during winter.

Density was moderately high in both survey areas during the calving survey, but during the June postcalving survey, densities decreased in the BTS survey area and increased in the BTN survey area, particularly the western portion of the BTN survey area, as females and males move north towards Teshekpuk Lake and the Beaufort Sea coast in anticipation of mosquito emergence. Transect surveys during the mosquito season are inefficient for describing caribou habitat use because caribou are typically aggregated in large groups and moving rapidly (Prichard et al. 2014), so variability within a survey area is very high. Caribou density during the oestrid fly surveys on 28 July was low in the BTN and moderately high in the BTS survey areas, as the majority of the herd moved inland

after the mosquito season. Densities decreased into the late summer season as caribou dispersed after insect harassment was predicted to have abated. During the fall migration season, densities decreased again in the BTN survey area and increased in the BTS survey area when large numbers of caribou migrated into or through the BTS survey area on their way to the south.

Compared to results from surveys in the BTN and BTS survey areas in 2018 and 2019, the densities in the area in 2020 were relatively high, indicating a shift in distribution towards the east compared to the previous 2 years. The only other surveys with densities higher than 1.0 caribou/km² were during the 2019 BTN and BTS fall migration surveys and 2019 BTN postcalving surveys (Prichard et al. 2020c). However, periodic shifts in distribution are common and moderately high densities have been recorded sporadically in the eastern NPRA in late winter (2.4 caribou/km² in April 2003) and the postcalving season (1.5 caribou/km² in late June 2001). These surveys on the eastern NPRA pre-dated the creation of the BTN and BTS survey areas (Burgess et al. 2002, Johnson et al. 2004, Lawhead et al. 2010).

The area near proposed Willow infrastructure is used more often than the area near existing and proposed ASDP and GMT infrastructure. Few crossings of the new GMT1/MT6 or GMT2/MT7 road alignments (constructed during the winters of 2017–2018 and 2018–2019 respectively) have occurred by collared caribou since 2004 (Prichard et al. 2018b, 2019c, 2020d, Welch et al. 2021). Approximately 14% of collared caribou crossed the proposed Willow alignment at least once during fall migration in a typical year (Table 3).

The harvest of caribou by Nuiqsut hunters tends to peak during the months of July and August, with lower numbers of caribou usually being taken in June and September–October and the smallest amount of harvest occurring in other months (Pedersen 1995, Brower and Opie 1997, Fuller and George 1997, Braem et al. 2011, SRB&A 2017). Using harvest data (Braem et al. 2011) and telemetry data from 2003–2007, Parrett (2013) estimated that TCH caribou comprised 86% of the total annual harvest by Nuiqsut hunters during those years. The construction of the Nuiqsut Spur Road, constructed during the winter of

2014–2015, and CD-5 access road, constructed during the winter of 2013–2014 resulted in increased use of those roads for subsistence harvest of caribou (SRB&A 2017) and the new GMT1/MT6 and GMT2/MT7 roads and the proposed Willow roads are likely to increase subsistence hunter access to seasonal ranges used consistently year-round by TCH caribou.

SPECIES DISTRIBUTION MODEL

We chose to use a machine learning approach to model caribou distributions and habitat associations in 2020 because caribou resource selection is likely complex and difficult to predict; the highly flexible machine learning approach that can model nonlinear relationships and variable interactions may be more effective at capturing that complexity. Maxent builds flexible models with combinations of variables, variable transformations, and multiple variable interactions, including correlated variables, to find the best model for predicting a species' distribution (Phillips et al. 2006, 2017, Elith et al. 2011, Merow et al. 2013). Maxent can produce maps with high predictive power, but interpretation of variable importance and influence becomes more difficult, if not impossible, as model complexity increases (Phillips et al. 2006, Phillips 2017). For this reason, we reduced the number of variables included by using only the spatial scale for each variable with the greatest difference between used and random locations and by eliminating variables highly correlated with other variables.

Response curves are provided by the program, but these are generalizations of how each variable affects modeled suitability (Phillips 2017) and are dependent on the relationships between not only the predictor and the response, but correlations with other variables. Variables with no causal relationship with caribou selection may be correlated with important variables in the model or with a different variable that was not included in the model which is actually driving the relationship. Maxent may then assign importance to the non-important variable, or split importance among correlated variables depending on the path the model takes to arrive at the optimal solution. The model can produce very similar and accurate predictions even if different variable combinations,

percent contributions, or responses are used (Phillips 2017). Therefore, Maxent is generally more suited towards modeling a predictive space rather than identifying causal relationships and care must be taken in interpreting the importance and modeled relationship of each variable.

The two data sets (aerial transect surveys and radio telemetry) that were combined for the Maxent analysis provided complementary information for investigating broad patterns of resource selection. Telemetry data have higher spatial accuracy than aerial survey data and are collected continuously throughout the year, albeit for a fairly small sample of individual caribou, mostly females. A single collared caribou that spends long periods of time within the study area can exert a large influence on distribution analysis. Because of the high variability in the amount of time spent in the study area by collared animals, we did not attempt to adjust for individual differences, other than limiting the frequency of locations in the analytical data set to one every 48 hours. In contrast, aerial transect survey data provide information on all caribou groups detected in the area (subject to sightability constraints) at the time of each survey, but the locations have lower spatial accuracy (~100 m) and surveys are conducted only periodically throughout the year. The lower spatial accuracy of aerial survey data was accommodated by using the mean proportion of habitats at spatial scales starting at 120m rather than the habitat types in individual 30-m pixels. Additionally, calculating mean proportions of habitat and other variables at multiple spatial scales allows evaluation of scale dependencies.

The two different data types also had different timing, especially during the winter season; only one aerial survey was conducted in that season in any given year (in mid-late April from 2002–2019 and in February 2020 for the BTS and BTN survey areas only), whereas telemetry locations were collected throughout the entire season. Despite these potential limitations, the combination of the two survey methods produced larger samples than were available for either data set alone and the resulting SDMs are broadly interpretable within the context of general patterns of caribou distributions on the central coastal plain.

Based on the guidelines on Hosmer and Lemeshow (2000), our mosquito season model performed excellently, our oestrid fly and spring migration models were adequate, and our winter, calving, postcalving, late summer, and fall migration models were below adequate, although better than a random model despite our large sample sizes collected over many years. This low ability to predict suitability during some seasons was not entirely unexpected. Caribou are not highly selective of specific landscape features like some species like mountain goats. As a highly mobile migratory species, caribou range over a wide array of habitats and forage on a variety of plants. The lower AUC values most likely reflect the generalist habitats or non-selective movement patterns during some seasons.

Use of the aerial survey areas by caribou varies widely among seasons. These differences are related to west-to-east and distance to coast distributions, distribution of habitat types, topography, snow cover, and forage availability. In general, broad geographic patterns in distribution (west-to-east, distance to coast) were the strongest predictors of caribou distribution in almost every season, due in large part to the seasonal distribution patterns during key life cycle stages, but other factors such as topography and habitat proportions were also important seasonally. The important variables were like those identified with our RSF models (Prichard et al. 2020c, 2020d). The flexible modeling framework of the Maxent, however, provides for better predictions and maps that more closely reflect where caribou have been recorded.

Because the survey areas are on the eastern edge of the TCH range, a natural west-to-east gradient of decreasing density occurs throughout much of the year. During calving, the highest densities of TCH females typically calve near Teshekpuk Lake outside of the study area (Person et al. 2007, Wilson et al. 2012, Parrett 2015a). The past 3 years of aerial survey data in the BTN and BTS survey areas, as well as previous years of surveys in the GMT survey area, suggest limited calving activity in survey areas. Therefore, our suitability results for the calving season likely reflect the distribution of non-parturient females and males, many of which are migrating north from the Brooks Range towards Teshekpuk Lake.

These migrations can last well into the postcalving season. Migrating caribou often cross the Colville River at Ocean Point and enter our study area near the southwest portion of GMT2/MT7.

During most seasons, the model was improved with some variable of topographic relief which tends to be higher along or adjacent to streams and creeks or lakes in the study area. Different studies have reported conflicting conclusions regarding the importance of topography, which may be related in part to the ways in which it has been calculated. Nellemann and Thomsen (1994) and Nellemann and Cameron (1996) reported that CAH caribou selected areas of greater terrain ruggedness (as calculated by hand from topographic maps) in the Milne Point calving concentration area, but Wolfe (2000) and Lawhead et al. (2004), using a digital method of calculating terrain ruggedness, found no consistent relationship with terrain ruggedness in a larger calving area used by CAH females during calving. We used a number of different topographic relief metrics because the flexible nature of machine learning algorithms allows inclusion of many variables and the model determines which variable(s) are the best predictors of caribou occurrence. However, because of the inherent similarities of the topographic relief variables and because the Maxent model often calculates models that perform similarly well using a combination of variables, many of the topographic relief variables could be interchangeable. For example, the oestrid fly season model used a combination of riverine habitat, aspect, and ruggedness to highlight the importance of streams as good insect relief habitat. Had ruggedness and aspect not been included in the model, Maxent may have arrived at a very similar model using, for example, greater contributions from local elevational difference and topographic position index. However, by including more variables, Maxent can create a map that likely has higher power for predicting suitability.

The avoidance of *Carex aquatilis*, Flooded Tundra, and Wet Tundra during fall and winter has been documented in previous years using different analyses (Lawhead et al. 2015, Prichard et al. 2020c, 2020d), as well as selection of areas along Fish and Judy creeks during the postcalving, oestrid fly, and late summer seasons and avoidance of riverine habitat during winter. The riparian

habitats along Fish and Judy creeks provide a complex interspersed of barren ground, dunes, and sparse vegetation that provide good oestrid fly-relief habitat near foraging areas (Nellemann and Thomsen 1994, Nellemann and Cameron 1996). Moss habitats are relatively rare on the landscape but are found primarily on the slopes adjacent to creeks and streams, an important area during the spring migration season.

Comparison of caribou habitat use across studies is complicated by the fact that different investigators have used different habitat classifications. Kelleyhouse (2001) and Parrett (2007) reported that TCH caribou selected wet graminoid vegetation during calving and Wolfe (2000) reported that CAH caribou selected wet graminoid or moist graminoid classes; those studies used the vegetation classification by Muller et al. (1998, 1999). Using a habitat classification similar to the one developed by Jorgenson et al. (2003), Lawhead et al. (2004) found that CAH caribou in the Meltwater study area in the southwestern Kuparuk oilfield and the adjacent area of concentrated calving selected Moist Sedge–Shrub Tundra, the most abundant type in their study area, during calving. Wilson et al. (2012) used TCH telemetry data and the habitat classification of BLM and Ducks Unlimited (2002), as in this study, to investigate summer habitat selection at two different spatial scales, and concluded that TCH caribou consistently selected sedge/grass meadow and avoided flooded vegetation. Prichard et al. (2020a) found that CAH caribou avoided *Carex aquatilis* and wet sedge and selected riparian areas during the oestrid fly season. In general, we also found that caribou appear to avoid wetter habitats (flooded tundra, *Carex aquatilis*) during most seasons.

We used NDVI to estimate vegetative biomass in this study because other researchers have reported significant relationships between caribou distribution and biomass variables (NDVI_Calving, NDVI_621, and NDVI_Rate) during the calving period (Wolfe 2000, Griffith et al. 2002, Kelleyhouse 2001). The first flush of new vegetative growth that occurs in spring among melting patches of snow is valuable to foraging caribou (Kuropat 1984, Klein 1990, Johnstone et al. 2002), but the spectral signal of snow, ice, and standing water complicates NDVI-based

inferences in patchy snow and recently melted areas. Snow, water, and lake ice all depress NDVI values. Therefore, estimates of NDVI variables change rapidly as snow melts and exposes standing dead biomass, which has positive NDVI values (Sellers 1985 [cited in Hope et al. 1993], Stow et al. 2004), and the initial flush of new growth begins to appear.

Johnson et al. (2018) used NDVI values as well as habitat type, distance to coast, and days from peak NDVI to develop models to predict biomass, nitrogen, and digestible energy for a given location on a given day. These models should, if successful, provide metrics that are more directly related to caribou forage needs than NDVI alone. In our Maxent models, however, biomass and nitrogen were generally not useful for predicting suitability. We did find evidence of a slight selection for areas that typically have higher biomass during the calving season, but permutation importance was never >5.2% in any season and the response curves were highly variable throughout the growing season. Similar to NDVI, these relationships may have had more to do with habitat associations and distributional shifts due to insect avoidance. These results suggest that these derived values may not be good predictors of caribou distribution in this area and at this scale of selection.

It is possible that these models do not predict biomass and nitrogen well in this area. Johnson et al. (2018) used a land cover map (Boggs et al. 2016) that was derived from a map created by Ducks Unlimited for the North Slope Science Initiative (NSSI 2013). That map has discontinuities in classification methodology and imagery used that could translate into inaccurate forage metrics in our analysis area. Alternatively, caribou may not be selecting for forage nitrogen or forage biomass at this scale of selection and caribou distribution may be better predicted by high NDVI values which tend to be correlated with locations that have both large amounts of vegetation and less surface water in the pixel. Caribou movements are influenced by many factors other than forage and only a portion of GPS locations represent caribou that are actively feeding. It does not appear that our study area is heavily used by calving caribou and the study area likely has many non-parturient and migrating

caribou present during this season. A demographically diverse local population could complicate modeling efforts, especially when one demographic is likely moving long distances and possibly not exhibiting highly selective behavior.

In this study, we found evidence that suitability in the winter and spring was consistent at low and moderate SWE levels but then dropped off quickly at higher levels, indicating an avoidance of deep snow. During the calving season, suitability increased as the median date of snowmelt increased, indicating selection for late melting areas which may have newly emergent vegetation. Previous studies have not produced consistent results concerning the calving distribution of northern Alaska caribou herds in relation to snow cover. Kelleyhouse (2001) concluded that TCH females selected areas of low snow cover during calving and Carroll et al. (2005) reported that TCH caribou calved farther north in years of early snow melt. Wolfe (2000) did not find any consistent selection for snow-cover classes during calving by the CAH, whereas Eastland et al. (1989) and Griffith et al. (2002) reported that calving PCH caribou preferentially used areas with 25–75% snow cover.

Interpretation of analytical results is complicated by the fact that caribou do not require snow-free areas in which to calve and are able to find nutritious forage even in patchy snow cover. The presence of patchy snow in calving areas is associated with the emergence of highly nutritious new growth of forage species, such as tussock cottongrass (Kuopat 1984, Griffith et al. 2002, Johnstone et al. 2002), and it also may increase dispersion of caribou and create a complex visual pattern that reduces predation (Bergerud and Page 1987, Eastland et al. 1989). Interpretation also is complicated by high annual variability in the extent of snow cover and the timing of snowmelt among years, as well as by variability in detection of snowmelt dates on satellite imagery because of cloud cover.

The current emphasis of this study is to compile predevelopment baseline data on caribou density and movements in relation to the proposed Willow developments. Detailed analyses of the existing patterns of seasonal distribution, density, and movements are providing important insights about the ways in which caribou currently use the

study area. Although both the TCH and CAH recently underwent sharp declines in population due to decreased survival of both adults and calves, particularly after the prolonged winter of 2012–2013, both herds increased in size in the latest counts from July 2017 (TCH) and July 2019 (CAH). In recent years, the TCH calving distribution has expanded both to the west and the southeast, whereas the winter distribution has varied widely among years (Parrett 2013, Prichard et al. 2019a).

We continue to compile data on caribou movements in the BTU area prior to road construction and assess distribution near the recently constructed roads in the GMT area (Welch et al. 2021) in order to understand pre-construction movements and possible impacts of road construction in the Willow Development. Seasonal patterns of movements can vary widely among years and the GMT area is near the eastern edge of the TCH range, but there was some preliminary indication of less use of areas near the roads during some seasons. We caution that these results should be considered preliminary. Because of the large annual variability in movements, multiple years of data are required to understand large spatial changes. The distribution of TCH caribou during fall migration, winter, and spring migration were influenced by the proportion of caribou wintering in the Brooks Range, which varied annually. Previous research on the CAH has found that caribou do avoid active roads and pads during the calving season (Cameron et al. 1989, Lawhead et al. 2004, Johnson et al. 2020, Prichard et al. 2020a), but this avoidance declines following calving (Smith et al. 1994, Lawhead et al. 2004, Johnson et al. 2020, Prichard et al. 2020a). Some avoidance may occur within 1 km of roads during the mosquito season (Johnson et al. 2020), although caribou cross roads frequently during that season (Prichard et al. 2020a). There is also evidence that impacts from development are largest right after construction and when caribou have had less previous exposure to infrastructure (Smith et al. 1994, Prichard et al. 2020a). Although it is unknown how quickly the degree of reactions to infrastructure decline in caribou, Smith et al. (1994) found some evidence of habituation to roads during mid-summer by the Central Arctic Herd within a decade of the first construction.

Caribou continued to avoid areas with high levels of traffic and maternal caribou continued to avoid areas of human activity during calving.

DISTRIBUTION NEAR ICE ROADS

The iSSA analysis indicated that caribou tended to select sedge/grass meadows and tussock tundra land cover classes and avoid riverine, water, and wet tundra classes relative to the reference class dwarf/low shrub tundra during winter. This is generally consistent with the Maxent analysis as well as other studies conducted for other seasons or areas (Wilson et al. 2012, Prichard et al. 2020a). Caribou also selected areas of high elevation, areas with high NDVI, and areas of high TPI. This could indicate selection for areas with more forage and/or lower snow depths. Areas with high TPI are likely to have more wind scouring and shallower snow. The selection for higher elevations could reflect additional selection for shallow snow not captured by TPI, selection for higher areas with better visibility to spot predators, or just indicate selection for areas farther inland.

It is unclear why there appeared to be avoidance of areas near the ice roads in 2018–2019 but not in 2019–2020. This could be related to the different location of ice roads (ice roads were located farther south in 2019–2020), different activity levels on ice roads, different motivation levels of caribou, or caribou could potentially have been more habituated to ice roads during 2019–2020. Assessing road avoidance in caribou can be somewhat complex because it depends on both the level of risk caribou associate with areas near roads as well as their degree of motivation to be near roads. During calving, female caribou and newborn calves are very vulnerable to predation and the perceived risk of being near roads and human activity is likely high. Caribou of the CAH have shown little indication of habituation to roads during the calving period even after about 40 years of exposure (Johnson et al. 2020, Prichard et al. 2020a), but there is more evidence of habituation to roads during other seasons (Smith et al. 1994, Prichard et al. 2020a, Prichard et al. *in press*). During the insect seasons, caribou calves are mobile, which decreases the perceived risk, and caribou are highly motivated to cross roads to reach the coast or use roads for oestrid fly relief.

Caribou of the CAH cross roads frequently during the insect seasons and some individuals will use roads and pads as oestrid fly relief (Pollard et al. 1996, Noel et al. 1998, Prichard et al. 2020a).

The northern coastal plain is largely in darkness during the winter months and the lights of drill pads and vehicle traffic are very visible from long distances. Caribou are also typically widely dispersed during this period and they move less than at any other time of year (Person et al. 2007, Prichard et al. 2014). Caribou may therefore have low motivation to use the areas near roads and ice roads unless there are especially favorable foraging conditions nearby. The perceived risk may also be low but could depend on the activity level and amount of hunting associated with the ice road.

OTHER MAMMALS

In 2020, a few sightings of grizzly bears and a single sighting of a wolverine comprised all the other mammal sightings in the BTU area. Bears are relatively commonly observed during surveys, while wolverine are observed far less frequently. Only 7 observations (6 singles, 1 pair) of wolverines have been recorded by ABR biologists in the region encompassing the BTU survey areas since 1993. Ten of those observations were near or west of the Colville River. Wolverines are found throughout the North Slope of Alaska but at low densities (Carroll 2013, Poley et al. 2018).

Muskoxen, which are more common to the east and are often found along the Colville River (Welch et al. 2021), have not been observed in the NPRA on ABR surveys since 2007. The muskox population on the North Slope of Alaska has declined since 1999, evidently due to a combination of predation by grizzly bears, human interactions, disease, and unusual mortality events such as drowning (Reynolds et al. 2002, Shideler et al. 2007, Lenart 2015b). The decline was noted first in the Arctic National Wildlife Refuge but later was documented farther west on the central coastal plain. Population surveys by ADFG in late winter (April) found 216 muskoxen in 2006. Since then, the population on the central North Slope has remained relatively stable at approximately 190–200 animals (Arthur and Del Vecchio 2017; Lenart 2015b). Predation by grizzly bears was the most common cause of death, responsible for an

estimated 58% of calf mortalities and 62% of adult mortalities when a cause of death could be determined (Arthur and Del Vecchio 2017).

CONCLUSION

The current emphasis of this study is to monitor caribou distribution and movements in relation to the proposed infrastructure in the BTN and BTS survey areas and to compile predevelopment baseline data on caribou density and movements. Detailed analyses of the existing patterns of seasonal distribution, density, and movements are providing important insights about the ways in which caribou currently use the study area and why. Although both the TCH and CAH recently underwent declines in population, possibly due to decreased survival of adults particularly after the prolonged winter of 2012–2013, both herds increased in size in the most recent counts. The TCH calving distribution has recently expanded to the west and the winter distribution has varied widely among years (Parrett 2013). The CAH has shown some changes in seasonal distribution, with more caribou remaining farther north during fall and early winter and more intermixing with adjacent herds (ADFG 2017, Prichard et al. 2020b).

For this report, we incorporated multiple types of data and several different analyses to better understand the seasonal distributions, movements, and habitat associations of caribou in the area. By conducting aerial surveys during different seasons over the course of 19 years in northeastern NPRA, we have compiled an extensive dataset that allows us to understand the seasonal patterns as well as the variability in caribou distribution over this specific area. The use of telemetry data provided high-resolution locations for a subset of caribou throughout the year. This large and growing database allows us to understand caribou movements through the area for the two different herds which use the area. It also allows us to put local caribou movements in the study area into the broader context of the annual herd ranges and seasonal herd distributions. Lastly, we incorporated aerial survey results and telemetry data with remote sensing information on land cover, vegetative biomass, forage nitrogen, and snow cover to better understand the factors determining

caribou seasonal distribution. This understanding of the underlying factors that are important to caribou will be useful when evaluating potential future changes in caribou distribution that may be attributable to development or a changing climate and in developing strategies or designs to minimize operational impacts on caribou.

LITERATURE CITED

- ADFG (Alaska Department of Fish and Game). 2017. Central Arctic caribou herd news. Winter 2016–17 edition. Alaska Department of Fish and Game, Division of Wildlife Conservation, Fairbanks, Alaska. 6 pp.
- Anderson, R. P., and I. Gonzalez Jr. 2011. Species-specific tuning increases robustness to sampling bias in models of species distributions: an implementation with Maxent. *Ecological Modeling* 222: 2796–2811.
- Arthur, S. M., and P. A. Del Vecchio. 2009. Effects of oil field development on calf production and survival in the Central Arctic Herd. Final research technical report, June 2001–March 2006. Federal Aid in Wildlife Restoration Project 3.46, Alaska Department of Fish and Game, Juneau, Alaska. 40 pp.
- Arthur, S. M., and P. A. Del Vecchio. 2017. Effects of grizzly bear predation on muskoxen in northeastern Alaska. *Ursus* 28: 81–91.
- Avgar, T., J. R. Potts, M. A. Lewis, and M. S. Boyce. 2016. Integrated step-selection analysis: Bridging the gap between resource selection and animal movement. *Methods in Ecology and Evolution* 7: 619–630.
- Bergerud, A. T., and R. E. Page. 1987. Displacement and dispersion of parturient caribou as antipredator tactics. *Canadian Journal of Zoology* 65: 1597–1606.
- Bieniek, P. A., U. S. Bhatt, J. E. Walsh, R. Lader, B. Griffith, J. K. Roach, and R. L. Thoman. 2018. Assessment of Alaska rain-on-snow events using dynamical downscaling. *Journal of Applied Meteorology and Climatology* 57: 1847–1863.
- BLM (Bureau of Land Management) and Ducks Unlimited. 2002. National Petroleum Reserve–Alaska earth-cover classification. U.S. Department of the Interior, BLM Alaska Technical Report 40, Anchorage, Alaska. 81 pp.
- Boggs, K., L. Flagstad, T. Boucher, T. Kuo, D. Fehringer, S. Guyer, and M. Aisu. 2016. *Vegetation Map and Classification: Northern, Western, and Interior Alaska*. Second edition. Alaska Center for Conservation Science, University of Alaska Anchorage, Anchorage, Alaska. 110 pp.
- Braem, N. M., S. Pedersen, J. Simon, D. Koster, T. Kaleak, P. Leavitt, J. Patkotak, and P. Neakok. 2011. Monitoring of annual caribou harvests in the National Petroleum Reserve in Alaska: Atqasuk, Barrow, and Nuiqsut, 2003–2007. Technical Paper No. 361, Alaska Department of Fish and Game, Division of Subsistence, Fairbanks, Alaska. 201 pp.
- Brower, H. K., and R. T. Opie. 1997. North Slope Borough subsistence harvest documentation project: data for Nuiqsut, Alaska, for the period July 1, 1994 to June 30, 1995. North Slope Borough Department of Wildlife Management, Barrow, Alaska.
- Brown, J., R. K. Haugen, and S. Parrish. 1975. Selected climatic and soil thermal characteristics of the Prudhoe Bay region. Pages 3–11 in J. Brown, editor. *Ecological investigations of the tundra biome in the Prudhoe Bay region, Alaska*. Biological Papers of the University of Alaska, Special Report No. 2, Fairbanks, Alaska.
- Burgess, R. M., C. B. Johnson, P. E. Seiser, A. A. Stickney, A. M. Wildman, and B. E. Lawhead. 2002. *Wildlife studies in the Northeast Planning Area of the National Petroleum Reserve–Alaska, 2001*. Report for Phillips Alaska, Inc., Anchorage, by ABR, Inc., Fairbanks, Alaska. 71 pp.
- Burnham, K. P., and D. R. Anderson. 2002. *Model Selection and Multimodel Inference: A Practical Information–Theoretic Approach*. 2nd edition. Springer–Verlag, New York City, New York. 488 pp.

- Cameron, R. D., W. T. Smith, and S. G. Fancy. 1989. Distribution and productivity of the Central Arctic Caribou Herd in relationship to petroleum development. Research progress report, Federal Aid in Wildlife Restoration Project 3.35, Alaska Department of Fish and Game, Juneau, Alaska. 52 pp.
- Cameron, R. D., W. T. Smith, S. G. Fancy, K. L. Gerhart, and R. G. White. 1993. Calving success of female caribou in relation to body weight. *Canadian Journal of Zoology* 71: 480–486.
- Cameron, R.D., W.T. Smith, R.G. White, and B. Griffith. 2005. Central Arctic caribou and petroleum development: distributional, nutritional and reproductive implications. *Arctic* 58: 1–9.
- Cao, Y., R.E. DeWalt, J. L. Robinson, T. Tweddale, L. Hinz, and M. Pessino. 2013. Using Maxent to model the historic distributions of stonefly species in Illinois streams: the effects of regularization and threshold selections. *Ecological Modelling*. 259: 30–39.
- Carroll, G. 2013. Unit 26A furbearer. Pages 355–363 in P. Harper, editor. Furbearer management report of survey and inventory activities 1 July 2009–30 June 2012. Alaska Department of Fish and Game, Species Management Report, ADF&G/DWC/SMR-2013-5, Juneau, Alaska.
- Carroll, G. M., L. S. Parrett, J. C. George, and D. A. Yokel. 2005. Calving distribution of the Teshekpuk caribou herd, 1994–2003. *Rangifer*, Special Issue 16: 27–35.
- CLS. 2016. Argos user's manual. CLS, Toulouse, France. Available online: <http://www.argos-system.org/manual/> (accessed 16 February 2018).
- Cox, C. J., R. S. Stone, D. C. Douglas, D. M. Stanitski, G. J. Divoky, G. S. Dutton, C. Sweeney, J. C. George, and D. U. Longenecker. 2017. Drivers and environmental responses to the changing annual snow cycle of northern Alaska. *Bulletin of the American Meteorological Society* 98: 2559–2577.
- Crookston N., and G. Rehfeldt. 2010. Degree-Days > 5 Degrees C (Based on Mean Monthly Temperature) Across All North America [raster digital data set]. U.S. Forest Service Rocky Mountain Research Station, Moscow Forestry Sciences Laboratory. Moscow, ID: <http://forest.moscowfsl.wsu.edu/climate/current/>.
- Dau, J. R. 1986. Distribution and behavior of barren-ground caribou in relation to weather and parasitic insects. M.S. thesis, University of Alaska, Fairbanks, Alaska. 149 pp.
- Dau, J. 2005. Two caribou mortality events in northwestern Alaska: possible causes and management implications. *Rangifer*, Special Issue 16: 37–50.
- Dick, B. L., S. L. Findholt, and B. K. Johnson. 2013. A self-adjusting expandable GPS collar for male elk. *Journal of Wildlife Management* 37: 887–892.
- Duong, T. 2017. *ks*: Kernel Smoothing. R package version 1.10.7. Available online: <https://CRAN.R-project.org/package=ks> (accessed 16 February 2018).
- Dunk, J. R., B. Woodbridge, T. M. Lickfett, G. Bedrosian, B. R. Noon, D. W. LaPlante, J. L. Brown, and J. D. Tack. 2019. Modelling spatial variation in density of golden eagle nest sites in the western United States. *PLoS ONE* 14(9). e0223143. <https://doi.org/10.1371/journal.pone.0223143>
- Eastland, W. G., R. T. Bowyer, and S. G. Fancy. 1989. Caribou calving sites relative to snow cover. *Journal of Mammalogy* 70: 824–828.
- Elith, J., C. H. Graham, R. P. Anderson, et al., 2006. Novel methods improve prediction of species' distributions from occurrence data. *Ecography*. 29: 129–151.
- Elith, J., S. J. Phillips, T. Hastie, M. Dudik, Y. E. Chee, and C. J. Yates. 2011. A statistical explanation of MaxEnt for ecologists. *Diversity and Distributions* 17: 43–57.
- Fancy, S. G. 1983. Movements and activity budgets of caribou near oil drilling sites in the Sagavanirktok River floodplain, Alaska. *Arctic* 36: 193–197.

- Fancy, S. G. 1986. Daily energy budgets of caribou: a simulation approach. Ph.D. dissertation, University of Alaska, Fairbanks, Alaska. 226 pp.
- Fancy, S. G., and R. G. White. 1985. Energy expenditure by caribou while cratering in snow. *Journal of Wildlife Management* 49: 987–993.
- Fancy, S. G., K. R. Whitten, N. E. Walsh, and R. D. Cameron. 1992. Population dynamics and demographics of caribou in developed and undeveloped areas of the Arctic Coastal Plain. Pages 1–21 in T. R. McCabe, D. B. Griffith, N. E. Walsh, and D. D. Young, editors. *Terrestrial research: 1002 Area, Arctic National Wildlife Refuge*. Interim report, 1988–1990. U.S. Fish and Wildlife Service, Anchorage, Alaska.
- Finstad, G. L., and A. K. Prichard. 2000. Climatic influence on forage quality, growth, and reproduction of reindeer on the Seward Peninsula, II: Reindeer growth and reproduction. *Rangifer*, Special Issue 12: 144.
- Fithian, W., J. Elith, T. Hastie, and D. A. Keith. 2015. Bias correction in species distribution models: pooling survey and collection data for multiple species. *Methods in Ecology and Evolution* 6: 424–438.
- Forester, J. D., H. K. Im, and P. J. Rathouz. 2009. Accounting for animal movement in estimation of resource selection functions: Sampling and data analysis. *Ecology* 90: 3554–3565.
- Fortin, D., H. L. Beyer, M. S. Boyce, D. W. Smith, T. Duchesne, and J. S. Mao. 2005. Wolves influence elk movements: behavior shapes a trophic cascade in Yellowstone National Park. *Ecology* 86: 1320–1330.
- Fuller, A. S., and J. C. George. 1997. Evaluation of subsistence harvest data from the North Slope Borough 1993 census for eight North Slope villages for calendar year 1992. North Slope Borough Department of Wildlife Management, Barrow, Alaska.
- Galante, P. J., B. Alade, R. Muscarella, S. A. Jansa, S. M. Goodman, and R. P. Anderson. 2018. The challenge of modeling niches and distributions for data-poor species: a comprehensive approach to model complexity. *Ecography*. 41: 726–736.
- Gasaway, W. C., S. D. DuBois, D. J. Reed, and S. J. Harbo. 1986. Estimating moose population parameters from aerial surveys. *Biological Papers of the University of Alaska*, No. 22, Fairbanks, Alaska. 108 pp.
- Gorelick, N., M. Hancher, M. Dixon, S. Ilyushchenko, D. Thau, and R. Moore. 2017. Google Earth Engine: planetary-scale geospatial analysis for everyone. *Remote Sensing of Environment* 202: 18–27.
- Gustine, D., P. Barboza, L. Adams, B. Griffith, R. Cameron, and K. Whitten. 2017. Advancing the match-mismatch framework for large herbivores in the Arctic: Evaluating the evidence for a trophic mismatch in caribou. *PLoS ONE* 12(2): e0171807. doi:10.1371/journal.pone.0171807
- Griffith, D. B., D. C. Douglas, N. E. Walsh, D. D. Young, T. R. McCabe, D. E. Russell, R. G. White, R. D. Cameron, and K. R. Whitten. 2002. Section 3: The Porcupine caribou herd. Pages 8–37 in D. C. Douglas, P. E. Reynolds, and E. B. Rhode, editors. *Arctic Refuge coastal plain terrestrial wildlife research summaries*. U.S. Geological Survey, Biological Resources Division, Biological Science Report USGS/BRD/BSR-2002-0001.
- Hijmans, R. J. (2020). raster: Geographic Data Analysis and Modeling. R package version 3.3-13. <https://CRAN.R-project.org/package=raster>
- Hope, A. S., J. S. Kimball, and D. A. Stow. 1993. The relationship between tussock tundra spectral properties and biomass and vegetation composition. *International Journal of Remote Sensing* 14: 1861–1874.
- Horne, J. S., E. O. Garton, S. M. Krone, and J. S. Lewis. 2007. Analyzing animal movements using Brownian bridges. *Ecology* 88: 2354–2363.

- Hosmer, D. S., and S. Lemeshow. 2000. Applied Logistic Regression, 2nd Ed. Chapter 5, John Wiley and Sons, New York, NY. 160–164.
- Jenness J., B. Brost, and P. Beier. 2013. Land Facet Corridor Designer: Extension for ArcGIS. Flagstaff, AZ: Jenness Enterprises. http://www.jennessent.com/arcgis/land_facets.htm.
- Jensen, P. G., and L. E. Noel. 2002. Caribou distribution in the northeast National Petroleum Reserve–Alaska, summer 2001. Chapter 3 in M. A. Cronin, editor. Arctic Coastal Plain caribou distribution, summer 2001. Report for BP Exploration (Alaska) Inc., Anchorage, by LGL Alaska Research Associates, Inc., Anchorage, Alaska.
- Johnson, C. B., R. M. Burgess, A. M. Wildman, A. A. Stickney, P. E. Seiser, B. E. Lawhead, T. J. Mabee, J. R. Rose, and J. E. Shook. 2004. Wildlife studies for the Alpine Satellite Development Project, 2003. Annual report for ConocoPhillips Alaska, Inc., and Anadarko Petroleum Corp., Anchorage, by ABR, Inc., Fairbanks, Alaska. 155 pp.
- Johnson, C. B., J. P. Parrett, T. Obritschkewitsch, J. R. Rose, K. B. Rozell, and P. E. Seiser. 2015. Avian studies for the Alpine Satellite Development Project, 2014. 12th annual report for ConocoPhillips Alaska, Inc., and Anadarko Petroleum Corp., Anchorage, by ABR, Inc., Fairbanks, Alaska. 124 pp.
- Johnson, H. E., T. S. Golden, L. G. Adams, D. D. Gustine, and E. A. Lenart. 2020. Caribou use of habitat near energy development in Arctic Alaska. *Journal of Wildlife Management* 84: 401–412.
- Johnson, H. E., D. D. Gustine, T. S. Golden, L. G. Adams, L. S. Parrett, E. A. Lenart, P. S. Barboza. 2018. NDVI exhibits mixed success in predicting spatiotemporal variation in caribou summer forage quality and quantity. *Ecosphere* 9: 10.
- Johnstone, J., D. E. Russell, and D. B. Griffith. 2002. Variations in plant forage quality in the range of the Porcupine caribou herd. *Rangifer* 22: 83–91.
- Jorgenson, M. T., J. E. Roth, E. R. Pullman, R. M. Burgess, M. Reynolds, A. A. Stickney, M. D. Smith, and T. Zimmer. 1997. An ecological land survey for the Colville River delta, Alaska, 1996. Report for ARCO Alaska, Inc., Anchorage, by ABR, Inc., Fairbanks, Alaska. 160 pp.
- Jorgenson, M. T., J. E. Roth, M. Emers, S. Schlentner, D. K. Swanson, E. R. Pullman, J. Mitchell, and A. A. Stickney. 2003. An ecological land survey for the Northeast Planning Area of the National Petroleum Reserve–Alaska, 2002. Report for ConocoPhillips Alaska, Inc., Anchorage, by ABR, Inc., Fairbanks, Alaska. 84 pp.
- Jorgenson, M. T., J. E. Roth, M. Emers, W. Davis, E. R. Pullman, and G. V. Frost. 2004. An ecological land survey for the Northeast Planning Area of the National Petroleum Reserve–Alaska, 2003. Addendum to 2002 report for ConocoPhillips Alaska, Inc., and Anadarko Petroleum Corporation, Anchorage, by ABR, Inc., Fairbanks, Alaska. 40 pp.
- Kelleyhouse, R. A. 2001. Calving-ground selection and fidelity: Teshekpuk Lake and Western Arctic herds. M.S. thesis, University of Alaska, Fairbanks, Alaska. 124 pp.
- Klein, D. R. 1990. Variation in quality of caribou and reindeer forage plants associated with season, plant part, and phenology. *Rangifer*, Special Issue 3: 123–130.
- Klimstra, R. 2018. Summary of Teshekpuk caribou herd photocensus conducted July 14, 2017. State of Alaska memorandum, Department of Fish and Game, Division of Wildlife Conservation (Northwest), Fairbanks, Alaska. 6 pp.
- Kranstauber, B., K. Safi, and F. Bartumeus. 2014. Bivariate Gaussian bridges: directional factorization of diffusion in Brownian bridge models. *Movement Ecology* 2: 5. doi.org/10.1186/2051-3933-2-5.

- Kranstauber, B., M. Smolla, and A.K. Scharf. 2017. *Move*: visualizing and analyzing animal track data. R package version 3.0.1. Available online: <https://CRAN.R-project.org/package=move> (accessed 16 February 2018).
- Kuropat, P. J. 1984. Foraging behavior of caribou on a calving ground in northwestern Alaska. M.S. thesis, University of Alaska, Fairbanks, Alaska. 95 pp.
- Lair, H. 1987. Estimating the location of the focal center in red squirrel home ranges. *Ecology* 68: 1092–1101.
- Lawhead, B. E. 1988. Distribution and movements of Central Arctic Herd caribou during the calving and insect seasons. Pages 8–13 *in* R. Cameron and J. Davis, editors. Reproduction and calf survival. Proceedings of the 3rd North American Caribou Workshop. Wildlife Technical Bulletin No. 8, Alaska Department of Fish and Game, Juneau, Alaska.
- Lawhead, B. E., J. P. Parrett, A. K. Prichard, and D. A. Yokel. 2006. A literature review and synthesis on the effect of pipeline height on caribou crossing success. BLM Alaska Open File Report 106, U.S. Department of the Interior, Bureau of Land Management, Fairbanks, Alaska, USA.
- Lawhead, B. E., A. K. Prichard, and M. J. Macander. 2006. Caribou monitoring study for the Alpine Satellite Development Program, 2005. First annual report for ConocoPhillips Alaska, Inc., Anchorage, by ABR, Inc., Fairbanks, Alaska. 102 pp.
- Lawhead, B. E., A. K. Prichard, and M. J. Macander. 2007. Caribou monitoring study for the Alpine Satellite Development Program, 2006. Second annual report for ConocoPhillips Alaska, Inc., Anchorage, by ABR, Inc., Fairbanks, Alaska. 75 pp.
- Lawhead, B. E., A. K. Prichard, and M. J. Macander. 2008. Caribou monitoring study for the Alpine Satellite Development Program, 2007. Third annual report for ConocoPhillips Alaska, Inc., Anchorage, by ABR, Inc., Fairbanks, Alaska. 89 pp.
- Lawhead, B. E., A. K. Prichard, and M. J. Macander. 2009. Caribou monitoring study for the Alpine Satellite Development Program, 2008. Fourth annual report for ConocoPhillips Alaska, Inc., Anchorage, by ABR, Inc., Fairbanks, Alaska. 91 pp.
- Lawhead, B. E., A. K. Prichard, and M. J. Macander. 2010. Caribou monitoring study for the Alpine Satellite Development Program, 2009. Fifth annual report for ConocoPhillips Alaska, Inc., Anchorage, by ABR, Inc., Fairbanks, Alaska. 101 pp.
- Lawhead, B. E., A. K. Prichard, and M. J. Macander. 2011. Caribou monitoring study for the Alpine Satellite Development Program, 2010. Sixth annual report for ConocoPhillips Alaska, Inc., Anchorage, by ABR, Inc., Fairbanks, Alaska. 101 pp.
- Lawhead, B. E., A. K. Prichard, and M. J. Macander. 2012. Caribou monitoring study for the Alpine Satellite Development Program, 2011. Seventh annual report for ConocoPhillips Alaska, Inc., Anchorage, by ABR, Inc., Fairbanks, Alaska. 90 pp.
- Lawhead, B. E., A. K. Prichard, M. J. Macander, and J. H. Welch. 2013. Caribou monitoring study for the Alpine Satellite Development Program, 2012. Eighth annual report for ConocoPhillips Alaska, Inc., Anchorage, by ABR, Inc., Fairbanks, Alaska. 88 pp.
- Lawhead, B. E., A. K. Prichard, M. J. Macander, and J. H. Welch. 2014. Caribou monitoring study for the Alpine Satellite Development Program, 2013. Ninth annual report for ConocoPhillips Alaska, Inc., Anchorage, by ABR, Inc., Fairbanks, Alaska. 94 pp.
- Lawhead, B. E., A. K. Prichard, M. J. Macander, and J. H. Welch. 2015. Caribou monitoring study for the Alpine Satellite Development Program, 2014. Tenth annual report for ConocoPhillips Alaska, Inc., Anchorage, by ABR, Inc., Fairbanks, Alaska. 100 pp.

- Lenart, E. A. 2009. GMU 26B and 26C, Central Arctic Herd. Pages 299–325 in P. Harper, editor. Caribou management report of survey and inventory activities, 1 July 2006–30 June 2008. Federal Aid in Wildlife Restoration Project 3.0, Alaska Department of Fish and Game, Juneau, Alaska.
- Lenart, E. A. 2015a. Units 26B and 26C, Central Arctic. Chapter 18 in P. Harper and L. A. McCarthy, editors. Caribou management report of survey and inventory activities, 1 July 2012–30 June 2014. Alaska Department of Fish and Game, Species Management Report ADF&G/DWC/SMR-2015-4, Juneau, Alaska.
- Lenart, E.A. 2015b. Units 26B and 26C — Muskox. Chapter 4, pp. 4-1 through 4-26 in P. Harper and L. A. McCarthy, editors. Muskox management report of survey and inventory activities 1 July 2012–30 June 2014. Alaska Department of Fish and Game, Species Management Report ADF&G/DWC/SMR-2015-2, Juneau, Alaska.
- Lenart, E. A. 2017. 2016 Central Arctic caribou photocensus results. State of Alaska memorandum, Department of Fish and Game, Division of Wildlife Conservation, Fairbanks, Alaska. 5 pp.
- Lenart, E. A. 2019. 2019 Central Arctic caribou photocensus results. State of Alaska Memorandum. Alaska Department of Fish and Game, Division of Wildlife Conservation. Fairbanks, Alaska. 8 pp.
- Lenart, E. 2021. Central Arctic caribou management report and plan, Game Management Unit 26B: Report period 1 July 2012–30 June 2017, and plan period 1 July 2017–30 June 2022. Alaska Department of Fish and Game, Species Management Report and Plan ADF&G/DWC/SMR&P-2021-2, Juneau.
- Macander, M. J., C. S. Swingley, K. Joly, and M. K. Reynolds. 2015. Landsat-based snow persistence map for northwest Alaska. *Remote Sensing of Environment* 163: 23–31.
- McNay, R. S., J. A. Morgan, and F. L. Bunnell. 1994. Characterizing independence of observations in movements of Columbian black-tailed deer. *Journal of Wildlife Management* 58: 422–429.
- Merow, C., M. J. Smith, and J. A. Silander, Jr. 2013. A practical guide to MaxEnt for modeling species' distributions: what it does, and why inputs and settings matter. *Ecography* 36: 1058–1069.
- Mörschel, F. M. 1999. Use of climatic data to model the presence of oestrid flies in caribou herds. *Journal of Wildlife Management* 63: 588–593.
- Muller, S. V., D. A. Walker, F. E. Nelson, N. A. Auerbach, J. G. Bockheim, S. Guyer, and D. Sherba. 1998. Accuracy assessment of a land-cover map of the Kuparuk River basin, Alaska: considerations for remote regions. *Photogrammetric Engineering and Remote Sensing* 64: 619–628.
- Muller, S. V., A. E. Racoviteanu, and D. A. Walker. 1999. Landsat-MSS-derived land-cover map of northern Alaska: extrapolation methods and a comparison with photo-interpreted and AVHRR-derived maps. *International Journal of Remote Sensing* 20: 2921–2946.
- Murphy, S. M., and B. E. Lawhead. 2000. Caribou. Chapter 4, pages 59–84 in J. Truett and S. R. Johnson, editors. *The Natural History of an Arctic Oil Field: Development and the Biota*. Academic Press, San Diego, California.
- Naimi B., N. Hamm, T. A. Groen, A. K. Skidmore, and A. G. Toxopeus. 2014. Where is positional uncertainty a problem for species distribution modelling. *Ecography* 37: 191–203. doi:10.1111/j.1600-0587.2013.00205.x (URL:<https://doi.org/10.1111/j.1600-0587.2013.00205.x>).
- Nellemann, C., and R. D. Cameron. 1996. Effects of petroleum development on terrain preferences of calving caribou. *Arctic* 49: 23–28.

- Nellemann, C., and M. G. Thomsen. 1994. Terrain ruggedness and caribou forage availability during snowmelt on the Arctic Coastal Plain, Alaska. *Arctic* 47: 361–367.
- Nicholson, K. L., S. M. Arthur, J. S. Horne, E. O. Garton, and P. A. Del Vecchio. 2016. Modeling caribou movements: seasonal ranges and migration routes of the Central Arctic Herd. *PLoS One* 11(4): e0150333. doi:10.1371/journal.pone.0150333.
- Noel, L. E. 1999. Calving caribou distribution in the Teshekpuk Lake area, June 1998. Data report for BP Exploration (Alaska) Inc., Anchorage, by LGL Alaska Research Associates, Inc., Anchorage, Alaska. 31 pp.
- Noel, L. E. 2000. Calving caribou distribution in the Teshekpuk Lake area, June 1999. Report for BP Exploration (Alaska) Inc., Anchorage, by LGL Alaska Research Associates, Inc., Anchorage, Alaska. 29 pp.
- Noel, L. E., and J. C. George. 2003. Caribou distribution during calving in the northeast National Petroleum Reserve–Alaska, June 1998 to 2000. *Rangifer*, Special Issue 14: 283–292.
- Noel, L. E., R. H. Pollard, W. B. Ballard, and M. A. Cronin. 1998. Activity and use of active gravel pads and tundra by caribou, *Rangifer tarandus granti*, within the Prudhoe Bay oil field, Alaska. *Canadian Field-Naturalist* 112: 400–409.
- North Slope Science Initiative (NSSI). 2013. North Slope Science Initiative land-cover mapping summary report. Report for NSSI by Ducks Unlimited, Inc., Rancho Cordova, California. 51 pp. + maps.
- Parrett, L. S. 2007. Summer ecology of the Teshekpuk caribou herd. M.S. thesis, University of Alaska, Fairbanks, Alaska. 149 pp.
- Parrett, L. S. 2013. Unit 26A, Teshekpuk Caribou Herd. Pages 314–355 in P. Harper, editor. Caribou management report of survey and inventory activities, 1 July 2010–30 June 2012. Alaska Department of Fish and Game, Species Management Report ADF&G/DWC/SMR-2013-3, Juneau, Alaska.
- Parrett, L. S. 2015a. Unit 26A, Teshekpuk caribou herd. Chapter 17 in P. Harper and L. A. McCarthy, editors. Caribou management report of survey and inventory activities, 1 July 2012–30 June 2014. Alaska Department of Fish and Game, Species Management Report ADF&G/DWC/SMR-2015-4, Juneau, Alaska.
- Parrett, L. S. 2015b. Summary of Teshekpuk caribou herd photocensus conducted July 6, 2015. State of Alaska memorandum, Department of Fish and Game, Division of Wildlife Conservation (Northwest), Fairbanks, Alaska. 6 pp.
- Pebesma, E. J. 2004. Multivariate geostatistics in S: the *gstat* package. *Computers & Geosciences* 30: 683–691.
- Pedersen, S. 1995. Nuiqsut. Chapter 22 in J. A. Fall and C. J. Utermohle, editors. An investigation of the sociocultural consequences of Outer Continental Shelf development in Alaska, Vol. V: Alaska Peninsula and Arctic. Technical Report No. 160, OCS Study MMS 95-014, Minerals Management Service, Anchorage, Alaska.
- Pennycuik, C. J., and D. Western. 1972. An investigation of some sources of bias in aerial transect sampling of large mammal populations. *East African Wildlife Journal* 10: 175–191.
- Person, B. T., A. K. Prichard, G. M. Carroll, D. A. Yokel, R. S. Suydam, and J. C. George. 2007. Distribution and movements of the Teshekpuk caribou herd, 1990–2005: prior to oil and gas development. *Arctic* 60: 238–250.
- Philo, L. M., G. M. Carroll, and D. A. Yokel. 1993. Movements of caribou in the Teshekpuk Lake herd as determined by satellite tracking, 1990–1993. North Slope Borough Department

- of Wildlife Management, Barrow; Alaska Department of Fish and Game, Barrow; and U.S. Department of Interior, Bureau of Land Management, Fairbanks, Alaska. 60 pp.
- Phillips, S. J. 2017. A brief tutorial on Maxent. Available from: http://biodiversityinformatics.amnh.org/open_source/maxent/. Accessed on 15 June 2020.
- Phillips, S. J., R. P. Anderson, and R. E. Schapire. 2006. Maximum entropy modeling of species geographic distributions. *Ecological Modelling* 190: 231–259.
- Phillips, S. J., and M. Dudík. 2008. Modelling of species distributions with Maxent: new extensions and a comprehensive evaluation. *Oecography*. 31: 161–259
- Phillips S. J., M. Dudík, and R. E. Schapire. 2020. Maxent software for modeling species niches and distributions (Version 3.4.1). Available from: http://biodiversityinformatics.amnh.org/open_source/maxent/. (accessed 15 September 2020)
- Poley, L. G., A. J. Magoun, M. D. Robards, and R. L. Klimstra. 2018. Distribution and occupancy of wolverines on tundra, northwestern Alaska. *Journal of Wildlife Management* 85: 991–1002. <https://doi.org/10.1002/jwmg.21439>
- Pollard, R. H., W. B. Ballard, L. E. Noel, and M. A. Cronin. 1996. Parasitic insect abundance and microclimate of gravel pads and tundra within the Prudhoe Bay oil field, Alaska, in relation to use by caribou, *Rangifer tarandus granti*. *Canadian Field-Naturalist* 110: 649–658.
- Prichard, A.K., R. L. Klimstra, B. T. Person, and L. S. Parrett. 2019a. Aerial survey and telemetry data analysis of a peripheral caribou calving area in northwestern Alaska. *Rangifer* 43–58.
- Prichard, A. K., B. E. Lawhead, E. A. Lenart, and J. H. Welch. 2020a. Caribou distribution and movements in a Northern Alaska Oilfield. Early View. *Journal of Wildlife Management*. <https://doi.org/10.1002/jwmg.21932>
- Prichard, A. K., M. J. Macander, J. H. Welch, and B. E. Lawhead. 2017. Caribou monitoring study for the Alpine Satellite Development Program, 2015 and 2016. Twelfth annual report for ConocoPhillips Alaska, Inc., Anchorage, by ABR, Inc., Fairbanks. 62 pp.
- Prichard, A. K., L. S. Parrett, E. A. Lenart, J. Caikoski, K. Joly, and B. T. Person. 2020b. Interchange and overlap among four adjacent Arctic caribou herds. *Journal of Wildlife Management*. Journal of Wildlife Management. Early View. <https://doi.org/10.1002/jwmg.21934>
- Prichard, A. K., and J. H. Welch. 2020. Mammal surveys in the Greater Kuparuk Area, northern Alaska, 2018–2019. Report for ConocoPhillips Alaska, Inc., and Greater Kuparuk Area, Anchorage, by ABR, Inc., Fairbanks.
- Prichard, A. K., and J. H. Welch. 2021. Caribou us of the Greater Kuparuk Area, northern Alaska, 2020. Report for ConocoPhillips Alaska, Inc. Greater Kuparuk Area, Anchorage, by ABR, Inc., Fairbanks. 53 pp.
- Prichard, A. K., J. H. Welch, and B. E. Lawhead. 2018a. Mammal surveys in the Greater Kuparuk Area, northern Alaska, 2017. Report for ConocoPhillips Alaska, Inc., Anchorage, by ABR, Inc., Fairbanks. 52 pp.
- Prichard, A.K., J.H. Welch, and B.E. Lawhead. *In press*. The effect of traffic levels on the distribution and behavior of calving caribou in an Arctic oilfield. *Arctic*.
- Prichard, A. K., J. H. Welch, M. J. Macander, and B. E. Lawhead. 2018b. Caribou monitoring study for the Alpine Satellite Development Program, 2017. Thirteenth annual report for ConocoPhillips Alaska, Inc., Anchorage, by ABR, Inc., Fairbanks. 63 pp.
- Prichard, A. K., J. H. Welch, M. J. Macander, and B. E. Lawhead. 2019b. Caribou monitoring study for the Bear Tooth Unit Program, Arctic Coastal Plain, Alaska, 2018. Annual report for ConocoPhillips Alaska, Inc., Anchorage, by ABR, Inc., Fairbanks. 96 pp.

- Prichard, A. K., J. H. Welch, M. J. Macander, and B. E. Lawhead. 2019c. Caribou monitoring study for the Alpine Satellite Development Program, 2018. Fourteenth annual report for ConocoPhillips Alaska, Inc., Anchorage, by ABR, Inc., Fairbanks. 88 pp.
- Prichard, A. K., J. H. Welch, and M. J. Macander. 2020c. Caribou monitoring study for the Bear Tooth Unit Program, Arctic Coastal Plain, Alaska, 2019. Annual report for ConocoPhillips Alaska, Inc., Anchorage, by ABR, Inc., Fairbanks.
- Prichard, A. K., J. H. Welch, and M. J. Macander. 2020d. Caribou monitoring study for the Alpine Satellite Development Program and Greater Moose's Tooth Unit, 2019. Annual report for ConocoPhillips Alaska, Inc., Anchorage, by ABR, Inc., Fairbanks.
- Prichard, A. K., D. A. Yokel, C. L. Rea, B. T. Person, and L. S. Parrett. 2014. The effect of frequency of telemetry locations on movement-rate calculations in arctic caribou. *Wildlife Society Bulletin* 38: 78–88.
- R Core Team. 2020. R: A language and environment for statistical computing. R Foundation for Statistical Computing, Vienna, Austria. URL: <http://www.R-project.org>.
- Radosavljevic, A. and R. P. Anderson. 2014. Making better Maxent models of species distributions: complexity, overfitting and evaluation. *Journal of Biogeography*. 41: 629–643.
- Riggs, G. A., and D. K. Hall. 2015. MODIS snow products Collection 6 user guide. National Snow and Ice Data Center. Available online: <https://nsidc.org/sites/nsidc.org/files/files/MODIS-snow-user-guide-C6.pdf>
- Reynolds, P. E., H. V. Reynolds, and R. A. Shideler. 2002. Predation and multiple kills of muskoxen by grizzly bears. *Ursus* 13: 79–84.
- Riggs, G. A., and D. K. Hall. 2015. MODIS snow products Collection 6 user guide. National Snow and Ice Data Center. Available online: <https://nsidc.org/sites/nsidc.org/files/files/MODIS-snow-user-guide-C6.pdf> (accessed 16 February 2018).
- Riley S. J., S. D. DeGloria, and R. Elliot. 1999. A Terrain Ruggedness Index That Quantifies Topographic Heterogeneity. *Intermountain Journal of Sciences* 5(1–4): 23–27.
- Rouse, J. W., R. H. Haas, J. A. Schell, and D. W. Deering. 1973. Monitoring vegetation systems in the Great Plains with ERTS. Third Earth Resources Technology Satellite Symposium, Greenbelt, MD, NASA (SP-351) 1: 309–317.
- Russell, D. E., A. M. Martell, and W. A. C. Nixon. 1993. Range ecology of the Porcupine caribou herd in Canada. *Rangifer*, Special Issue 8. 167 pp.
- Salomonson, V. V., and I. Appel. 2004. Estimating fractional snow cover from MODIS using the normalized difference snow index. *Remote Sensing of Environment* 89: 351–360.
- Sappington, J., K. M. Longshore, and D. B. Thompson. 2007. Quantifying landscape ruggedness for animal habitat analysis: a case study using bighorn sheep in the Mojave Desert. *Journal of Wildlife Management* 71: 1419–1426.
- Schaaf, C., and Z. Wang. 2015. MCD43A4 MODIS/Terra+Aqua BRDF/Albedo Nadir BRDF Adjusted Ref Daily L3 Global - 500m V006. Distributed by NASA EOSDIS Land Processes DAAC, <https://doi.org/10.5067/MODIS/MCD43A4.006>
- Sellers, P. J. 1985. Canopy reflectance, photosynthesis, and transpiration. *International Journal of Remote Sensing* 21: 143–183. [original not reviewed; cited in Hope et al. 1993]
- Shideler, R., P. Reynolds, S. Arthur, E. Lenart, and T. Paragi. 2007. Decline of eastern North Slope muskoxen. *The Alaskan Wildlifer*: 5–6.
- Signer, J., J. Fieberg, and T. Avgar. 2018. Animal Movement Tools (amt): R-Package for managing tracking data and conducting habitat selection analyses. <<https://CRAN.R-project.org/package=amt>>. Accessed 16 Oct 2019.

- Smith, W. T., R. D. Cameron, and D. J. Reed. 1994. Distribution and movements of caribou in relation to roads and pipelines, Kuparuk Development Area, 1978–1990. Alaska Department of Fish and Game Wildlife Technical Bulletin 12, Juneau, USA.
- SRB&A. 2017. Nuiqsut caribou subsistence monitoring project: results of year 8 hunter interviews and household harvest surveys. Report for ConocoPhillips Alaska, Inc., Anchorage, by Stephen R. Braund & Associates, Anchorage, Alaska. 47 pp. + appendices.
- Stow, D. A., A. Hope, D. McGuire, D. Verbyla, J. Gamon, F. Huemmrich, S. Houston, C. Racine, M. Sturm, K. Tape, L. Hinzman, K. Yoshikawa, C. Tweedie, B. Noyle, C. Silapaswan, D. Douglas, B. Griffith, G. Jia, H. Epstein, D. Walker, S. Daeschner, A. Pertersen, L. Zhou, and R. Myneni. 2004. Remote sensing of vegetation and land-cover change in arctic tundra ecosystems. *Remote Sensing of Environment* 89: 281–308.
- Theobald, D. 2011. *Landscape Connectivity & Pattern Tools: Toolbox for ArcGIS*. Fort Collins, CO: Colorado State University.
- Therneau, T. 2015. A package for survival analysis in S. Version 2.44. <<https://CRAN.R-project.org/package=survival>>. Accessed 16 Oct 2019.
- Thornton, P. E., M. M. Thornton, B. W. Mayer, Y. Wei, R. Devarakonda, R. S. Vose, and R. B. Cook. 2016. Daymet: Daily Surface Weather Data on a 1-km Grid for North America, Version 3. ORNL DAAC, Oak Ridge, Tennessee, USA. doi:10.3334/ORNLDAAC/1328
- Thurfjell, H., S. Ciuti, and M. S. Boyce. 2014. Applications of step-selection functions in ecology and conservation. *Movement Ecology* 2: 4.
- Walker, H. J., and H. H. Morgan. 1964. Unusual weather and riverbank erosion in the delta of the Colville River, Alaska. *Arctic* 17: 41–47.
- Warren, D. L. and S. N. Seifert. 2011. Ecological niche modeling in Maxent: the importance of model complexity and the performance of model selection criteria. *Ecological Applications*. 21: 335–342.
- Weladji, R. B., G. Steinheim, Ø. Holand, S. R. Moe, T. Almøy, and T. Ådnøy. 2003. Use of climatic data to assess the effect of insect harassment on the autumn weight of reindeer (*Rangifer tarandus*) calves. *Journal of Zoology* 260: 79–85.
- Welch, J. H., A. K. Prichard, and M. J. Macander. 2021. Caribou monitoring study for the Alpine Satellite Development Program and Greater Moose's Tooth Unit, 2020. Annual report for ConocoPhillips Alaska, Inc., Anchorage, by ABR, Inc., Fairbanks.
- White, R. G., B. R. Thomson, T. Skogland, S. J. Person, D. E. Russell, D. F. Holleman, and J. R. Luick. 1975. Ecology of caribou at Prudhoe Bay, Alaska. Pages 151–201 in J. Brown, editor. *Ecological investigations of the tundra biome in the Prudhoe Bay region, Alaska*. Biological Papers of the University of Alaska, Special Report No. 2, Fairbanks, Alaska.
- Wilson, M. F. J., B. O'Connell, C. Brown, J. C. Guinan, and A. J. Grehan. 2007. Multiscale Terrain Analysis of Multibeam Bathymetry Data for Habitat Mapping on the Continental Slope. *Marine Geodesy* 30: 3–35. doi: 10.1080/01490410701295962.
- Wilson, R. R., A. K. Prichard, L. S. Parrett, B. T. Person, G. M. Carroll, M. A. Smith, C. L. Rea, and D. A. Yokel. 2012. Summer resource selection and identification of important habitat prior to industrial development for the Teshekpuk caribou herd in northern Alaska. *PLoS One* 7(11): e48697. doi:10.1371/journal.pone.0048697.
- Wolfe, S. A. 2000. Habitat selection by calving caribou of the central arctic herd, 1980–95. M.S. thesis, University of Alaska, Fairbanks. 83 pp.
- Yokel, D. A., A. K. Prichard, G. Carroll, L. Parrett, B. Person, and C. Rea. 2009. Teshekpuk caribou herd movement through narrow corridors around Teshekpuk Lake, Alaska. *Alaska Park Science* 8(2): 64–67.

We analyzed 2020 snow cover and 2000–2020 vegetation greenness using gridded, daily reflectance and snow-cover products from MODIS Terra and Aqua sensors. The snow-cover data were added to the data compiled for 2000–2019 (see Lawhead et al. 2015 and Prichard et al. 2017 and 2018b for detailed description of methods). The entire vegetation index record, based on atmospherically corrected surface reflectance data, was processed to ensure comparability of greenness metrics.

For data from 2000–2015, we applied a revised cloud mask that incorporated snow-cover history to reduce false cloud detection during the active snowmelt season. However, the revised cloud mask did not work on the 2016–2020 imagery, probably due to changes in the data and data format from the aging MODIS sensors. For 2016–2020, we applied manual cloud masks for the snowmelt season and applied the standard cloud mask for images collected in June and later.

We analyzed and summarized the data using Google Earth Engine, a cloud computing service (Gorelick et al. 2017). For final analysis and visualization, we exported the results to the Alaska Albers coordinate system (WGS-84 horizontal datum) at 240-m resolution.

SNOW COVER

Snow cover was estimated using the fractional snow algorithm developed by Salomonson and Appel (2004). Only MODIS Terra data were used for snow mapping through 2016 because MODIS Band 6, which was used in the estimation of snow cover, was not functional on the MODIS Aqua sensor. However, a Quantitative Image Restoration algorithm has been applied to restore the missing Aqua Band 6 data to a scientifically usable state for snow mapping (Riggs and Hall 2015). The Terra sensor was no longer reliable for snow mapping in 2017, so we used MODIS Aqua data for snow mapping in 2017–2020. The 2018–2020 analysis was based on MYD10A1.006 data (MODIS/Aqua Snow Cover Daily L3 Global 500m Grid).

- A time series of images covering the April–June period was analyzed for each year during 2000–2020. Pixels with >50% water (or ice) cover were excluded from the analysis. For each pixel in each year, we identified:
- The first date with 50% or lower snow cover (i.e., “melted”)
- The closest prior date with >50% snow cover (i.e., “snow”)
- The midpoint between the last observed date with >50% snow cover and the first observed date with <50% snow cover, which is an unbiased estimate of the actual snowmelt date (the first date with <50% snow cover)
- The duration between the dates of the two satellite images with the last observed “snow” date and the first observed “melted” date, providing information on the uncertainty in the estimate of snowmelt date. When the time elapsed between those two dates exceeded one week because of extensive cloud cover or satellite sensor malfunction, the pixel was assigned to the “unknown” category.

VEGETATIVE BIOMASS

The Normalized Difference Vegetation Index (NDVI; Rouse et al. 1973) is used to estimate the biomass of green vegetation within a pixel of satellite imagery at the time of image acquisition (Rouse et al. 1973). The rate of increase in NDVI between two images acquired on different days during green-up has been hypothesized to represent the amount of new growth occurring during that time interval (Wolfe 2000, Kelleyhouse 2001, Griffith et al. 2002). NDVI is calculated as follows (Rouse et al. 1973; <http://modis-atmos.gsfc.nasa.gov/NDVI/index.html>):

$$\text{NDVI} = (\text{NIR} - \text{VIS}) \div (\text{NIR} + \text{VIS})$$

where:

NIR = near-infrared reflectance (wavelength 0.841–0.876 μm for MODIS), and

VIS = visible light reflectance (wavelength 0.62–0.67 μm for MODIS).

We derived constrained view-angle (sensor zenith angle $\leq 40^\circ$) maximum-value composites from daily surface reflectance composites acquired over targeted portions of the growing season in 2000–2020. The data products used were MOD09GA.006 (Terra Surface Reflectance Daily Global 1km and 500m) and MYD09GA.006 (MYD09GA.006 Aqua Surface Reflectance Daily L2G Global 1km and 500m). NDVI during the calving period (NDVI_Calving) was calculated from a 10-day composite period (1–10 June) for each year during 2000–2020 (adequate cloud-free data were not available to calculate NDVI_Calving over the entire study area in some years). NDVI values near peak lactation (NDVI_621) were interpolated based on the linear change from two composite periods (15–21 June and 22–28 June) in each year. NDVI_Rate was calculated as the linear change in NDVI from NDVI_Calving to NDVI_621 for each year. Finally, NDVI_Peak was calculated from all imagery obtained between 21 June and 31 August each year during 2000–2020. Due to the availability of new forage models, NDVI_Calving, NDVI_621, NDVI_Rate, and NDVI_Peak were not included in analyses of caribou distribution in 2020, but we included summaries of these metrics in this report for comparison with previous reports.

FORAGE MODELING

We applied forage models from Johnson et al. (2018) that incorporate daily NDVI values as well as habitat type, distance to coast, and days from peak NDVI to predict biomass, nitrogen, and digestible energy for a given location on a given day. These models may provide metrics that are more directly related to caribou forage needs than NDVI alone.

We used the MCD43A4.Version 6 daily product at 500-m resolution (Schaaf and Wang 2015). This is the Nadir Bidirectional Reflectance Distribution Function Adjusted Reflectance (NBAR) product, and it provides 500-meter reflectance data that are adjusted using a bidirectional reflectance distribution function (BRDF) to model the reflectance values as if they were collected from a nadir view (i.e., viewed from directly overhead). The NBAR data are produced daily within 16-day retrieval periods using data from both MODIS platforms (i.e., the Terra and Aqua satellites). The product is developed using a single observation from each 16-day period for each 500-m pixel, with priority given to the central day in each compositing period (i.e., the ninth day) to provide the most representative information possible for each period of the year. Other observations in the period are used to parameterize the BRDF model that is required to adjust the observation to nadir. Similar to other MODIS vegetation index products such as MOD13Q1, it has a 16-day composite period, but unlike other products it has a temporal frequency of one day, with the 16-day window shifting one day with each new image. Thus it avoids any artificial steps at

the break between composite intervals, and is a good tool to assess daily phenology normals. It is more likely to provide an observation for a given day than true daily products such as the MOD09GA.006/MYD09GA.006 products used for the NDVI composite metrics (above).

Johnson et al. (2018) calibrated the forage models for 4 broad vegetation classes (tussock tundra, dwarf shrub, herbaceous mesic, and herbaceous wet). Following their approach, we used the Alaska Center for Conservation Science (ACCS) land cover map for Northern, Western, and Interior Alaska (Boggs et al. 2016), aggregated on the “Coarse_LC” attribute. This map is based on the North Slope Science Initiative (NSSI 2013) with the addition of the aggregation field. We calculated the modal land cover class for each 500-m pixel.

Snow water equivalent (SWE) estimates were obtained from the Daymet Version 3 model output data (Thornton et al. 2016), which provided gridded estimates of daily weather parameters for North America and Hawaii at 1 km resolution. Daymet output variables include minimum temperature, maximum temperature, precipitation, and snow water equivalent. The dataset currently covers the period from January 1, 1980 to December 31, 2019 (2020 data will become available sometime in late winter of 2021). SWE was extracted based on the location and date.

For each date from the start of the calving season through the end of the late summer season (30 May–15 September) and for each year with telemetry locations (2002–2020) we mapped NDVI, annual NDVIMax, and days to NDVIMax. Then, we applied the equations from Johnson et al. (2018) to calculate forage nitrogen content and forage biomass for the 4 broad vegetation classes. We set the forage metrics to zero for water, snow/ice, and barren classes and set it to undefined for other vegetation classes that were not included in the Johnson et al. (2018) models. The areas with undefined forage metrics within the study area were primarily low and tall shrub types which comprise a small proportion of the surface area.

HABITAT CLASSIFICATION

We used the NPRA earth-cover classification created by BLM and Ducks Unlimited (2002; Figure 3) to classify habitats for analyses. The NPRA survey area contained 15 cover classes from the NPRA earth-cover classification (Appendix A), which we lumped into nine types to analyze caribou habitat use. The barren ground/other, dunes/dry sand, low shrub, and sparsely vegetated classes, which mostly occurred along Fish and Judy creeks, were combined into a single riverine habitat type. The two flooded-tundra classes were combined as flooded tundra and the clear-water, turbid-water, and *Arctophila fulva* classes were combined into a single water type; these largely aquatic types are used very little by caribou, so the water type was excluded from the analysis of habitat preference.

Some previous reports (e.g., Lawhead et al. 2015) used a land-cover map created by Ducks Unlimited for the North Slope Science Initiative (NSSI 2013); however, discontinuities in classification methodology and imagery bisected our survey area and potentially resulted in land-cover classification differences in different portions of the survey area, and so we reverted to the BLM and Ducks Unlimited (2002) classification instead.

Appendix B. Cover-class descriptions of the NPRA earth-cover classification (BLM and Ducks Unlimited 2002).

Cover Class	Description
Clear Water	Fresh or saline waters with little or no particulate matter. Clear waters typically are deep (>1 m). This class may contain small amounts of <i>Arctophila fulva</i> or <i>Carex aquatilis</i> , but generally has <15 surface coverage by these species.
Turbid Water	Waters that contain particulate matter or shallow (<1 m), clear waterbodies that differ spectrally from Clear Water class. This class typically occurs in shallow lake shelves, deltaic plumes, and rivers and lakes with high sediment loads. Turbid waters may contain small amounts of <i>Arctophila fulva</i> or <i>Carex aquatilis</i> , but generally have <15 surface coverage by these species.
<i>Carex aquatilis</i>	Associated with lake or pond shorelines and composed of 50–80 % clear or turbid water >10 cm deep. The dominant species is <i>Carex aquatilis</i> . Small percentages of <i>Arctophila fulva</i> , <i>Hippuris vulgaris</i> , <i>Potentilla palustris</i> , and <i>Caltha palustris</i> may be present.
<i>Arctophila fulva</i>	Associated with lake or pond shorelines and composed of 50–80% clear or turbid water >10 cm deep. The dominant species is <i>Arctophila fulva</i> . Small percentages of <i>Carex aquatilis</i> , <i>Hippuris vulgaris</i> , <i>Potentilla palustris</i> , and <i>Caltha palustris</i> may be present.
Flooded Tundra– Low-centered Polygons	Polygon features that retain water throughout the summer. This class is composed of 25–50% water; <i>Carex aquatilis</i> is the dominant species in permanently flooded areas. The drier ridges of polygons are composed mostly of <i>Eriophorum russeolum</i> , <i>E. vaginatum</i> , <i>Sphagnum</i> spp., <i>Salix</i> spp., <i>Betula nana</i> , <i>Arctostaphylos</i> spp., and <i>Ledum palustre</i> .
Flooded Tundra– Non-patterned	Continuously flooded areas composed of 25–50% water. <i>Carex aquatilis</i> is the dominant species. Other species may include <i>Hippuris vulgaris</i> , <i>Potentilla palustris</i> , and <i>Caltha palustris</i> . Non-patterned class is distinguished from low-centered polygons by the lack of polygon features and associated shrub species that grow on dry ridges of low-centered polygons.
Wet Tundra	Associated with areas of super-saturated soils and standing water. Wet tundra often floods in early summer and generally drains of excess water during dry periods, but remains saturated throughout the summer. It is composed of 10–25% water; <i>Carex aquatilis</i> is the dominant species. Other species may include <i>Eriophorum angustifolium</i> , other sedges, grasses, and forbs.
Sedge/Grass Meadow	Dominated by the sedge family, this class commonly consists of a continuous mat of sedges and grasses with a moss and lichen understory. The dominant species are <i>Carex aquatilis</i> , <i>Eriophorum angustifolium</i> , <i>E. russeolum</i> , <i>Arctagrostis latifolia</i> , and <i>Poa arctica</i> . Associated genera include <i>Cassiope</i> spp., <i>Ledum</i> spp., and <i>Vaccinium</i> spp.
Tussock Tundra	Dominated by the tussock-forming sedge <i>Eriophorum vaginatum</i> . Tussock tundra is common throughout the arctic foothills north of the Brooks Range and may be found on well-drained sites in all areas of the NPRA. Cottongrass tussocks are the dominant landscape elements and moss is the common understory. Lichen, forbs, and shrubs are also present in varying densities. Associated genera include <i>Salix</i> spp., <i>Betula nana</i> , <i>Ledum palustre</i> , and <i>Carex</i> spp.
Moss/Lichen	Associated with low-lying lakeshores and dry sandy ridges dominated by moss and lichen species. As this type grades into a sedge type, graminoids such as <i>Carex aquatilis</i> may increase in cover, forming an intermediate zone.
Dwarf Shrub	Associated with ridges and well-drained soils and dominated by shrubs <30 cm in height. Because of the relative dryness of the sites on which this cover type occurs, it is the most species-diverse class. Major species include <i>Salix</i> spp., <i>Betula nana</i> , <i>Ledum palustre</i> , <i>Dryas</i> spp., <i>Vaccinium</i> spp., <i>Arctostaphylos</i> spp., <i>Eriophorum vaginatum</i> , and <i>Carex aquatilis</i> . This class frequently occurs over a substrate of tussocks.

Appendix B. Continued.

Cover Class	Description
Low Shrub	Associated with small streams and rivers, but also occurs on hillsides in the southern portion of the NPRA. This class is dominated by shrubs 0.3–1.5 m in height. Major species include <i>Salix</i> spp., <i>Betula nana</i> , <i>Alnus crispa</i> , and <i>Ledum palustre</i> .
Dunes/Dry Sand	Associated with streams, rivers, lakes and coastal beaches. Dominated by dry sand with <10% vegetative cover. Plant species may include <i>Poa</i> spp., <i>Salix</i> spp., <i>Astragalus</i> spp., <i>Carex</i> spp., <i>Stellaria</i> spp., <i>Arctostaphylos</i> spp., and <i>Puccinellia phryganodes</i> .
Sparsely Vegetated	Occurs primarily along the coast in areas affected by high tides or storm tides, in recently drained lake or pond basins, and in areas where bare mineral soil is being recolonized by vegetation. Dominated by non-vegetated material with 10–30% vegetative cover. The vegetation may include rare plants, but the most common species include <i>Stellaria</i> spp., <i>Poa</i> spp., <i>Salix</i> spp., <i>Astragalus</i> spp., <i>Carex</i> spp., <i>Arctostaphylos</i> spp., and <i>Puccinellia phryganodes</i> .
Barren Ground/ Other	Associated with river and stream gravel bars, mountainous areas, and human development. Includes <10% vegetative cover. May incorporate dead vegetation associated with salt burn from ocean water.

Appendix C. Snow depth (cm) and cumulative thawing degree-days ($^{\circ}\text{C}$ above freezing) at the Kuparuk airstrip, 1983–2019.

Year	Snow Depth (cm)			Cumulative Thawing Degree-days ($^{\circ}\text{C}$)						
	1 April	15 May	31 May	1–15 May	16–31 May	1–15 June	16–30 June	1–15 July	16–31 July	1–15 August
1983	10	5	0	0	3.6	53.8	66.2	74.7	103.8	100.3
1984	18	15	0	0	0	55.6	75.3	122.8	146.4	99.5
1985	10	8	0	0	10.3	18.6	92.8	84.7	99.4	100.0
1986	33	20	10	0	0	5.0	100.8	112.2	124.7	109.4
1987	15	8	3	0	0.6	6.7	61.4	112.2	127.8	93.1
1988	10	5	5	0	0	16.7	78.1	108.3	143.1	137.5
1989	33	–	10 ^a	0	5.6	20.6	109.4	214.7	168.1	215.8
1990	8	3	0	0	16.1	39.7	132.2	145.0	150.0	82.5
1991	23	8	3	0	7.8	14.4	127.6	73.3	115.0	70.6
1992	13	8	0	0.3	20.3	55.0	85.3	113.9	166.1	104.2
1993	13	5	0	0	8.6	33.6	94.4	175.8	149.7	96.1
1994	20	18	8	0	4.4	49.2	51.7	149.7	175.8	222.2
1995	18	5	0	0	1.1	59.4	87.5	162.8	106.9	83.3
1996	23	5	0	8.1	41.7	86.1	121.1	138.9	168.1	95.8
1997	28	18	8	0	20.8	36.1	109.7	101.7	177.8	194.2
1998	25	8	0	3.6	45.8	74.2	135.0	158.9	184.4	174.4
1999	28	15	10	0	1.4	30.3	67.8	173.3	81.1	177.5
2000	30	23	13	0	0	36.7	169.7	113.3	127.5	118.6
2001	23	30	5	0	0.8	51.9	72.2	80.0	183.9	131.7
2002	30	trace	0	4.2	30.3	57.8	70.3	92.2	134.4	106.1
2003	28	13	trace	0	10.8	23.6	77.5	140.0	144.7	91.9
2004	36	10	5	0	8.9	26.4	185.6	148.1	151.4	153.3
2005	23	13	0	0	2.5	14.2	78.1	67.5	79.4	176.7
2006	23	5	0	0	23.3	93.3	153.1	82.2	186.1	109.7
2007	25	46	5	0	0	46.4	81.7	115.0	138.9	134.4
2008	20	18	0	0	32.8	71.7	138.9	172.2	132.5	86.1
2009	36	13	0	0	16.7	71.7	44.4	142.8	126.4	133.6
2010	41	43	13	0	1.4	53.3	51.1	126.7	168.9	149.2
2011 ^a	25	18	0	0	27.8	12.5	101.2	122.4	171.6	143.2
2012 ^a	48	53	2	0	1.7	26.8	137.3	140.2	195.2	143.5
2013	33	18	2	0	4.2	79.2	131.7	112.8	188.0	185.4
2014	33	0 ^b	0 ^b	11.1	4.2	28.6	82.0	127.2	102.3	67.9

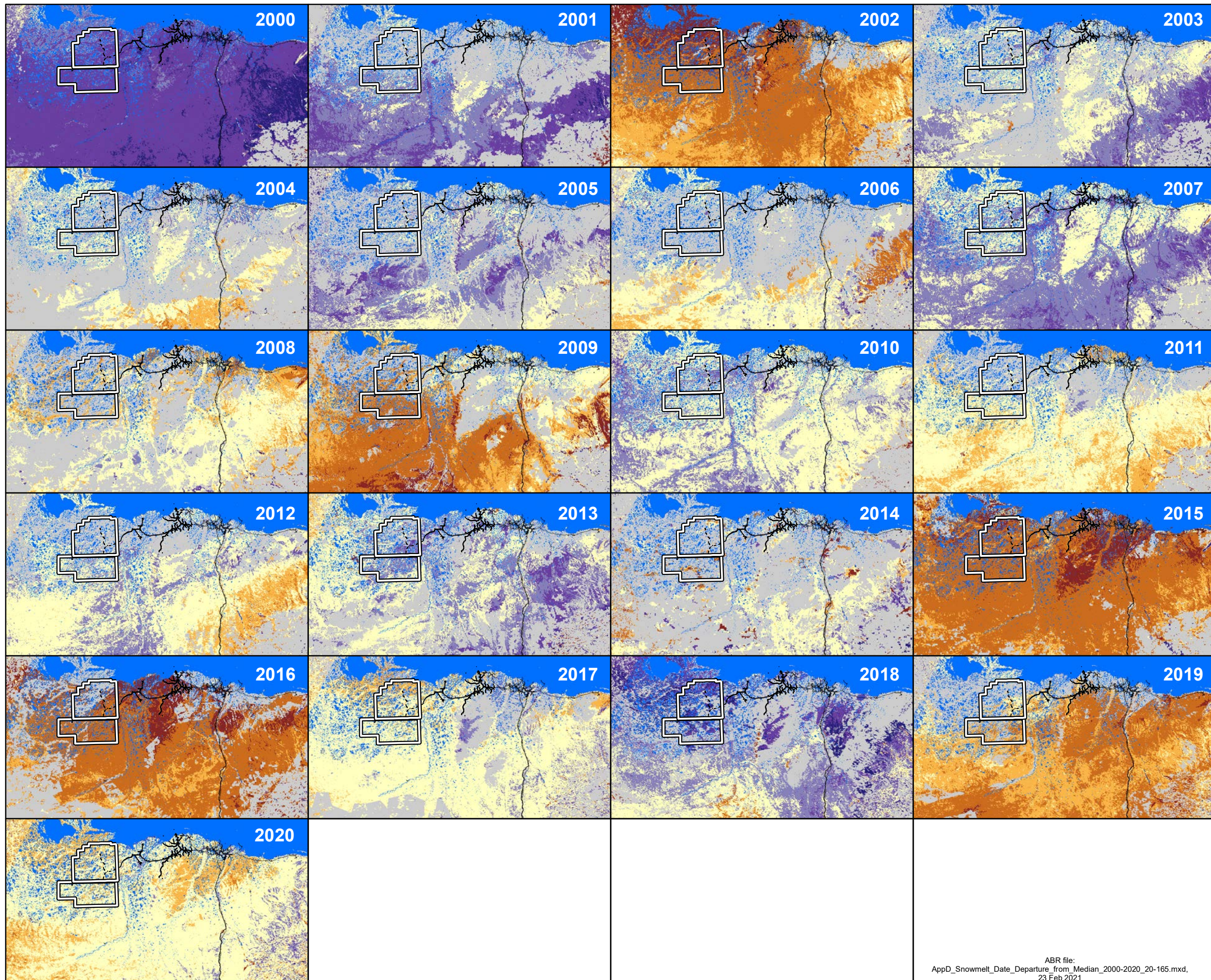
Appendix C. Continued.

Year	Snow Depth (cm)			Cumulative Thawing Degree-days (°C)						
	1 April	15 May	31 May	1–15 May	16–31 May	1–15 June	16–30 June	1–15 July	16–31 July	1–15 August
2015	38	14	3	1.4	46.4	78.9	197.2	117.9	95.7	106.9
2016	25	0	0	15.6	12.4	63.7	131.2	174.7	130.8	98.1
2017	36	14	0	0	12.1	5.2	121.3	173.4	174.5	150.5
018	41	20	15	1.35	0	6.6	47.7	137.0	195.9	55.25
2019	23	13	0	1.1	11.9	31.1	108.5	180.3	181.3	118.0
Mean	25	14	3	1.3	11.8	41.5	102.1	129.5	145.8	125.0

^a Kuparuk weather data were not available for 17 June–9 December 2011, 4–14 August 2012, and 30–31 August 2012, so cumulative TDD for those periods were estimated by averaging Deadhorse and Nuiqsut temperatures (Lawhead and Prichard 2012).

^b Kuparuk airport station reported no snow after 8 May 2014, whereas other weather stations nearby reported snow until 31 May and patchy snow was present in the GKA survey areas into early June. Therefore, if accurate, the airport information was not representative of the study area.

Page intentionally left blank.

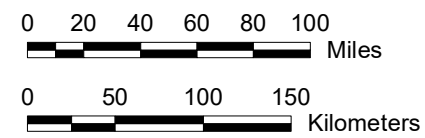
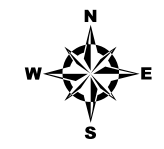


Timing of Snow Melt

Compared to Median (2000–2020)

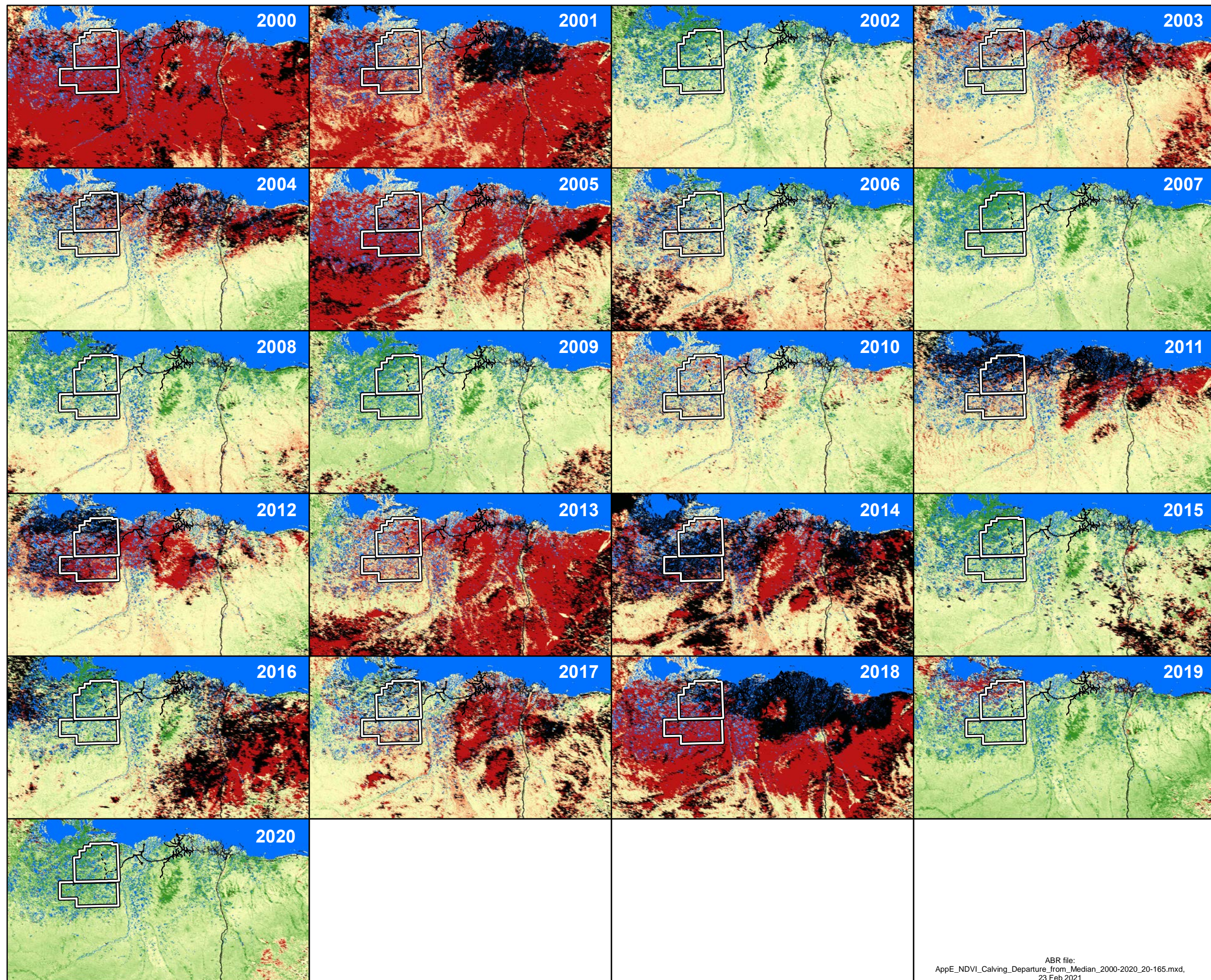
- Date not known within one week
- > 14 days earlier than median
- 8–14 days earlier than median
- 4–7 days earlier than median
- Within 3 days of median
- 4–7 days later than median
- 8–14 days later than median
- > 14 days later than median
- >= 50% Water Cover

Aerial Survey Area



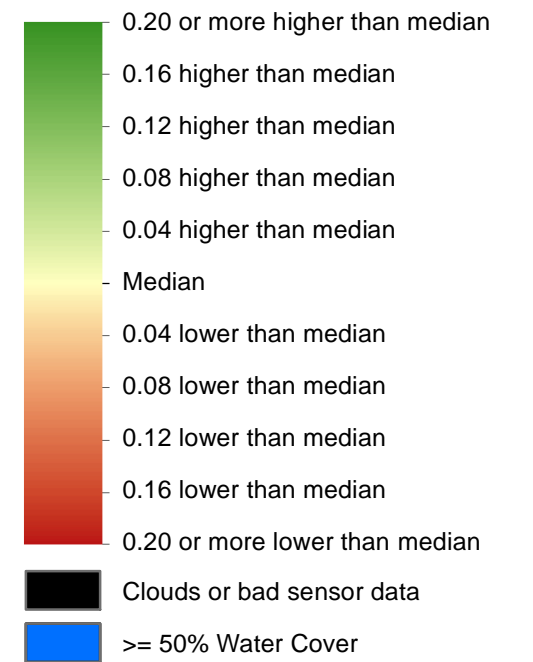
Appendix D.
Timing of annual snowmelt (<50% snow cover), compared with median date of snowmelt, on the central North Slope of Alaska during 2000–2020, as estimated from MODIS satellite imagery.


ABR file:
 AppD_Snowmelt_Date_Departure_from_Median_2000-2020_20-165.mxd,
 23 Feb 2021

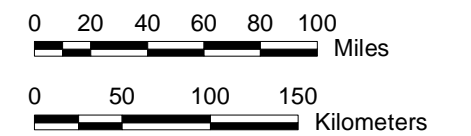
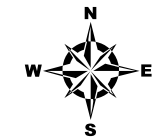


NDVI_Calving

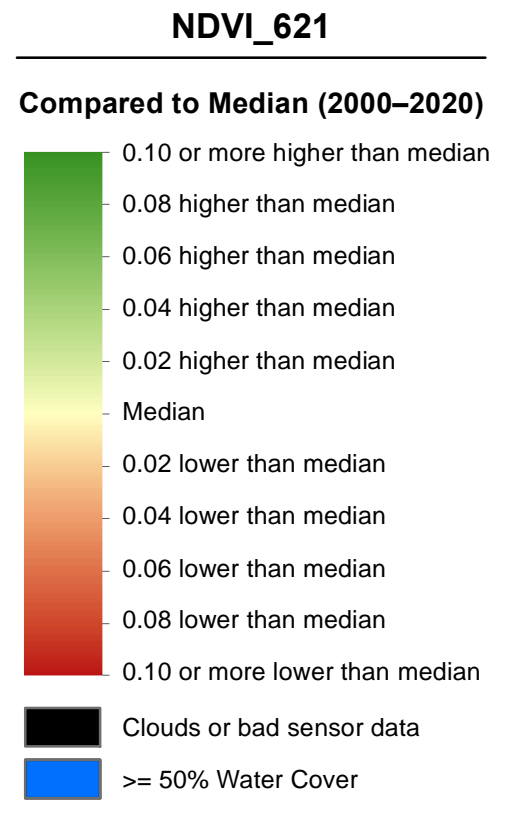
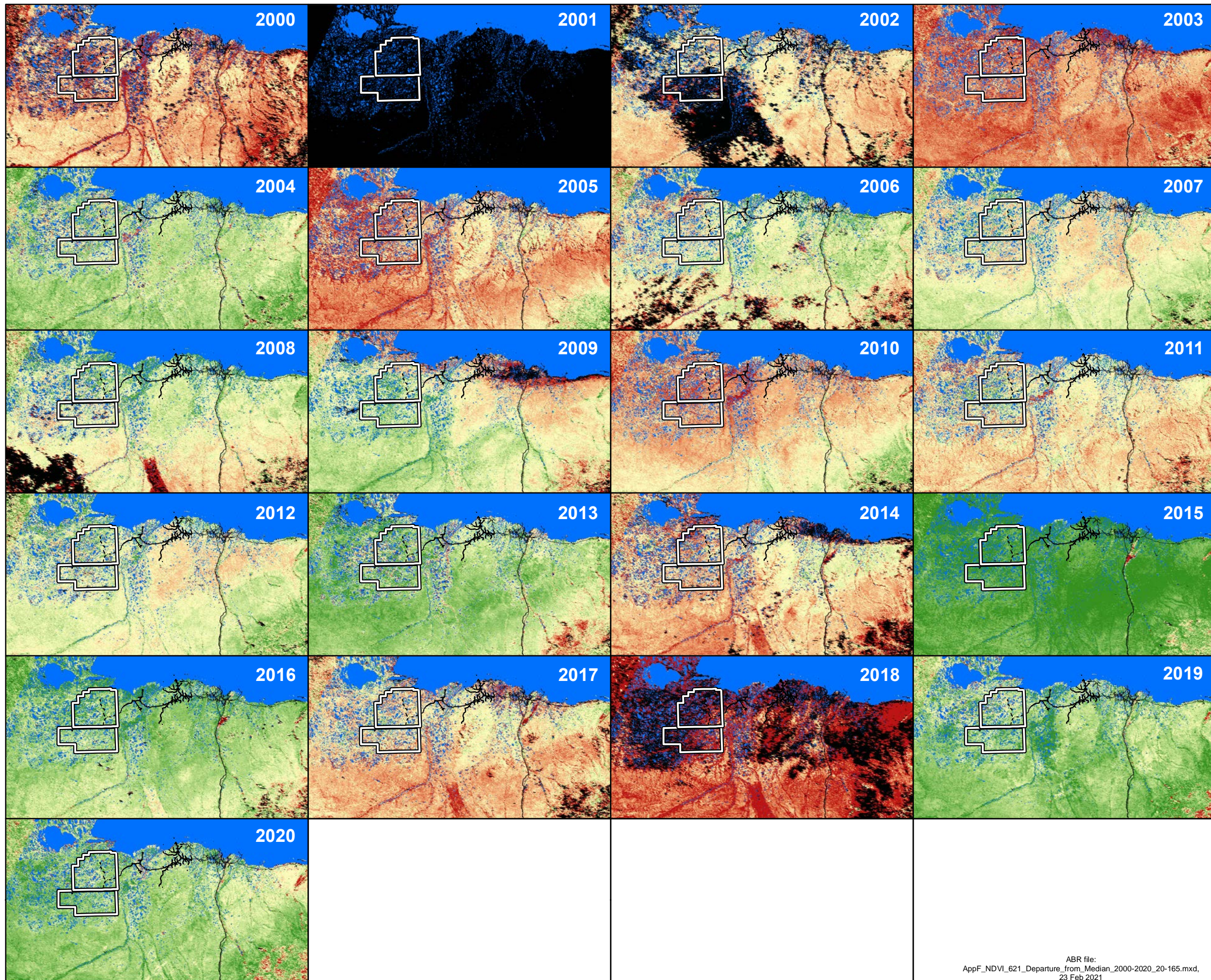
Compared to Median (2000–2020)




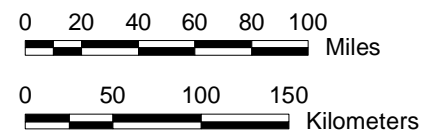
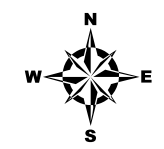
 Aerial Survey Area



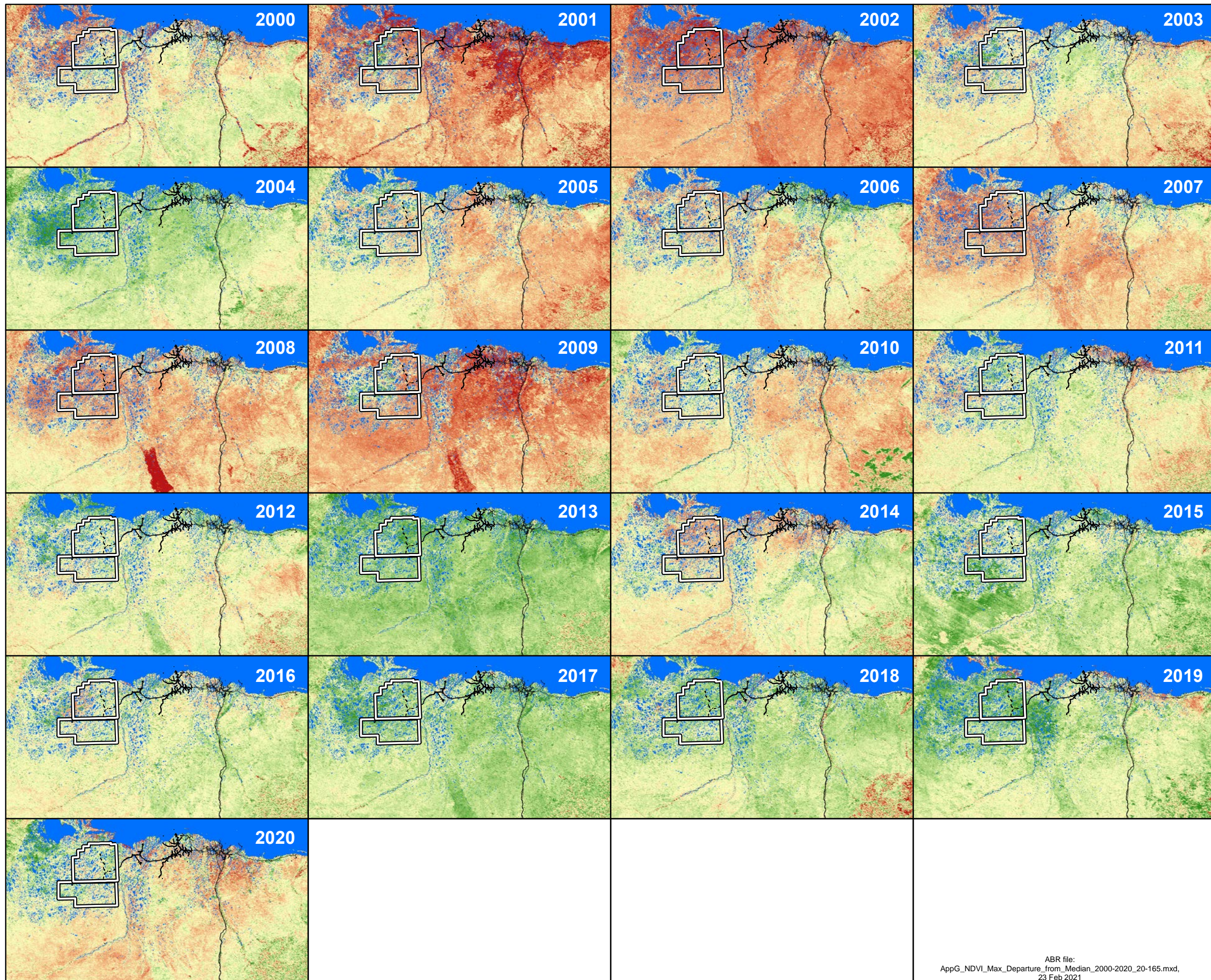
Appendix E.
Differences between annual relative vegetative biomass values and the 2000–2020 median during the caribou calving season (1–10 June) on the central North Slope of Alaska, as estimated from NDVI calculated from MODIS satellite imagery.



 Aerial Survey Area

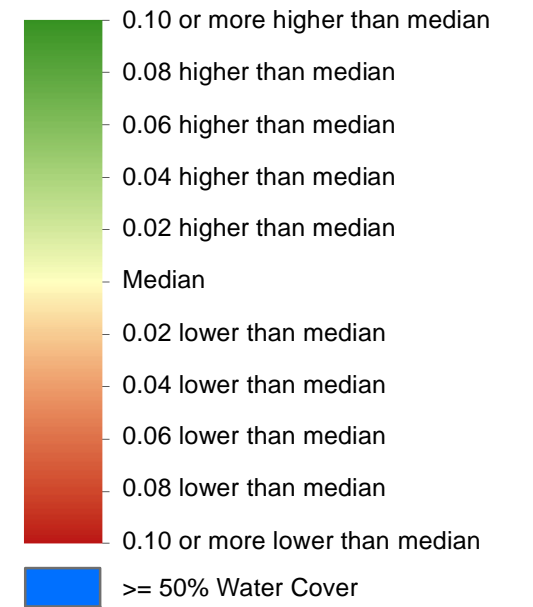



Appendix F.
Differences between annual relative vegetative biomass values and the 2000–2020 median at estimated peak lactation for caribou (21 June) on the central North Slope of Alaska, as estimated from NDVI calculated from MODIS satellite imagery.

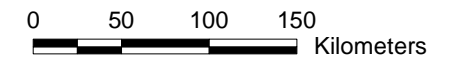
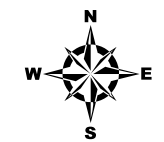


NDVI_Peak

Compared to Median (2000–2020)



 Aerial Survey Area



Appendix G.
Differences between annual relative vegetative biomass values and the 2000–2020 median for estimated peak biomass on the central North Slope of Alaska, as estimated from NDVI calculated from MODIS satellite imagery.

ABR file:
 AppG_NDVI_Max_Departure_from_Median_2000-2020_20-165.mxd,
 23 Feb 2021